CHARACTERIZATION OF NON-CANONICAL HETEROTRIMERIC G PROTEIN COMPONENTS IN MAIZE PATHOGEN *FUSARIUM VERTICILLIOIDES*

A Dissertation

by

HUIJUAN YAN

Submitted to the Office of Graduate and Professional Studies of
Texas A&M University
in partial fulfillment of the requirements for the degree of

DOCTOR OF PHILOSOPHY

Chair of Committee,	Won-Bo Shim
Committee Members,	Daniel J. Ebbole
	Libo Shan
	Charles M. Kenerley
Head of Department,	Leland S. Pierson III

May 2020

Major Subject: Plant Pathology

ABSTRACT

Fusarium verticillioides is a fungal pathogen of maize causing ear rot and stalk rot diseases. Importantly, the fungus also produces carcinogenic mycotoxins, fumonisins, on infested maize. Unfortunately, we still lack a clear understanding of how the pathogen responds to host and environmental stimuli to trigger fumonisin B1 (FB1) biosynthesis. In this study, we hypothesized that G-protein coupled receptors (GPCRs), heterotrimeric G proteins and regulators of G protein signaling (RGS) proteins play important roles in sensing environmental cues and activate signaling pathways. Previously, we demonstrated that Gβ protein FvGbb1 directly impacts FB1 regulation but no other physiological aspects in *F. verticillioides*. In this study, we identified and characterized Receptor for Activated C Kinase 1 (RACK1) homolog FvGbb2 as a putative Gβ-like protein in *F. verticillioides.* The mutant exhibited severe defects not only in FB1 biosynthesis but also in vegetative growth and conidiation. FvGbb2 was positively associated with carbon source utilization and stress agents but negatively regulated general amino acid control. As for RGS proteins, *F. verticillioides* has two FvFlbA paralogs, namely FvFlbA1 and FvFlbA2, unlike yeast and *Aspergillus* species with a single copy of FlbA. Previously, we demonstrated that FlbA2 protein negatively impacts FB1 regulation in *F. verticillioides*. In this study, we further characterized the role and association of two FvFlbA paralogs. We learned that FvFlbA1 deletion did not lead to significant physiological defects, but FvflbA2/A1 double mutation resulted in severe growth defects and elevated FB1 production than those observed in single mutants. Taken together, our data suggest that

heterotrimeric G proteins and RGS proteins perform unique functions in regulating *F. verticillioides* growth, virulence and FB1 biosynthesis by associating with different proteins and signaling pathways. Additionally, the characterization of a small GTPase FvSec4 showed critical functions in asexual development, pathogenicity, stress responses and mycotoxin biosynthesis. GFP-FvSec4 is localized to growing hyphal tips and raised the possibility that FvSec4 is involved in protein trafficking and endocytosis.

DEDICATION

This dissertation is dedicated to my parents, Longhe Yan and Minglian Liu for their unconditional love and support during this work.

ACKNOWLEDGEMENTS

Firstly, I would like to express my sincere gratitude to my advisor Dr. Won-Bo Shim for his expertise, patience, guidance and continuous support of my Ph.D. study. Without his help, this work would not have been possible. I would also like to thank my committee members: Dr. Daniel J. Ebbole, Dr. Libo Shan and Dr. Charles M. Kenerley for their advice, insightful discussions and comments.

I would like to extend my sincere thanks to my current and former members of Dr. Shim's lab, especially Huan Zhang and Angelyn Hilton, who passed knowledge to me when I joined in the lab and Jun Huang for his friendship and sharing the knowledge with me. I also would like to thank the faculties, staff and students of the Department of Plant Pathology and Microbiology for making my time at Texas A&M University so memorable. Special thanks to Dr. Brian Shaw and Dr. Zach Schultzhaus.

Finally, I would like to thank my mom and dad for their unconditional love and support, and my boyfriend Yuanning Zheng for his encouragement and accompany.

CONTRIBUTORS AND FUNDING SOURCES

Contributors

This work was supervised by a dissertation committee consisting of Professor Won-Bo Shim [major advisor] of plant pathology and microbiology and Professors and Daniel J. Ebbole, Charles M. Kenerley of the Department of Plant Pathology and Microbiology and Professor Libo Shan of the Department of Molecular & Environmental Plant Science. All other work conducted for the dissertation was completed by the candidate independently.

Funding Sources

This work was supported by a Teaching Assistantship from the Department of Plant Pathology and Microbiology and in part by the Agriculture and Food Research Initiative (No. 2013-68004-20359) from the US Department of Agriculture.

NOMENCLATURE

FB1	Fumonisin B_1
PCR	Polymerase chain reaction
HPLC	High performance Liquid Chromatography
GPCR	G protein-coupled receptors
RGS	Regulator of G protein signaling

TABLE OF CONTENTS

Page

LIST OF FIGURES

Page

CHAPTER I

INTRODUCTION

Fusarium verticillioides is a major pathogen of maize

Fusarium species is a major group of filamentous fungi associated with plant diseases and mycotoxin contamination (Ma et al., 2013). These fungi cause a wide variety of plant diseases including wilts, rots and blights in many agriculturally important plants worldwide. For example, *F. oxysporum f. sp. cubense* tropical race 4 (*Foc* TR4) is a devastating pathogen for Cavendish bananas in subtropic and tropic areas worldwide (Warman and Aitken, 2018). *F. oxysporum f. sp. vasinfectum* Race 4, known as FOV4, is a newly introduced pathogen that is causing devastating wilt in Pima cotton in California and Texas (Cox et al., 2019; Seo et al., 2020). Furthermore, *Fusarium* is notorious for producing a large number of toxic mycotoxins including fumonisins, trichothecenes, zearalenone, and fusarins. The genes associated with biosynthesis of these secondary metabolites typically occur in clusters. To date, forty-six secondary metabolite clusters were identified in key *Fusarium* plant pathogens, including *F. verticillioides*, *F. graminearum* and *F. oxysporum* (Ma et al., 2010).

Maize is widely cultivated and one of the most important crops in the world, mainly used for human and animal consumption. *F. verticillioides* (teleomorph: *Gibberella moniliformis* Wineland) is a fungal pathogen of maize that causes ear rot and stalk rot

diseases and thus poses significant food safety and security risks. This fungus utilizes asexual spores, *i.e.* microconidia and macroconidia, to rapidly reproduce and spread through infested seeds and plant debris. Typically, microconidia are the predominant inoculum source for dissemination and infection. *F. verticillioides* can infect all developing stages of maize, and in some cases does not exhibit any recognizable symptoms prompting some scientists to designate the pathogen as facultative endophyte (Blacutt et al., 2018). *F. verticillioides* is known to cause ear rot on maize primarily through silk infection (Duncan and Howard, 2010).

Fumonisins gene cluster and biosynthesis

F. verticillioides produces a variety of mycotoxins and biologically active secondary metabolites including fusaric acid, fusarins, and fumonisins on infested maize. Production of fumonisins are notable in several *Fusarium* species, but *F. verticillioides* is recognized as the most prevalent species with critical economic impact. Fumonisins consist of A, B, C and P series with 28 fumonisin analogs identified in total (Rheeder et al., 2002). The B series fumonisin B1, B2, B3 and B4 are more thoroughly studied, and fumonisin B1 (FB1) is recognized as the most prevalent and toxic form in nature. Fumonisins are a group of polyketide-derived mycotoxins structurally similar to sphinganine, which are associated with esophageal cancer and neural tube defect in humans and also toxic to animals (Gelderblom et al., 1988; Nelson et al., 1993). Due to these health risks, the levels of

fumonisins in grains and foodstuffs for human and animal consumptions are regulated by governmental agencies worldwide.

Structurally, fumonisins are 19-20 carbon backbone polyketide secondary metabolites. The fumonisin biosynthesis gene cluster (referred to as the "*FUM* cluster") was first proposed by Proctor et al (1999), which consists of 16 genes encoding biosynthetic enzymes and regulatory proteins (Proctor et al., 2013). Except for four *FUM* genes (*FUM15*, *FUM16*, *FUM17*, *FUM18*) which were reported to have no impacts on fumonisns production, all other *FUM* genes (*FUM1*, *FUM2, FUM3, FUM6, FUM7*, *FUM8*, *FUM10*, *FUM11*, *FUM13*, *FUM14*, *FUM19*, *FUM21*) were determined to be required for fumonisins production in *F. verticillioides*. More specifically, *FUM1*, which encodes a polyketide synthase (PKS), contributes to the first step in fumonisin production, followed by *FUM8*, an aminotransferase gene. *FUM6*, a cytochrome P450 monixygenase is proposed to be responsible for the third step in FB1 biosynthesis pathway. Fumonisins production were completely abolished in *fum1*, *fum8* and *fum6* knockout mutants. (Proctor et al., 1999; Seo et al., 2001). Additionally, *FUM21* is a Zn(II)2Cys6 transcription factor that positively regulated *FUM* cluster gene expression and fumonisins production (Brown et al., 2007).

It is well documented that polyketide synthases (PKSs) and non-ribosomal peptide synthases (NRPSs) are responsible for a large number of structurally diverse secondary metabolites in bacteria, fungi and plants. Fungal PKSs are multifunctional proteins which

harbor multiple functional domains required for synthesizing polyketides that are precursors of numerous pigments and toxins (Hopwood and Sherman, 1990; Staunton and Weissman, 2001; Kroken et al., 2003). To date, 16 PKSs and 16 NRPSs are identified in the *F. verticillioides* genome (Hansen et al., 2015). Particularly, *PKS11* (also known as *FUM1*) is the essential PKS gene for initiating fumonisin biosynthesis. Some additional PKS genes have been characterized in *F. verticillioides* responsible for secondary metabolisms, e.g. *PKS3* (*PGL1*) required for the dark violet pigment production in perithecia. *PKS21* (*FUB1*) is required for fusaric acid biosynthesis (Brown et al., 2012). *PKS10* (*FUS1*), a NRPS-PKS hybrid, is also responsible for fusarin C production (Song et al., 2004). However, the majority of PKS gene functions remain uncharacterized (Hansen et al., 2015).

In addition to *FUM* gene cluster, a number of genetic components have been demonstrated to be positively or negatively associated with FB1 regulation. Disruption of *FCC1* gene, a yeast Ssn8 (Ume3 or Srb11) homolog, led to significantly lower FB1 and microconidia production (Shim and Woloshuk, 2001). Later, it was revealed that *Fcc1* interacts with a cyclin-dependent kinase 8, Fck1 and that inactivation of *FCK1* results in similar phenotypes as *FCC1* mutant (Bluhm and Woloshuk, 2006). Another study identified a transcription factor, *ZFR1*, which is highly suppressed in the Δfcc1 deletion mutant. Disruption of *ZFR1* gene led to a drastic reduction in fumonisin B1(FB1) production but there was minimal negative impacts on physiological growth and development (Flaherty and Woloshuk, 2004). Two MADS-box transcription factors deletion mutants, Δmads1

and Δmads2, further showed significant alterations in FB1 production and PKS genes expression. A recent study on *FUG1*, a Fungal Unknown Gene 1, implies that there are still a number of uncharacterized genetic factors associated with *FUM* genes expression and fumonisin biosynthesis (Ridenour and Bluhm, 2017).

A select number of negative regulators including *PAC1*, *CPP1*, *PPR2, GBP1*, *FLBA2* have also been reported. Molecular characterization of *PAC1*, a PH regulatory gene showed significant higher FB1 production when grown on maize kernels and in acidic synthetic medium (Flaherty et al., 2003). *CPP1* is a protein phosphatase 2A (PP2A) catalytic subunit, negatively associated with FB1 production, *FUM1* expression level but positively involved in growth and hyphal polarity (Choi and Shim, 2008). Similarly, deletion of *PPR2*, a gene encoding regulatory subunit of PP2A, showed elevated FB1 production (Shin et al., 2013). *GBP1*, a monomeric G protein, was upregulated in *fcc1* mutant in expressed sequence tag (EST) test. Gene deletion mutant of Δgbp1 demonstrated increases in FB1 production, *FUM1* and *FUM8* gene expressions compared to WT (Sagaram et al., 2006).

GPCRs and non-receptor guanine nucleotide exchange factors

All living organisms have the task of sensing and responding to fluctuating environmental cues. G protein-coupled receptors (GPCRs) are the largest group of receptors containing seven transmembrane (TM) domains that transduce signals from the external environment

to the cell, enabling the organism to adjust to its environment. In addition to 7 TM domains, GPCRs have N-terminus exposed to the external cell while the C-terminus is extending to cytoplasm. GPCRs are roughly half of drug targets accounted for in human disease treatments or under development (Marchese et al., 2008). To date, 15,147 GPCRs are predicted in 3,547 species in GPCRdb (Munk et al., 2016). The number of GPCRs varies in different organisms; more than 800 GPCRs were identified in the human genome while over 1300 were found in the mouse genome. By contrast, three GPCRs are present in *Saccharomyces cerevisiae* and nine in *S. pombe*. Surprisingly, GPCR was not identified in plants such as *Arabidopsis thaliana*.

GPCRs bind to heterotrimeric G proteins that consist of α, β, and γ subunits. The α subunit is bound to GTP or GDP and is capable of GTP hydrolysis stimulated by RGS proteins. When activated by specific stimuli including hormones, amino acid and nutrients, GPCRs will go through a conformational change. This will lead to the exchange of GTP for GDP on the Gα subunit triggering dissociation of the heterotrimer G proteins (Hanlon and Andrew, 2015). Both Gα subunit and Gβγ dimer are responsible for initiating the signaling pathway. Typically, Gβγ dimer is not dissociated during nondenaturing circumstances (Neves et al., 2002).

Gα subunit GDP–GTP exchange can also be regulated by nonreceptor guanine echange factors (GEFs), including Ric8 and Get3/Arr4 (Miller et al., 2000; Tall et al., 2003; Lee and Dohlman, 2008). Ric8 (resistant to inhibitors of cholinesterase 8 protein) was firstly

identified in *Caenorhabditis elegans*, mediating GEF activity to several G proteins (Miller et al., 2000; Tall et al., 2003). Ric8 orthologs are found in filamentous fungi, but are absent in *S. cerevisiae*. Recent studies have characterized five putative Ric8 orthologs in filamentous fungi, including *Neurospora crassa*, *Aspergillus nidulans*, *A. fumigatus*, *Magnaporthe oryzae* and *F. gramniearum*, associated with many different biological processes (Li et al., 2010; Eaton et al., 2012; Kwon et al., 2012; Wu et al., 2015). For instance, in *F. graminearum*, FgRic8 has physical interaction with group I and Group II Gα proteins (Wu et al., 2015). Gene expression levels of heterotrimeric G protein components were all significantly inhibited in FgRic8 deletion mutant except *FgGPA2* which was elevated (Wu et al., 2015). Significantly, the deletion mutant exhibited defects in radial growth, conidiation, mycotoxin production and virulence (Wu et al., 2015).

Arr4, a homolog of ArsA ATPase in bacteria was initially named due to the similarity to Arsenicals Resistance proteins in bacterial species (Shen et al., 2003). Get3/Arr4 is responsible for tail-anchored (TA) proteins inserting into the endoplasmic reticulum (Schuldiner et al., 2008). Get3 showed interaction with Gpa1 and promoted GEF activity on Gpa1 protein in *S. cerevisiae* (Lee and Dohlman, 2008). Get3/Arr4 is important for stress tolerance, proper MAPK signaling, gene expression, and mating efficiency in *S. cerevisiae* (Shen et al., 2003; Lee and Dohlman, 2008). Additionally, a recent study revealed that Get3 acts as a ATP-Independent chaperone under oxidative stresses preventing cells from detrimental oxidative damage (Voth et al., 2014). Get3 has been

shown to be an essential protein in mouse (Mukhopadhyay et al., 2006), however its ortholog has not been studied in the filamentous fungi to date.

Heterotrimeric G proteins signaling components

In general, canonical heterotrimerc G protein complex in vast majority of filamentous fungi contains three Gα, one Gβ, and one Gγ subunits (Li et al., 2007). However, this is not always the case; *S. cerevisiae* has two Gα proteins while *Ustilago maydis* has a fourth Gα protein Gpa4. Similar to many fungi, *Fusarium* species contain three Gα proteins. Gα group I is the most conserved Gα proteins in key *Fusarium* species, with 100% identity at the protein level, and is responsible for negatively regulating secondary metabolisms in *F. graminearum* and *F. fujikuroi* (Yu et al., 2008b; Studt et al., 2013). In addition, the mutants showed mating defects in both *F. graminearum* and *Fusarium fujikuroi*. Gα group II did not impact the phenotypes in *F. graminearum*, while Gα group III was shown to be involved in pathogenicity and cell wall chitin content in *F. graminearum* but associated with the fusarubin biosynthesis in *F. fujikuroi*.

It is widely accepted that fungi contain one canonical Gβ protein. However, studies have shown that Gβ function is not conserved in fungi. For instance, the deletion of Gβ protein in *F. graminearum* and *F. fujikuroi* showed significant reduction in host virulence while the mutation did not impact *F. verticillioides* maize stalk pathogenicity (Delgado-Jarana

et al., 2005; Sagaram and Shim, 2007; Yu et al., 2008a). *F. graminearum* ΔFggpb1 mutant produced significantly higher DON and ZEA biosynthesis, while *F. verticillioides* ΔFvgbb1 mutant produced significantly less FB1. To date, the function of Gγ subunit in *Fusarium* species has not been characterized but we know it is highly conserved in four select *Fusarium* species (*F. verticillioides*, *F. graminearum*, *F. fujikuroi*, and *F. oxysporum*).

Accumulating evidences demonstrate that non-canonical Gβ subunit, Receptor for Activated C Kinase 1 (RACK1) homologue, interacts with canonical heterotrimeric G protein components in various fungi. For instance, Gβ-like protein RACK1 interacts with Gα group III in *S. cerevisiae*, *C. neoformans* and *M. oryzae* (Zeller et al., 2007; Wang et al., 2014; Yin et al., 2018). In addition, RACK1 homologue Gib2 in *C. neoformans* also showed interaction with two Gγ subunits (Gpg1 and Gpag2) (Wang et al., 2014). RACK1 protein has seven WD40 repeats that are about 40 amino acids motifs typically ending with Trp(W)-Asp(D) dipeptide (Wang et al., 2016). WD40 proteins mainly exist in eukaryotes while some are present in bacteria. In *F. verticillioides*, HMMER (version 3.2.1) search showed 109 WD40-containing proteins. WD proteins often function as scaffolding proteins and are associated with many fundamental biological processes, such as signal transduction, autophagy and transcription regulation (Xu and Min, 2011).

Regulator of G protein signaling (RGS) proteins

GPCR signaling is attenuated by G-protein-coupled receptor kinases (GRKs) and β-arrestin in animals (Dohlman, 2009). However, GRKs and β-arrestin were not found in fungi. In contrast, studies showed regulator of G protein signaling (RGS) proteins in fungi acts as GTPase-activating proteins that promote GTP hydrolysis and leads Gα subunit back to GDP-bound inactivated form to terminate GPCR and G protein signaling pathways (Dohlman, 2009). RGS proteins typically contain a 130 amino acid RGS domain, which promote RGS protein binding to the Gα subunit. Notably, RGS proteins also contain diverse non-RGS domains, such as DEP (*Dishevelled*, *Egl-10* and *Pleckstrin*), PX (phox), PXA, nexin C and TM, which are linked to various signaling pathways. For instance, the DEP domain is found in a well-known yeast RGS protein Sst2 that is known to interact with pheromone sensing Ste2 and mediate GPCR signaling responses (Ballon et al., 2006).

S. cerevisiae Sst2 was the first RGS protein investigated in fungi. Since then, RGS proteins have also been identified and studied in other fungi. Amongst *Fusarium* species, RGS proteins were first identified and studied in *F. verticillioides*; when investigating the function of Gβ protein FvGbb1, transcription of four RGS genes *FvFLBA1*, *FvFLBA2*, *FvRGSB* and *FvRGSC1* were significantly altered compared to the WT strain (Mukherjee et al., 2011). Intriguingly, FvFlbA2 and FvRgsB knockout mutants exhibited increase in FB1 production. In *F. graminearum*, FgFlbA exhibited similar impacts on DON and ZEA production while FgRgsB and FgRgsC were associated with sexual development. No

evidence indicated the function of RGS proteins in virulence on corn stalk rot in *F. verticillioides* but *F. graminearum* FgFlbA, FgRgsA and FgRgsb were shown to be involved in the pathogenicity.

Objectives of this study

The discovery of *FUM* gene cluster allowed researchers to gain a better understanding of the biosynthetic mechanism associated with fumonisins contamination in *Fusarium* ear rot of maize. However, further studies suggested that fumonisins are not critical for maize ear rot virulence (Desjardins et al., 2002). Thus, it is intriguing to ask why, when, and how *F. verticillioides* triggers fumonisin biosynthesis. While there are a number of genes shown to be involved in regulating fumonisin biosynthesis, our knowledge of the cellular and genetic networks underpinning the mechanisms of fumonisin regulation is still very limited. Previous studies demonstrated that there are multiple components, environmental and epigenetic factors, involved in this complex biological process (Woloshuk and Shim, 2013; Blacutt et al., 2018). For instance, Bluhm & Woloshuk (2005) showed that amylopectin in synthetic media supported the higher FB1 levels when compared to a medium with glucose or maltose as the carbon source. How does *F. verticillioides* sense the differences in carbon source and trigger *FUM* genes? Based on earlier studies, it is reasonable to hypothesize GPCRs, heterotrimeric G proteins and RGS proteins play important roles in sensing environmental cues and activating signaling pathways. The goal

of my research is to further understand fumonisins regulatory mechanism, particularly the roles heterotrimeric G proteins and RGS proteins play, in *F. verticillioides*.

CHAPTER II

CHARACTERIZATION OF NON-CANONICAL G BETA-LIKE PROTEIN FVGBB2 AND ITS RELATIONSHIP WITH HETEROTRIMERIC G PROTEINS IN *FUSARIUM VERTICILLIOIDES*

Summary

Fusarium verticillioides is a fungal pathogen that is responsible for maize ear rot and stalk rot diseases worldwide. The fungus also produces carcinogenic mycotoxins, fumonisins, on infested maize. Unfortunately, we still lack clear understanding of how the pathogen responds to host and environmental stimuli to trigger fumonisin biosynthesis. The heterotrimeric G protein complex, consisting of canonical Gα, Gβ, and Gγ subunits, is involved in transducing signals from external stimuli to regulate downstream signal transduction pathways. Previously, we demonstrated that Gβ protein FvGbb1 directly impacts fumonisin regulation but no other physiological aspects in *F. verticillioides*. In this study, we identified and characterized a RACK1 (Receptor for Activated C Kinase 1) homolog FvGbb2 as a putative Gβ-like protein in *F. verticillioides.* The mutant exhibited severe defects not only in fumonisin biosynthesis but also vegetative growth and

* This chapter is reprinted with permission from "Characterization of non-canonical G beta-like protein FvGbb2 and its relationship with heterotrimeric G proteins in *Fusarium verticillioide*" by Yan, H.J. and Shim, W.B. 2020. Environmental Microbiology 22(2), 615-628. Copyright © (2020) John Wiley & Sons, Inc.

conidiation. FvGbb2 was also positively associated with various carbon source utilization and stress agents. While FvGbb2 does not interact with canonical G protein subunits, it may associate with diverse proteins in the cytoplasm to regulate vegetative growth, virulence, fumonisin biosynthesis, and stress response in *F. verticillioides*.

Introduction

Fusarium verticillioides (teleomorph: *Gibberella moniliformis* Wineland) is a widely distributed fungal pathogen associated with every stage of maize life cycle, from seed germination to harvest and post-harvest storage (Blacutt et al., 2018). The most common maize diseases caused by this fungus are stalk rot, ear rot and seedling blight. Importantly, *F. verticillioides* produces a variety of mycotoxins including fusaric acid, fusarins, and fumonisins. Fumonisin B1 is the most abundant and toxic form among fumonisins, a group of polyketide-derived secondary metabolites, that contaminate cereals and grains, leading to health and food safety risks for humans and animals (Marin et al., 2013). Note that a wide variety of secondary metabolites are synthesized in microbes, plants, and even certain marine animals. Polyketide synthases (PKSs) and non-ribosomal peptide synthases (NRPSs) are mainly responsible for the biosynthesis of diverse secondary metabolites. To date, 16 PKSs and 16 NRPSs are identified in *F. verticillioides* genome (Hansen et al., 2015). Particularly, *PKS11* (also known as *FUM1*) is the essential PKS gene for initiating fumonisin biosynthesis. While some PKS genes have been characterized in *F. verticillioides* secondary metabolism, *e.g*. *PKS3* (*PGL1*) required for the dark violet

pigment production in perithecia and *PKS10* contributing to fusarin biosynthesis, the majority of PKS gene functions remain unclear (Hansen et al., 2015). Furthermore, these secondary metabolites are not required for normal fungal growth, survival, or virulence but are known to provide certain physiological benefits, including protection against UV damage, defense against abiotic and biotic stresses (Ma et al., 2013; Keller, 2019). It is also important to note that there is still a significant gap in our knowledge on how these secondary metabolites, including fumonisins, are regulated for biosynthesis.

Canonical heterotrimeric G protein complex, which consists of α, β, and γ subunits (Neves et al., 2002), is critical for sensing environmental stimuli, including pheromones, nutrients and host infection. When activated by their cognate ligands, seven transmembrane domain receptors, *i.e.* G protein-coupled receptors (GPCRs), will go through a conformational change. This leads to the exchange of GTP for GDP in Gα subunit triggering the dissociation of G protein complex (Xue et al., 2008). Both Gα subunit and Gβγ dimer are responsible for initiating downstream signaling pathway including cAMP and MAPK kinase pathways. Multiple Gα subunits are identified in filamentous fungi, while only one canonical Gβ subunit is found in fungal species (Li et al., 2007). Gβ subunit is the most extensively studied WD40-repeat protein. In addition to harboring seven WD40-repeat domains, Gβ subunit also contains a short coiled-coil motif in the N-terminus region responsible for interacting with Gγ subunit (Zeller et al., 2007). In addition to Gβ subunit, 12 out of 55 WD proteins have seven WD40-repeat domains in *S. cerevisiae*, but only one

Gβ and one Gβ-like protein were identified (Smith et al., 1999). Studies suggest that Gβ-like protein is associated with diverse physiological functions in fungi (Zhang et al., 2016).

Putative Gβ-like protein RACK1 (Receptor for Activated C Kinase 1) was first identified from a chicken liver cDNA library. Later, RACK1 was also identified as a receptor protein for activated Protein Kinase C (PKC) (Mochlyrosen et al., 1991; Ron et al., 1994). In *Aspergillus fumigatus*, the deletion of RACK1 homolog CpcB led to defects in hyphal growth, virulence and gliotoxin biosynthesis (Kong et al., 2013; Cai et al., 2015). In rice blast pathogen *Magnaporthe oryzae*, RACK1 homolog Mip11 was identified as a Mst50- and MoRgs7-binding protein, which is critical in cAMP signaling and plant infection (Li et al., 2017; Yin et al., 2018). RACK1 homologs were shown to interact directly with one of the Gα subunits in multiple fungi, including *S. cerevisiae*, *Cryptococcus neoformans* and *M. oryzae* (Palmer et al., 2006; Zeller et al., 2007). Furthermore, a recent study in *Arabidopsis thaliana* demonstrated that RACK1 actually serves as a scaffolding protein for Gβ subunit and a downstream MAPK cascade component involved in plant immunity (Cheng et al., 2015). If RACK1 were to be recognized as a Gβ-like protein in *F. verticillioides*, one question we can ask is whether this protein physically interacts with heterotrimeric G protein subunits.

In *F. graminearum*, the deletion mutant of Gβ protein GzGpb1 facilitated ZEA and DON production but was defective in hyphal growth and pathogenicity (Yu et al., 2008b). Our previous study demonstrated that Gβ subunit FvGbb1 positively regulated FB1

biosynthesis, but otherwise showed very limited role in *F. verticillioides* vegetative growth and virulence (Sagaram and Shim, 2007). Significantly, as described earlier, Gβ-like protein RACK1 is involved in diverse functions in multiple eukaryotic organisms. The outcomes from our FvGbb1 study led us to hypothesize that an alternative non-conventional Gβ subunit may compensate for the main Gβ subunit functions in *F. verticillioides*. In this study, we characterized the functional role of putative Gβ-like protein FvGbb2, a RACK1 homolog, in *F. verticillioides* development and secondary metabolism. Additionally, we investigated the relationship between FvGbb2 and canonical heterotrimeric G protein components.

Results

Identification of RACK1 homolog in *F. verticillioides*

We used Asc1 protein sequence from the *S. cerevisiae* genome database (http://www.yeastgenome.org/) to search for RACK1 homolog in *F. verticillioides* database using BLASTP algorithm. Our search led to the identification of FVEG_02582, which was designated as FvGbb2. The *FvGBB2* gene is 1,465 bp in length with 3 predicted introns, encoding a 316-amino-acid protein. To identify FvGbb2 orthologs in other species, *F. verticillioides* FvGbb2 protein sequence was used in BLAST query. Sequence alignment indicated that FvGbb2 protein shares a high amino acid identity with its orthologs (Figure A-1). Both FvGbb2 and FvGbb1 are predicted to contain seven WD-40

repeat motifs, while FvGbb1 has an extra coiled-coil domain. FvGbb2 did not share high protein similarity with FvGbb1, but this is not surprising when you consider structural diversity of WD-40 repeat motifs and the difficulty associated with predicting secondary structure information (Wang et al., 2016). But, to further study FvGbb2 against canonical Gβ subunit in fungi, amino acid sequences of candidate proteins were aligned using ClustalW software (Larkin et al., 2007), and the phylogenetic tree was built with bootstrap 1000 replicates using MEGA 7 (Kumar et al., 2016). Domain information was retrieved from SMART and presented by EvolView (Letunic et al., 2015; He et al., 2016; Letunic and Bork, 2018) (Figure 2.1). Phylogenetic tree analysis suggested that FvGbb2 and its homologs are distinct from canonical Gβ subunit in various species.

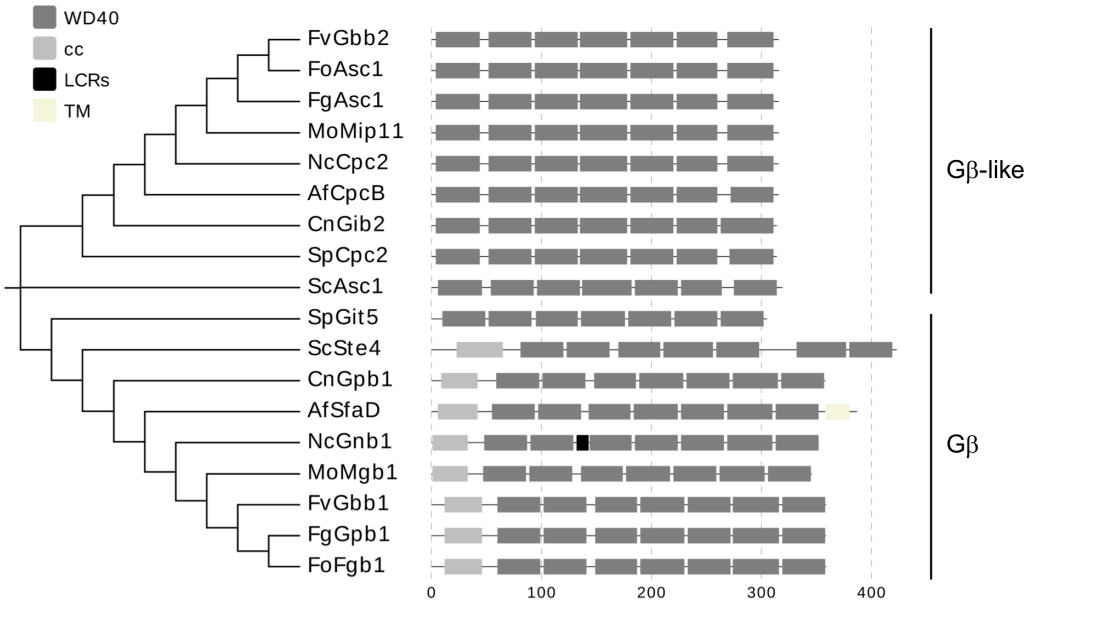

Figure 2.1 Phylogenetic and domain analysis of Gβ-like and Gβ proteins in multiple fungi.

Protein names with fungal species, NCBI locus tag, and protein similarity against FvGbb2 used in the figure are; FvGbb2 (*Fusarium verticillioides*, FVEG_02582, 100% identity), FoAsc1 (*F. oxysporum* f. sp. *lycopersici* 4287, FOXG_05557, 100% identity), FgAsc1 (*F. graminearum,* FGSG_09870, 99% identity), MoMip11 (*Magnaporthe oryzae,* MGG_04719, 97% identity), NcCpc2 (*Neurospora crassa* OR74A, NCU05810, 95% identity), AfCpcB (*Aspergillus fumigatus* A1163, AFUB_070060, 90% identity), CnGib2 (*Cryptococcus neoformans var. grubii H99*, CNAG_05465, 73% identity), SpCpc2 (*Schizosaccharomyces pombe,* SPAC6B12.15, 70% identity), ScAsc1 (*Saccharomyces cerevisiae*, YMR116C, 59% identity), SpGit5 (*S. pombe*, SPBC32H8.07, 22% identity), ScSte4 (*S. cerevisiae*, YOR212W, 26% identity), CnGpb1 (*C. neoformans var. grubii H99*, CNAG 01262, 22% identity), AfSfaD (*A. fumigatus* A1163, AFUB_059800, 23% identity), NcGnb1 (*N. crassa* OR74A, NCU00440, 23% identity), MoMgb1 (*M. oryzae*, MGG_05201, 22% identity), FvGbb1 (*F. verticillioides*, FVEG_10291, 22% identity), FgGpb1 (*F. graminearum*, FGSG_04104.1, 27% identity), FoFgb1 (*F. oxysporum* f. sp. *lycopersici* 4287, FOXG_11532, 22% identity).

ΔFvgbb2 had severe defects in vegetative growth and conidia on agar plates but showed more vigorous mycelial growth in liquid YEPD medium

To study the functional role of FvGbb2, we generated a null mutant of *FvGBB2* (ΔFvgbb2) by replacing the gene with hygromycin-resistance gene (Figure A-2A). *FvGBB2* transcript in the mutant was tested by qPCR, and the complete loss of *FvGBB2* expression indicated successful gene deletion (Figure A-2D). The ΔFvgbb2 mutant grew significantly slower and less fluffy compared to the wild type (WT) on V8, 0.2xPDA, myro and YEPD agar plates (Figure 2.2A). In addition, 7-day-old YEPD liquid cultures of double deletion mutants ΔFvgbb2-gbb1, ΔFvgbb2-gpa2 showed extremely high levels of undetermined dark pigment (Figure 2.2A).

Additionally, when examined under the microscope, ΔFvgbb2 exhibited shorter but noticeable hyper-branching hyphae (Figure 2.2B). Gene complementation strains ΔFvgbb2-Com and ΔFvgbb2-Gbb2-GFP showed full recovery of growth defects in ΔFvgbb2 strain. These results indicated that FvGbb2 is important for vegetative growth in *F. verticillioides*. Moreover, we measured the number of conidia after 8 days of incubation on V8 plates at room temperature. ΔFvgbb2 exhibited dramatic inhibition of conidia production and germination (Figure 2.3A and 2.3C). Interestingly, we found that ΔFvgbb2 mycelial mass (fresh weight) in YEPD liquid media was significantly higher than WT (Figure 2.3B). To further understand the molecular basis of these defects, we studied expression levels of conidia-related genes including *FvBRLA*, *FvWETA*, *FvABAA* and

FvSTUA. Total RNA was extracted from WT and mutant mycelia collected from YEPD liquid cultures incubated for 20 h with agitation (150 rpm). Transcript levels of conidia-related genes were all significantly down-regulated in ΔFvgbb2 in myro and YEPD liquid media (Figure 2.3D and A-3A). We also tested whether FvGbb2 is essential for sexual reproduction, but all mutant strains were capable of perithecia production (Figure A-3B).

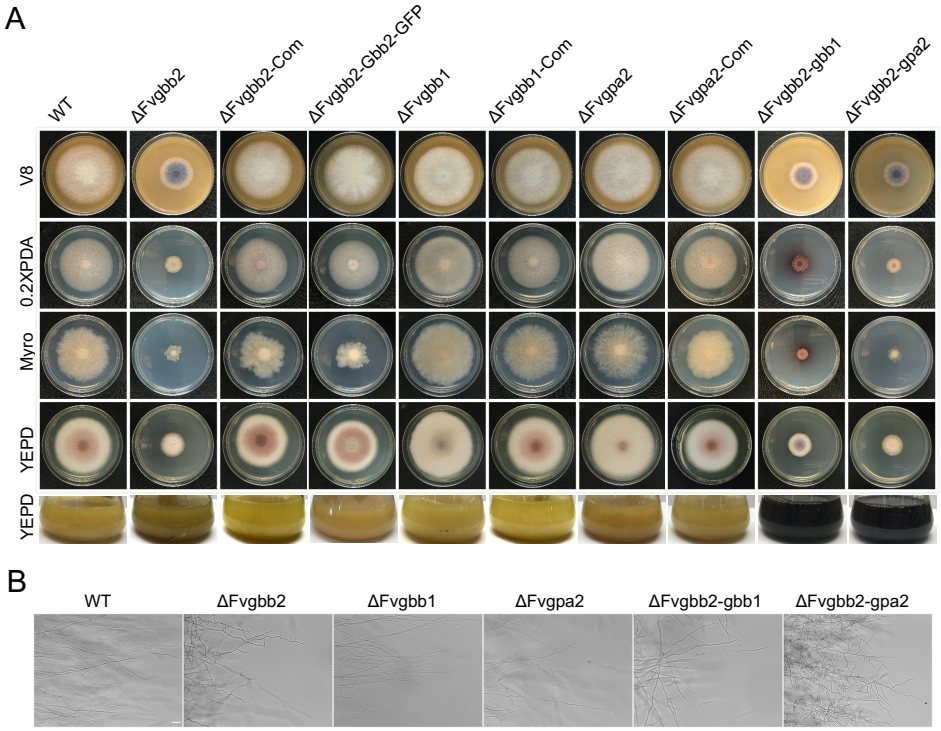

Figure 2.2 Mycelial growth and morphology of ΔFvgbb2, ΔFvgbb1, ΔFvgpa2, ΔFvgbb2-gbb1, and ΔFvgbb2-gpa2 mutants.
(A) Colonies of the wild-type (WT), ΔFvgbb2, ΔFvgbb2-Com, ΔFvgbb2-Gbb2-GFP, ΔFvgbb1, ΔFvgbb1-Com, ΔFvgpa2, ΔFvgpa2-Com, ΔFvgbb2-gbb1, ΔFvgbb2-gpa2 mutants grown on V8 agar, 0.2xPDA, myro agar, YEPD agar plates for 8 days at room temperature. Strains were also cultured in YEPD liquid medium for 7 days with agitation at 150 rpm. (B) Hyphal growth and branching were examined on 0.2xPDA after 3 days of incubation at room temperature. Bar = 100 μm

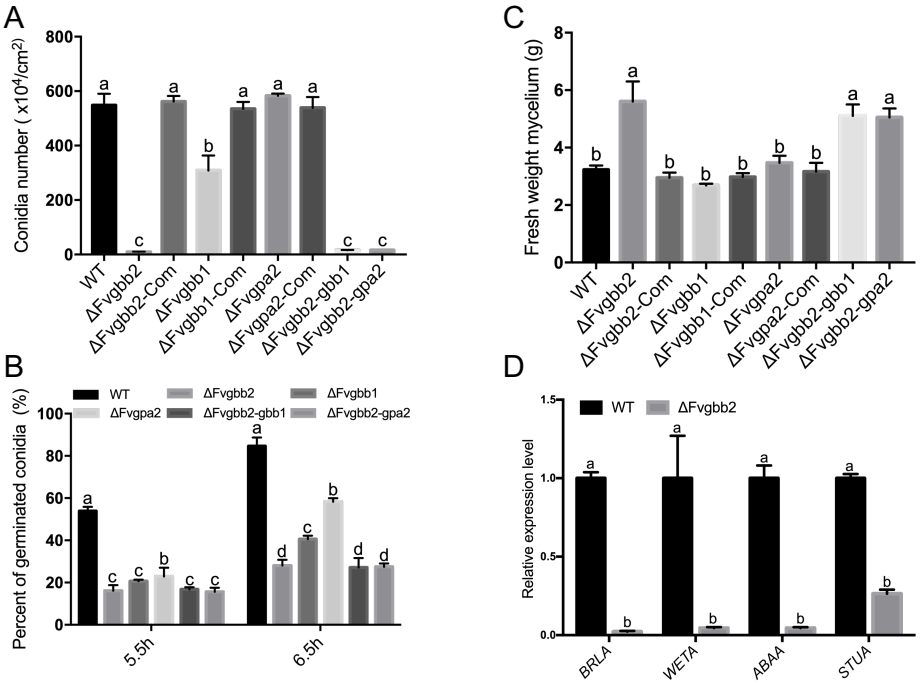

Figure 2.3 Impacts of gene deletion (ΔFvgbb2, ΔFvgbb1, ΔFvgpa2, ΔFvgbb2-gbb1, ΔFvgbb2-gpa2) on conidiation and vegetative growth.

(A) Conidia production was assayed after 8 days of incubation on V8 agar plates. Error bars indicate standard deviation from three replicates. The letters indicate statistically significant differences analyzed by Ordinary One-way ANOVA Fisher's LSD test ($p < 0.05$). (B) WT, ΔFvgbb2, ΔFvgbb1, ΔFvgpa2, ΔFvgbb2-gbb1, ΔFvgbb2-gpa2 strains were suspended in 0.2xPDB liquid medium. Conidia showing germination were counted after incubating for 5.5 h and 6.5 h with gentle shaking. Different letters indicate significant difference according to a Two-Way ANOVA Fisher's LSD test ($P < 0.05$). (C) Conidia (10^6) from each strain were inoculated into 100 ml YEPD liquid medium, and images were taken after 7 days of incubation with shaking at 150 rpm. Fresh mycelia were harvested by filtering through Miracloth. Three replicates were performed for each strain. (D) The differences in transcription of conidia regulation genes were observed in WT versus ΔFvgbb2 when cultured in myro liquid medium. Three replicates were performed for each sample.

FvGBB2, *FvGBB1* and *FvGPA2* play important roles in secondary metabolism

Fumonisin B1 (FB1) is the most important mycotoxin produced by *F. verticillioides* in maize (Marin et al., 2013). Here, we assayed FB1 production in ΔFvgbb2, ΔFvgbb1, and ΔFvgpa2 in autoclaved kernels and surface-sterilized kernels (Silver Queen hybrid, Burpee Seeds) after 8 days of incubation (Figure A-4A and A-4B). Interestingly, we noticed differences in pigment production (Figure 2.4A and B). Additionally, FB1 production levels were dramatically lower in ΔFvgbb2, ΔFvgbb1 and ΔFvgpa2 mutants when compared to WT and complemented strains (Figure 2.4C and D). To verify the role of FvGbb2 in *F. verticillioides* secondary metabolism, we used qPCR to test transcription of 15 PKS genes. Total RNA samples were extracted from mycelia grown in myro broth, in which we noticed intense carmine red pigment production after 7 days of culturing with 150 rpm shaking (Figure A-4C). Consistently, all tested PKS genes showed significantly altered expressions in ΔFvgbb2. Notably, *PKS11* (*FUM1*), which is responsible for the first step of FB1 biosynthesis, was significantly downregulated in ΔFvgbb2 and ΔFvgbb1 (Table A-1). Taken together, FvGbb2 is positively associated with FB1 production and necessary for maintaining proper regulation of other pigment productions.

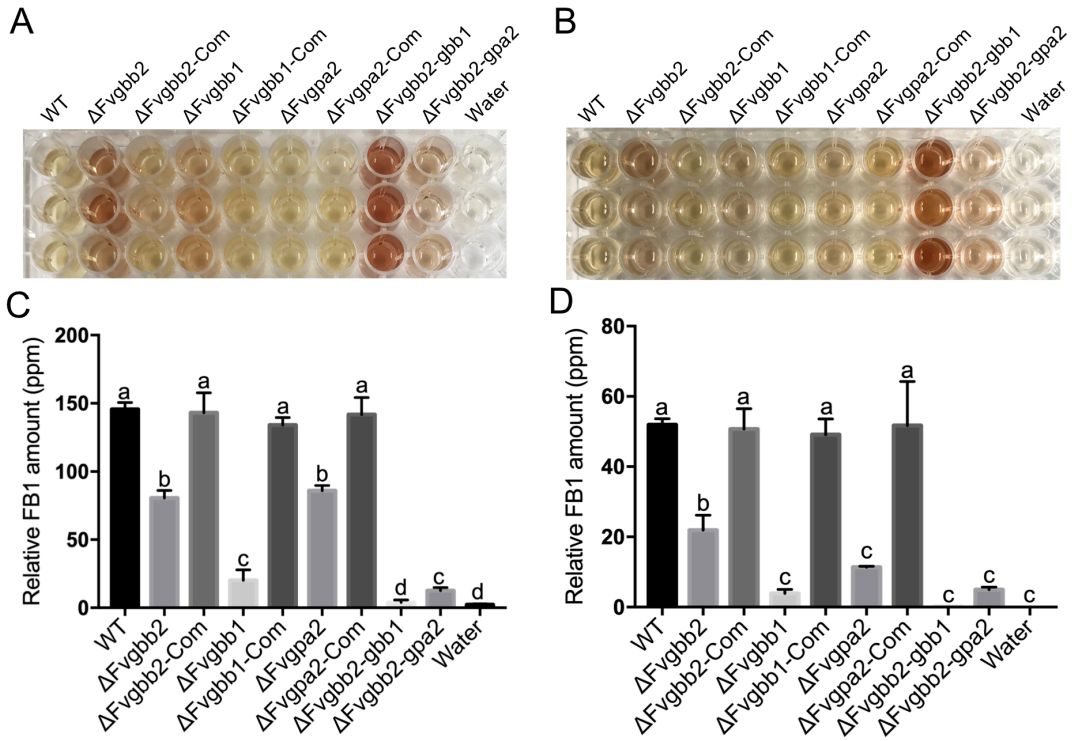

Figure 2.4 Role of *FvGBB2*, *FvGBB1*, *FvGPA2* on fumonisin B1 (FB1) and pigment productions.

Pigment production observed in WT and deletion mutant strains grown on (A) autoclaved kernels and (B) surface sterilized kernels for 8 days. Samples were extracted overnight with 50 % acetonitrile (5 ml) and retrieved in a 96-well plate for the photograph. Three replicates were conducted for each strain. FB1 production in WT, mutants and complemented strains grown on (C) autoclaved kernels and (D) surface sterilized kernels for 8 days at room temperature. FB1 levels were normalized with fungal ergosterol levels.

Subcellular localization of FvGbb2, FvGbb1, and FvGpa2

To study the subcellular localization of FvGbb2, we fused GFP to the C-terminus of FvGbb2 with its native promoter (Figure A-5A). We observed strong FvGbb2-GFP signals widely distributed in *F. verticillioides* cells grown on both 0.2xPDA and myro agar media (Figure A-5B~D). To further uncover the relationship between FvGbb2 and G protein subunits, we examined colocalizations of FvGbb2 with FvGbb1 and FvGpa2. Briefly, mCherry-FvGbb1 and FvGpa2-mCherry were independently transformed into FvGbb2-GFP strain. Unfortunately, we were not able to determine mCherry signals of FvGbb1 and FvGpa2 in growing hyphae tips (18 h) at room temperature due to very low signal intensity (data not shown). However, FvGbb1 and FvGpa2 mCherry signals from 0- and 10-h post-inoculation samples were clearly visible in plasma membrane and vacuoles (Figure 2.5A and B). Significantly, our observations showed that GFP-FvGbb2 does not colocalize with mCherry-FvGbb1 and FvGpa2-mCherry, suggesting that FvGbb2 does not physically interact with FvGbb1 and FvGpa2 in selected time points in *F. verticillioides*.

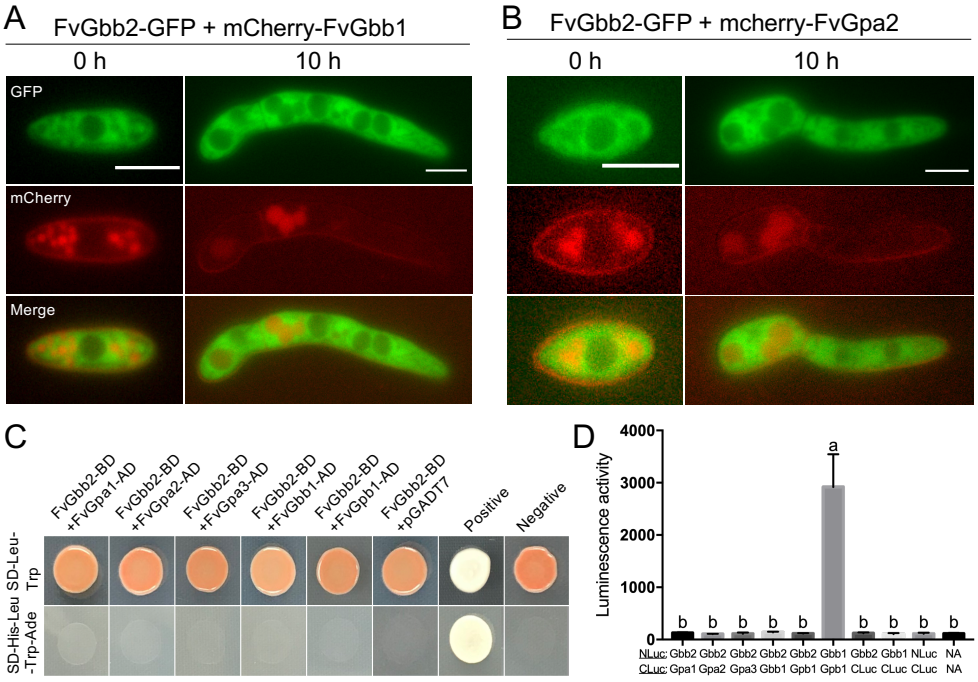

Figure 2.5 FvGbb2 localization and protein-protein interaction assays with FvGbb1 and FvGpa2 in *F. verticillioides*.
Colocalization of (A) FvGbb2-GFP and mCherry-FvGbb1 and (B) FvGbb2-GFP and FvGpa1-mCherry are shown. We inoculated conidia ($1x10^6$) on 0.2xPDA agar plates, cultivated at room temperature, and took images at 0 h and 10 h post inoculation. Images were processed by ImageJ. Bar = 5 μm. (C) Testing physical interaction between FvGbb2 and canonical heterotrimeric G protein components by yeast two-hybrid assay. FvGbb2 was co-introduced with Gα (FvGpa1, FvGpa2, and FvGpa3), Gβ (FvGbb1) and Gγ (FvGpb1) into AH109 strain. Yeast transformants were grown on SD–His–Leu–Trp–Ade plates amended with 3 mM 3-AT. A pair of plasmids pGBKT7–53 and pGADT7-T was used as a positive control. A pair of plasmids pGBKT7–Lam and pGADT7-T was used a negative control. Images were taken after incubating at 30°C for 3 days. (D) Yeast two-hybrid assay results were further verified by split luciferase complementation assays. Luminescence activity was acquired from three replicates and shown as relative light units (RLUs). A pair of FvGbb1-NLuc and FvGpb1-CLuc was used as a positive control. Multiple negative controls (FvGbb2-CLuc, FvGbb1-CLuc, NLuc-CLuc, no vector (NA)-NA) were also included in the study.

Gβ-like protein FvGbb2 does not physically interact with *F. verticillioides* canonical heterotrimeric G protein components

Our localization study led us to ask the relationship between FvGbb2 and canonical heterotrimeric G protein subunits. We used yeast two-hybrid system to test the interaction between these proteins *in vivo*. Results showed that FvGbb2 does not physically interact with heterotrimeric G protein subunits (FvGpa1, FvGpa2, FvGpa3, FvGbb1, FvGpb1) in yeast cells (Figure 2.5C). To further verify these results and to circumvent the limitations known in yeast two-hybrid system, we performed *in vivo* split luciferase complementation assay. However, we did not observe luciferase activity in all samples tested, confirming that FvGbb2 and key heterotrimeric G protein subunits (FvGpa1, FvGpa2, FvGpa3, FvGbb1, and FvGpb1) do not interact in *F. verticillioides* (Figure 2.5D). FvGbb1 (Gβ subunit) and FvGpb1 (Gγ subunit) were used as a positive control in split luciferase complementation assay.

FvGbb2 is important for corn seedling virulence

Our previous study demonstrated that Gβ subunit is dispensable for the stalk rot virulence in *F. verticillioides* (Sagaram and Shim, 2007). FvGbb1 was fully capable of causing stalk rot disease when inoculated into maize B73 inbred stalks. To further investigate the function of Gβ-like protein in pathogenicity, we performed seedling rot assay with

ΔFvgbb2, ΔFvgbb1, ΔFvgpa2, ΔFvgbb2-gbb1, ΔFvgbb2-gpa2 strains along with WT and complemented strains. The single mutant ΔFvgbb2 exhibited reduced virulence, but double mutants ΔFvgbb2-gbb1 and ΔFvgbb2-gpa2 were far less virulent when compared to the WT progenitor (Figure 2.6A and 2.6B). These results suggest that FvGbb1, while physically not interacting with FvGbb2, plays a supplementary role in *F. verticillioides* seedling rot virulence.

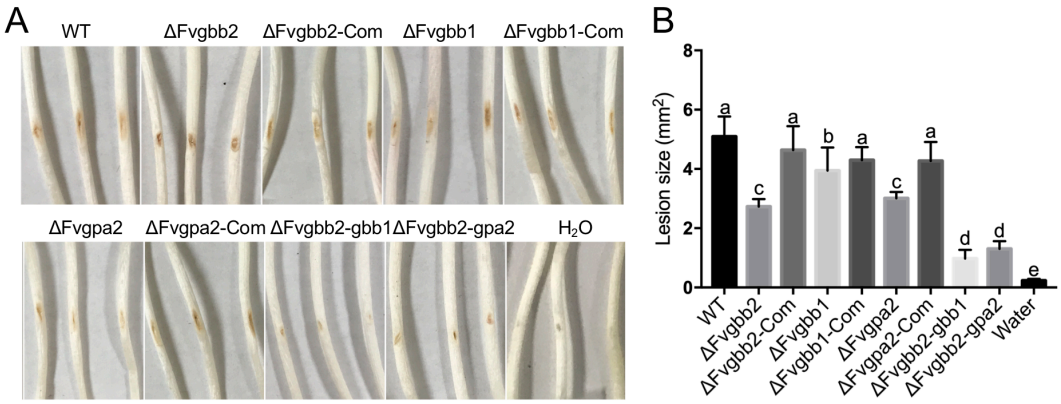

Figure 2.6 Attenuated virulence of Fvgbb2 mutant strain in corn seedling rot assay. (A) Seedlings were grown in the dark room and inoculated with fungal spore suspension from each strain. The images were taken after one week of incubation. (B) The lesion size of seedling rot was examined and measured by image J. At least three biological and three technical replicates were performed for each strain.

FvGbb2 is associated with carbon source utilization and stress response

Yeast RACK1 homolog ScAsc1 is positively associated with glucose sensing (Zeller et al., 2007). Here, we cultured mutant strains on different carbon sources to test whether FvGbb2 plays a similar role in *F. verticillioides*. In addition to dextrose, we tested sucrose, fructose and xylose as the sole carbon source in Czapek-Dox agar plates (Figure 2.7A and C). While ΔFvgbb2 showed general vegetative growth defect, we learned that the negative impact on mycelial growth was more severe in dextrose when compared to sucrose, fructose and xylose. This result was in agreement with the study in *S. cerevisiae*.

Moreover, in *S. cerevisiae*, MAPK Slt2 phosphorylation level was enhanced in *Scasc1* mutant (Chasse et al., 2006). Thus, we hypothesized that FvGbb2 is associated with stress responses in *F. verticillioides*. As shown in Figure 7B and D, ΔFvgbb2 exhibited increased sensitivity to SDS (cell wall stress) and H_2O_2 (oxidative stress) but enhanced tolerance to NaCl (salt stress). This result indicates that FvGbb2 is positively associated with cell wall stress response but negatively with salt tolerance. To test whether FvGbb2 regulates stress response via interacting with MAP kinase pathways, we performed yeast two-hybrid and split luciferase complementation assays to test possible interactions between FvGbb2 with three cell wall integrity MAPK kinase cascade proteins (FvSlt2, FvMkk1/2, FvBck1) (Figure A-6A and A-6B). However, these studies did not reveal direct physical interactions.

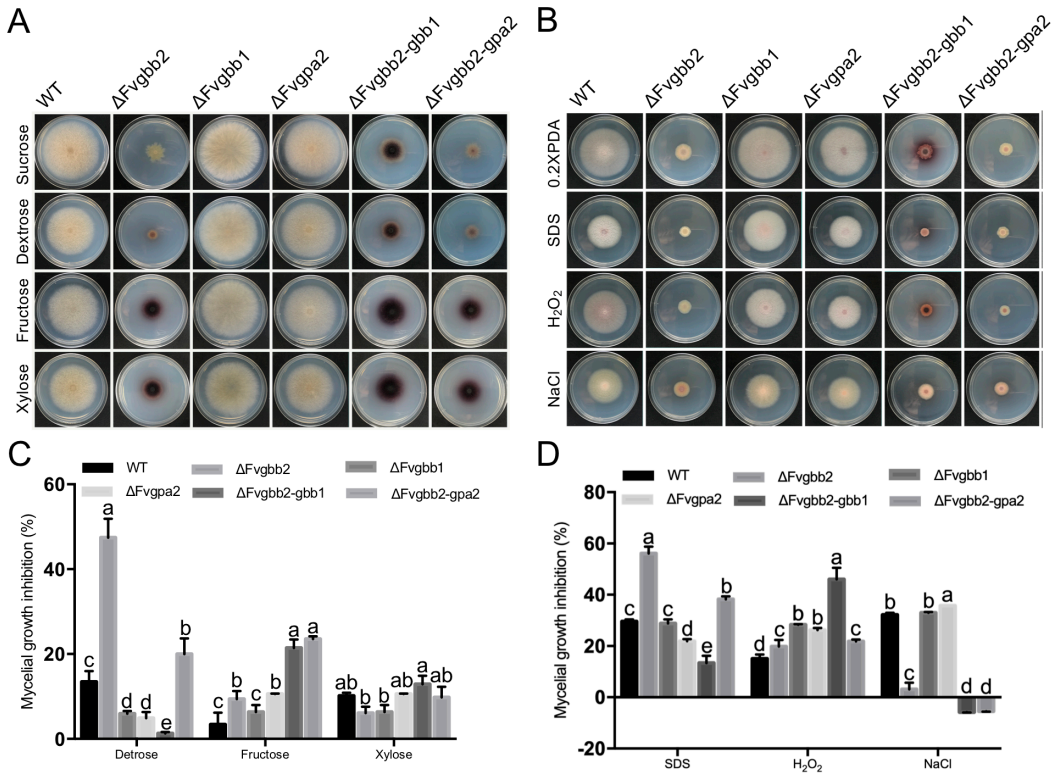

Figure 2.7 Impact of *FvGBB2*, *FvGBB1*, *FvGPA2* on carbon utilization and stress response.

Strains were cultivated on modified Czapek-Dox agar with different carbon sources, including sucrose, dextrose, fructose, and xylose, and incubated at room temperature for 8 days. (B) Radial growth of WT and deletion mutants with various stress agents amended in 0.2xPDA plates incubated for 8 days at room temperature. (C) The growth inhibition rate was analyzed by comparing the growth on Czapek-Dox agar with sucrose against other carbon amendments. The mycelial growth inhibition rate (%) was measured by ((sucrose growth diameter - designated carbon diameter) / sucrose growth diameter) x 100. Bar indicates standard deviation of three replicates. (D) The inhibition rate (%) of strains of stress responses was measured by ((0.2xPDA growth diameter - designated stress growth diameter) / 0.2xPDA growth diameter) x 100. Bar indicates standard deviation of three replicates.

Discussion

Our previous study characterized *F. verticillioides* Gβ protein FvGbb1, a key component in the heterotrimeric G protein complex, that demonstrated an important role for FB1 biosynthesis. However, despite the roles Gβ subunit is known to play in the heterotrimeric G protein complex, we were quite baffled by the fact that FvGbb1 null mutation had little impact on vegetative growth, sexual and asexual reproduction, and pathogenicity in *F. verticillioides* (Sagaram and Shim, 2007), particularly when Gβ protein subunits in other fungal species are known to play some critical roles (Rosen et al., 1999; Wang et al., 2000; Nishimura et al., 2003; Yu et al., 2008b). For instance, mutational inactivation studies in *M. oryzae*, *C. neoformans, F. graminearum* and *N. crassa* indicated that Gβ proteins are directly associated with sexual mating or virulence. Namely, *M. oryzae* Mgb1 deletion mutant showed defects in appressorium formation and thus failed to penetrate host plant leaves. It was also observed that the mutation led to cAMP level reductions in *M. oryzae* cells and that exogenous application of cAMP failed to restore appressorium functions. Moreover, we must recognize that Gβ protein is one of the best characterized WD40-repeat proteins, and numerous published reports demonstrate important physiological and genetic roles WD40-repeat proteins play in filamentous fungi. For instance, fungal striatin-like proteins are important WD40-repeat proteins known to function as a scaffolding protein required for fungal anastomosis, sexual development and virulence in *N. crassa*, *Sordaria macrospora*, and *Fusarium* species (Shim et al., 2006; Bloemendal et al., 2012; Dettmann et al., 2013)

Based on our experimental data and literature, we hypothesized that the presence of a Gβ-like protein can supplement or perhaps substitute canonical Gβ subunit in *F. verticillioides*. In this study, we identified FvGbb2, which shares structural similarity with FvGbb1 with seven WD40 repeat domains. As we mentioned earlier, since Gβ protein FvGbb1 does not play a critical role in *F. verticillioides* growth and virulence (Sagaram and Shim, 2007), we tested whether FvGbb2 serve these functions. Gβ subunit is a well-recognized regulator of asexual development and secondary metabolism in fungi. As shown in this study, the deletion mutant of *FvGBB2* exhibited severe defects in growth and conidiation in solid medium. Our qPCR results also revealed that transcription of conidia-related genes including putative *BRLA* are highly suppressed in tested media. In *Aspergillus* species, transcriptional and metabolic studies indicated that *BRLA* is associated with regulating secondary metabolisms in addition to asexual development (Adams and Yu, 1998; Lind et al., 2018). This outcome raised a question whether secondary metabolites such as mycotoxins and pigments in *F. verticillioides* also follow the same pattern of regulation as in *Aspergillus*. Additionally, earlier studies also demonstrated that Gβ-like proteins positively regulate mycotoxin production in *F. graminearum* and *A. fumigatus*. Similarly, we found that the deletion of *FvGBB2* led to a reduction in FB1 production while showing enhanced pigment production in maize kernels (Figure 2.4A), myro liquid medium (Figure 2.4C), and 0.2xPDB (data not shown). However, it is interesting to note that the pigment biosynthesis was not altered in *F. graminearum* when Fgasc1 was cultured in PDB (Tang et al., 2018). When we performed

expression analyses of 15 PKS genes, we learned that most PKS genes are significantly downregulated, including *PKS11* (*FUM1*). And we also saw overexpression of select PKS genes which may explain why we observed a high level of pigment production in ΔFvgbb2 cultures. This is contradictory to results observed in *A. nidulans*; Gβ-like protein inactivation did not alter mycotoxin sterigmatocystin (ST) biosynthesis *stcU* gene expression in *A. nidulans* (Kong et al., 2013). We concluded that FvGbb2 regulates transcriptional activities of key conidia-related genes and impacts fungal secondary metabolism and asexual reproduction, as is the case with canonical heterotrimeric Gβ subunit.

Previous studies in *Candida albicans* and *A. fumigatus* demonstrated that the deletion of RACK1 leads to a dramatic reduction of virulence when tested in animal models (Liu et al., 2010; Cai et al., 2015). Consistent with these results, ΔFvgbb2 exhibited approximately 50% reduction in virulence when tested for maize seedling rot. The virulence defect is likely due to impaired vegetative growth on seedlings. However, we did not rule out the possibility that ΔFvgbb2 virulence deficiency is also due to impaired response against stress factors. In *S. cerevisiae* and *M. oryzae*, RACK1 deletion mutants showed higher sensitivity when exposed to cell wall stress agents (Rachfall et al., 2013; Li et al., 2017). Notably, *A. thaliana* RACK1 homolog has been shown to interact with three tiers of MAPK cascade components, while in *M. oryzae* the protein interacts with MoBck1 (Cheng et al., 2015; Li et al., 2017). These MAPK pathways are known to be important signal transduction pathways in eukaryotes (Hamel et al., 2012). Similar to *S.*

cerevisiae and *M. oryzae*, ΔFvgbb2 exhibited sensitivity towards SDS stress, but we found no experimental evidence that FvGbb2 physically interacts with MAPK kinase cascade components FvBck1, FvMkk1/2, and FvSlt2. However, we are further investigating this due to the possibility that FvGbb2-MAPK interactions may occur in a specific, yet-to-be determined condition. On another note, *S. pombe* RACK1 homolog Cpc2 was positively involved in cytoplasmic catalase production, which in turn mediates the detoxification of hydrogen peroxides (Nunez et al., 2009). In line with this previous study, ΔFvgbb2 exhibited greater sensitivity to oxidative stress agents. Moreover, a prior study demonstrated that rice OsRACK1A has negative impacts on salt tolerance and interacts physically with salt stress-related proteins (Zhang et al., 2018a). Our analysis also revealed that ΔFvgbb2 mutant strain showed a higher level of tolerance against NaCl treatment. In *A. fumigatus,* the mutation in *AfcpcB* gene showed no such effect (Cai et al., 2015). These stress responses observed in *F. verticillioides* could be explained by *S. cerevisiae* proteome and transcriptome studies since the mutation in RACK1 homolog Asc1 impacted the expression of various regulatory response components including those in MAPK kinase signal pathways (Rachfall et al., 2013).

RACK1 shares structural similarity, and therefore is hypothesized to function as a Gβ subunit and physically interact with Gα subunits. In yeast, the interaction with one of the two Gα subunits, Gpa2, was documented while RACK1 homolog in *F. graminearum* Gib2 was shown to interact with one of the three Gα subunits, Gpa1, and two Gγ subunits (Palmer et al., 2006; Zeller et al., 2007). Interestingly, two studies in *A. thaliana* were not

in agreement when characterizing the relationship between RACK1 homolog and canonical heterotrimeric G protein components. While one previous report in *A. thaliana* using yeast two-hybrid and *in vivo* Co-IP assays failed to detect interactions between RACK1 and G proteins, the other research group showed that the scaffolding protein RACK1 interacts with Gβ protein in *A. thaliana* through bimolecular fluorescence, split firefly luciferase complementation and co-immunoprecipitation assays (Guo et al., 2009; Cheng et al., 2015). In our study, the direct interaction between FvGbb2 with canonical heterotrimeric G proteins could not be established by yeast two-hybrid and split luciferase complementation assays. We also could not observe colocalization of FvGbb2-GFP with mCherry-FvGbb1 and FvGpa2-mCheery. However, ΔFvgbb2-gbb1 and ΔFvgbb2-gpa2 showed more severe defects in FB1 production and pathogenicity when compared to single mutant strains. We propose that although Gβ protein FvGbb1 and Gβ-like protein FvGbb2 share similarity, their localizations and functions are distinct. While FvGbb1 is expressed mostly in the vacuole in conidia and early hyphal elongation stage, FvGbb2 is highly expressed in the cytoplasm constitutively. We observed diverse roles FvGbb2 plays in *F. verticillioides*, and this may be explained by how FvGbb2-GFP signal is distributed broadly in the cytoplasm. Thus, it would be reasonable to hypothesize that FvGbb2 interacts with diverse partners in the cell concurrently or sequentially, and in turn regulates differential gene expression and translation of downstream proteins associated with vegetative growth, virulence, mycotoxin biosynthesis, carbon utilization and stress response in *F. verticillioides*.

Materials and methods

Fungal strains and growth study

F. verticillioides strain M3125 was used as the wild-type strain in this study (Sagaram and Shim, 2007). All strains in this study were cultivated on V8, 0.2x potato dextrose agar (PDA) and myro agar plates as described previously (Yan et al., 2019). For spore gemination assay, equal amounts of newly harvested microconidia grown on V8 agar plates for 8 days were cultivated in 0.2x potato dextrose broth (PDB) (Sigma-Aldrich) for 5.5 h and 6.5 h with gentle shaking. For stress assay, 4 µl of 1×10^6 conidial suspension of each strain was inoculated on 0.2xPDA agar plates amended with various stressors including 0.01% SDS, 2 mM H_2O_2, and 0.75 M NaCl. For carbon utilization assay, four different carbon sources were used in Czapek-Dox agar, *i.e.*, sucrose (30g/L), dextrose (10g/L), fructose (10g/L) and xylose (10g/L) (Yan et al., 2019). Fungal growth diameters were determined after 8 days of incubation at room temperature. Perithecia formation was conducted by applying equal amount of spores obtained from V8 agar plates and spreading onto the strain m3120 grown on carrot agar plates following our earlier method (Sagaram and Shim, 2007). For amino-acid starvation assay, 0.2xPDA with 3mM 3-amino-l,2,4-triazole (3AT) was used for testing growth impact. All experiments had at least three replicates.

Gene deletion and complementation

Knockout mutants ΔFvgbb2, ΔFvgbb1, ΔFvgpa2 were generated in *F. verticillioides* M3125 strain via homologous recombination using the split-marker approach. Partial hygromycin B phosphotransferase gene (*HPH*) designated as *PH* (929bp) and *HP* (765bp) or partial geneticin resistance gene (*GEN*) designated as *GE* (1183 bp) and *EN* (1021 bp) were used to fuse with left and right flanking regions of the targeted gene with joint-PCR approach (Figure A-2). For generating double knockout mutants, *FvGPA2* and *FvGBB1* genes were replaced with *GEN* gene in ΔFvgbb2 background using the same strategy as described above. For complementation, we amplified the target gene with its native promoter and terminator and cotransformed with either pBSG (*GEN*) or pBP15 (*HPH*) plasmid to the mutant protoplast. All knockout constructs and complementation fragments in this study were amplified using Phusion Flash High-Fidelity PCR Master Mix (Thermo Scientific) following the manufacturer's instructions. All transformants were screened by PCR using Phire Plant Direct PCR Kit (Thermo Scientific) and Taq DNA polymerase (New England Biolabs) to identify putative mutant strains. qPCR was used for further confirmations. All primers used in this study are listed in Table S2.

Construction of fluorescent strains

For constructing FvGbb2-GFP plasmid, *FvGBB2* fragment (2818 bp) was amplified from *F. verticillioides* genomic DNA of with primers FvGbb2-GFP-F/R using Q5 High-Fidelity

DNA Polymerase (New England Biolabs). The amplicon was introduced to pKNTG plasmid *Kpn*I and *Hind*III sites via In-Fusion-HD cloning kit (Clontech). We sequenced plasmids and subsequently transformed these into ΔFvgbb2 and WT strains resulting in ΔFvgbb2-Gbb2-GFP and FvGbb2-GFP strains. To construct the mCherry-FvGbb1 plasmid, *FvGBB1* native promoter was amplified from *F. verticillioides* genomic DNA, while *FvGBB1* coding sequence and 3' UTR was amplified from *F. verticillioides* cDNA. pKNT-mCherry was used for mCherry fragment amplification. These three PCR products were cloned into *Kpn*I and *Bam*HI sites of pKNT. Based on suggestions for Gα protein florescent strain construction, mCherry was tagged in the amino acid 114 site to construct FvGpa2-mCherry plasmid (Eaton et al., 2012; Ramanujam et al., 2013). mCherry-FvGbb1 and FvGpa2-mCherry were independently cotransformed with hygromycin marker into the FvGbb2-GFP strain. All DNA fragments used in this study were purified using GeneJET Gel Extraction Kit (Thermo Scientific). Plasmids in this study were isolated using GeneJET Plasmid Miniprep Kit (Thermo Scientific).

Yeast two-hybrid and split luciferase complementation assay

Coding sequences of *FvGPA1* (FVEG_06962), *FvGPA2* (FVEG_04170), *FvGPA3* (FVEG_02792), *FvGPB1*(FVEG_05349), *FvGBB1* (FVEG_10291), *FvMKK1/2* (FVEG_05280), *FvSLT2* (FVEG_03043), and *FvBCK1*(FVEG_05000) were used to construct plasmids for yeast two-hybrid assay. These were amplified from *F. verticillioides* cDNA using Q5 High-Fidelity DNA Polymerase and inserted in pGADT7

as prey vectors (Clontech). The full coding region of *FvGBB2* was cloned into pGBKT7 as the bait vector. The resulting plasmids were verified by sequencing. The pair of yeast two-hybrid plasmids were transformed into yeast strain AH109 following the manufacturer's instruction. We added 5 µl of transformants (10^7 cells/mL) on SD/–Leu/–Trp and SD/–Ade/–His/–Leu/–Trp (3 mM 3-AT) agar plates.

Split luciferase complementation assay plasmids in this study were described previously (Kim et al., 2012). Coding region of each gene was amplified from WT strain cDNA by Q5 High-Fidelity DNA Polymerase and inserted into pFNLucG or pFCLucH via In-Fusion HD Cloning (Clontech). The resulting constructs were validated by sequencing. Transformation, selection and luciferin assay methods were described previously (Zhang et al., 2018b).

Fumonisin B1 and pathogenicity assays

For determining FB1 production, cracked corn kernels (2 g) were put in 20-mL scintillation vials and hydrated with 1 mL sterilized water overnight followed by autoclaving. Additionally, silver queen kernels (Burpee Seeds) were surface sterilized using a method previously described (Christensen et al., 2012). Sterilized kernels were placed on sterilized 90 mm Whatman filter paper, wounded on the endosperm area by a scalpel, and four kernels were put in each scintillation vial. Fungal spore solutions (200 µL, 10^6/mL) were inoculated in each vial and cultivated at room temperature for eight

days. FB1 and ergosterol extraction methods were described previously (Christensen et al., 2012), but in this study we used 5 mL of acetonitrile:water (1:1, v/v) for FB1 extraction while 5 ml of chloroform: methanol (2:1, v/v) for ergosterol extraction. HPLC analyses of FB1 and ergosterol were performed as described (Shim and Woloshuk, 1999). FB1 levels were normalized to ergosterol contents. These experiments were carried out with three biological replicates. Stalk rot virulence assay was conducted using silver queen hybrid seeds as previously described with minor modifications (Kim et al., 2018b). Spores solutions (5 μL, 10^7/mL) were collected from V8 plates. Seedlings were harvested and imaged after one-week growth in the dark room.

RNA extraction and relative gene expression study

For PKS gene qPCR assay, 200-μl conidia solution (10^6 conidia/ml) was inoculated into 100 ml YEPD liquid medium for 3 days. Subsequently, mycelial samples were harvested through Miracloth (EMD Millipore), weighed (0.3 g), and inoculated into 100-ml myro liquid medium. Samples were collected after 7 days of incubation at 150 rpm. All experiments had at least three replicates. Total RNA was isolated using Qiagen RNA Plant Mini kit following the manufacturer's instruction. For qPCR, cDNA was synthesized using Verso cDNA synthesis kit (Thermo Scientific). qPCR analyses were conducted by Step One plus real-time PCR system using the DyNAmo ColorFlash SYBR Green qPCR Kit (Thermo Scientific). Relative expression levels of each gene were calculated using a $2^{-\Delta\Delta CT}$ method and normalized with *F. verticillioides* β-tubulin gene (FVEG_04081). All

qPCR assays were performed three times. Primers for *F. verticillioides* polyketide synthase (PKS) genes were from a previous study (Ortiz and Shim, 2013).

Microscopy

For hyphal branching imaging, minor modifications were made from a previously described method (Schultzhaus et al., 2015). Briefly, strains were cultivated on 0.2xPDA agar plates for three days. A block of agar was cut and put on a glass slide. Sterilized water (10 μL) was added followed by a coverslip. The sample was incubated at room temperature for 20 mins and examined by a microscope (Olympus BX60). Images were processed using ImageJ software (Schneider et al., 2012).

CHAPTER III

TWO FVFLBA PARALOGS FVFLBA1 AND FVFLBA2 DIFFERENTIALLY REGULATE FUMONISIN BIOSYNTHSIS IN *FUSARIUM VERTICILLIOIDES*

Summary

Fusarium verticillioides is a fungal pathogen causing maize ear rot and fumonisins contamination. While fumonisins are recognized as mycotoxins posing health concerns to humans and animals, we still do not have a clear understanding of the mechanism of fumonisins regulation during maize ear rot pathogenesis. The heterotrimeric G protein complex, which consists of Gα, Gβ, and Gγ subunits, plays an important role in transducing signals under environmental stress. Furthermore, regulators of G-protein signaling (RGS) proteins are well known to act as negative regulators of the heterotrimeric G protein signaling pathway. Our previous study demonstrated that Gα and Gβ subunits are positive regulators of fumonisin B1 (FB1) biosynthesis and that two RGS genes, FvFlbA1 and FvFlbA2, were highly upregulated in Gβ deletion mutant ΔFvgbb1. *Saccharomyces cerevisiae* and *Aspergillus nidulans* contain a single copy of FlbA, but *F. verticillioides* has two FvFlbA paralogs, FvFlbA1 and FvFlbA2. Importantly, FvFlbA2 plays a negative role in FB1 regulation. In this study, we further characterized the relationship between the two FvFlbA paralogs. While the FvFlbA1 single deletion mutant had no significant defects, the ΔFvflbA2 and ΔFvflbA2/A1 mutants showed thinner aerial growth but promoted fumonisin B1 production. Consistently, we learned that FvFlbA2 is

required for proper expression of key conidia regulation genes, including putative *FvBRLA*, *FvWETA*, and *FvABAA*. FvFlbA2 is also critical for suppressing *FUM21*, *FUM1*, and *FUM8* gene transcription. However, two FvFlbA paralogs were not associated with carbon source utilization and stress agents. When two FvFlbA paralogs localization and protein interaction partner studies are completed, we will have a better understanding of how FvFlbA1 and FvFlbA2 differentially regulate fumonisin B1 biosynthesis in *F. verticillioides.*

Introduction

Fusarium verticillioides (teleomorph: *Gibberella moniliformis* Wineland) is a fungal pathogen capable of causing ear rot, stalk rot and seedling blight in maize worldwide. The fungus primarily utilizes conidia for dissemination, and the pathogen is capable of infecting and colonizing all developmental stages of maize plants (Blacutt et al., 2018). Importantly, kernel infections by *F. verticillioides* lead to the production of fumonisins, a group of carcinogenic mycotoxins. Fumonisin B1 (FB1) is the most abundant and toxic form among fumonisin analogs, and long-term exposure to FB1 is linked to severe human and animal diseases including esophageal cancer and neural tube defects. Fumonisins contain a 19-20 carbon polyketide backbone, and usually multiple genes are involved in the biosynthesis of these complex secondary metabolites. A number of studies have demonstrated that genes involved in microbial secondary metabolite biosynthesis are

organized as gene clusters (Alexander et al., 2009). The fumonisin biosynthesis gene cluster (referred to as the "*FUM* cluster") was first discovered by Proctor et al (1999), which consists of 16 genes encoding biosynthetic enzymes and regulatory proteins (Proctor et al., 2013). Inactivation of each of the key genes, e.g. *FUM1*, *FUM6*, *FUM8*, and *FUM21*, completely abolished production of fumonisins. Notably, previous studies demonstrated that these fumonisins-non-producing mutant strains did not significantly reduce maize ear rot in field tests (Desjardins and Plattner, 2000; Desjardins et al., 2002), which demonstrated that fumonisins are not essential for *Fusarium* ear rot pathogenicity.

G protein-coupled receptors (GPCRs) are the largest group of membrane receptors containing seven transmembranes (TMs) that transduce signals from the external environment to the cell, enabling the organism to adjust to its environment (Xue et al., 2008). The canonical heterotrimeric G protein complex, which consists of α, β and γ subunits, plays important roles in transducing signals from GPCRs. When activated by specific ligands, GPCRs stimulate GDP to GTP exchange on the Gα subunit. Then, heterotrimeric G proteins are dissociated into Gα subunit and Gβγ dimer, which triggers downstream various signaling pathways. GPCR signaling is known to be attenuated by G-protein-coupled receptor kinases (GRKs) and β-arrestin in animals, which are absent in filamentous fungi (Dohlman, 2009). However, the studies showed regulators of G protein signaling (RGS) proteins in fungi act as GTPase activating proteins, which promotes GTP hydrolysis of Gα subunit back to GDP-bound inactivated form terminating GPCR and G protein signaling pathways. RGS proteins typically contain 130-amino-acid RGS

domains, which promotes the binding of RGS proteins to the Gα subunit. Notably, other than the RGS domain, RGS proteins are known to contain diverse non-RGS domains such as DEP (*Dishevelled*, *Egl-10* and *Pleckstrin*), PX, PXA, nexin C and TM, which are linked to various signaling pathways. For instance, the DEP domain in *Saccharomyces cerevisiae* ScSst2 was shown to interact with pheromone sensing Ste2 and mediated regulation of pheromone signaling responses (Ballon et al., 2006).

In *Aspergillus nidulans*, *flbA* (for fluffy low brlA expression) was the first RGS protein identified in filamentous fungi, which is positively associated with conidiophore development and sterigmatocystin accumulation (Lee and Adams, 1994; Hicks et al., 1997a). The deletion mutant of *flbA* was incapable of facilitating the transition from vegetative growth to conidiophore development. Conversely, overexpression of *flbA* led to premature *stcU* gene expressions and sterigmatocystin biosynthesis (Hicks et al., 1997a). In *Magnaporthe oryzae*, an AnFlbA1 ortholog MoRgs1 was shown to be involved in asexual development, pathogenicity, and thigmotropism (Liu et al., 2007). Additionally, MoRgs1 had physical interactions with a non-canonical GPCR, MoPth11 and colocalize with Rab7, a late endosome marker (Ramanujam et al., 2013). The other well studied RGS protein, MoRgs7 comprises of N-terminal GPCR seven-transmembrane domain and a C-terminal RGS domain, which is critical for germ tube growth, cAMP signaling, and virulence in *M. oryzae* (Zhang et al., 2011a). Similarly, a GPCR protein in *Arabidopsis thaliana*, AtRgs1 is important for plant cell proliferation and sugar signaling pathway (Chen and Jones, 2004).

We previously studied Gβ and Gβ-like proteins were positively associated with FB1 production in *F. verticillioides* (Sagaram and Shim, 2007; Yan and Shim, 2020). Transcription of four RGS genes *FLBA1*, *FLBA2*, *RGSB*, and *RGSC1* were significantly altered in Gβ deletion mutant Fvgbb1 when compared to the wild-type *F. verticillioides* strain (Mukherjee et al., 2011). In this earlier study, we learned that unlike in *A. nidulans*, *F. verticillioides* contains two putative FvFlbA paralogs which we designated as FvFlbA1 and FvFlbA2. Intriguingly, FvFlbA2 deletion mutation showed a drastic increase in FB1 production (Mukherjee et al., 2010). Also, FlbA1 and FlbA2 were important for regulating host response during the fungal infection in surface-sterilized viable maize kernels. In this study, we further examined the regulatory mechanisms of the two FlbA genes in *F. verticillioides*. In particular, we focused on a deeper study of how each gene plays unique roles in FB1 biosynthesis.

Results

Identification and sequence analyses of FlbA1 and FlbA2 in *F. verticillioides*

Our previous study identified two FvFlbA paralogs in *F. verticillioides* including FvFlbA1 (FVEG_08855) and FvFlbA2 (FVEG_06192) (Mukherjee et al., 2011). The new annotation predicts that FvFlbA1 encodes a 499-amino-acid protein while FvFlbA2 contains 517-amino-acid. FvFlbA1 and FvFlbA2 share 52% identity at the amino-acid

level. To identify FlbA orthologs in other fungi, *F. verticillioides* FvFlbA2 protein sequence was used in a BLAST query. Among the fungal species we searched, only *Fusarium* species showed multiple copies of FlbA genes. Both *F. verticillioides* and *F. graminearum* have two FlbA genes, and surprisingly, *F. oxysporum* has five FlbA paralogs. All FlbA orthologs are predicted to contain both DEP and RGS domain except that FvFlbA2 does not contain the RGS domain in the new annotation. Notably, FvFlbA1 and FvFlbA2 belong to different branches in our phylogenetic tree analysis (Figure 3.1), which indicated that FvFlbA paralogs may have a distinct evolutionary origin. Phylogenetic tree and domain analysis followed a previous description (Yan and Shim, 2020).

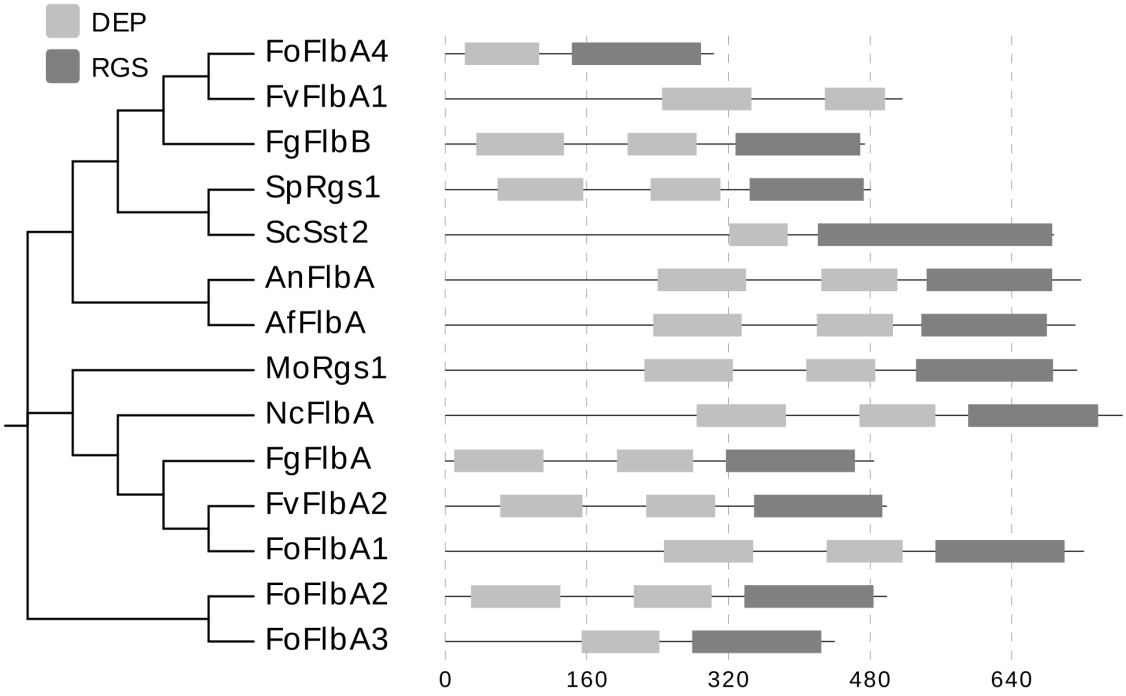

Figure 3.1 Phylogenetic and domain analysis of FlbA proteins in multiple fungi. Organism names and NCBI locus tag: FvFlbA2 (FVEG_06192, 100% identify), FvFlbA1 (FVEG_08855, 52% identify), FoFlbA1 (FOXG_08482, 98% identity), FoFlbA2 (FOXG_06495, 74% identity), FoFlbA3 (FOXG_17640, 64% identity), FoFlbA4 (FOXG_09613, 53% identity), FoFlbA5 (FOXG_07099, 53% identity) in *F. oxysporum f. sp. lycopersici 4287*, FgFlbA (FGSG_06228, 98% identity), FgFlbB (FGSG_03597, 50% identity) in *F. graminearum*, MoRgs1 in *Magnaporthe oryzae* (MGG_14517, 63% identity), NcFlbA in *Neurospora crassa* OR74A (NCU08319, 74% identity), AnFlbA in *Aspergillus nidulans* FGSC A4 (An5893, 66% identity), AfFlbA in *A. fumigatus* Af293 (AFUA_2G11180,77%), SpRgs1 in *Schizosaccharomyces pombe* (SPAC22F3.12c, 31% identity), ScSst2 in *Saccharomyces cerevisiae S288C* (YLR452C, 36% identity). Notably, we failed to perform the tree analysis of FoFlbA5 with other proteins in this analysis.

ΔFvflbA1 and ΔFvflbA2 mutants exhibit limited defects in vegetative growth

The two FvFlbA paralogs null mutants were generated by the split-marker approach (Figure B-2A). *FvFLBA1* and *FvFLBA2* transcriptional expression in the mutants were tested by qPCR method (Figure B-2D). The mutant ΔFvflbA1 showed no obvious defect in terms of growth and conidiation on three different agar media. However, the ΔFvflbA2 mutant showed slower growth on these media and also produced less conidia compared to the wild type (Fig. 3.2). To further understand the relationship of two FvFlbA paralogs in *F. verticillioides*, we generated a ΔFvflbA2/A1 double mutant. ΔFvflbA2/A1 exhibited more severe defects in aerial hyphae and conidia production when compared to ΔFvflbA2 (Fig. 3.3A). Surprisingly, we discovered that ΔFvflbA2 and ΔFvflbA2/A1 had precocious conidial germination which was not observed in wild type or other mutants (Fig. 3.3B). Gene complementation strain ΔFvflbA2-Com demonstrated full recovery of growth defects observed in ΔFvflbA2 strain.

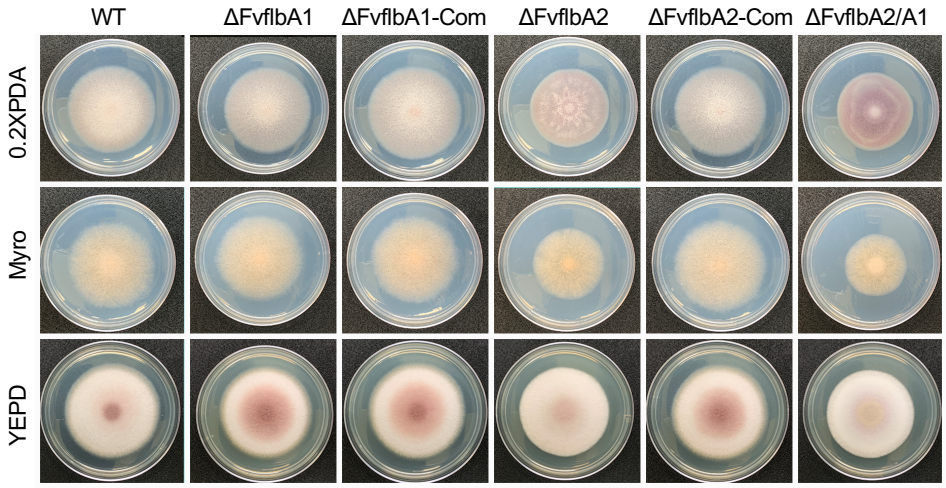

Figure 3.2 Hyphal growth of ΔFvflbA1, ΔFvflbA1-Com, ΔFvflbA2, ΔFvflbA2-Com, ΔFvflbA2/A1 strains.
Colonies of the wild-type (WT), ΔFvflbA1, ΔFvflbA1-Com, ΔFvflbA2, ΔFvflbA2-Com, ΔFvflbA2/A1 strains on 0.2xPDA, myro and YEPD agar incubated at room temperature for 8 days.

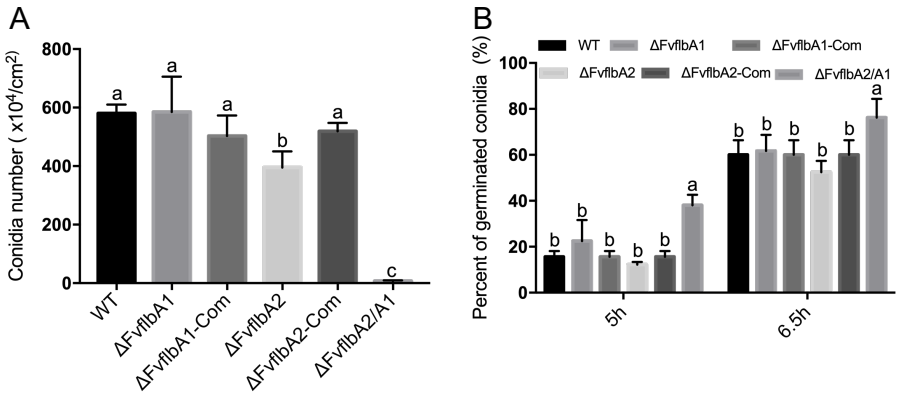

Figure 3.3 FvFlbA2 impacts on conidiation and germination.
(A) Conidia were harvested from V8 agar plates after 8 days at room temperature incubation. The letters suggest statistically significant differences analyzed by Ordinary One-way ANOVA Fisher's LSD test ($p < 0.05$). (B) WT, ΔFvflbA1, ΔFvflbA1-Com, ΔFvflbA2, ΔFvflbA2-Com, ΔFvflbA2/A1 strains were cultured in 0.2xPDB liquid medium with gentle shaking. Conidial germination rate was counted under microscope.

FvFlbA2 is negatively associated with FB1 production

Fumonisn B1 (FB1) is the most widely distributed and toxic form of fumonisins produced by *F. verticillioides*. Our previous studies showed RGS protein FvFlbA2 is negatively associated with FB1 production, while Gβ and one of the Gα proteins positively regulate FB1 biosynthesis (Mukherjee et al., 2011; Yan and Shim, 2020). To further understand the impact and relationship of the two FvFlbA paralogs in FB1 production, we studied FB1 biosynthesis in mutant strains. We performed FB1 assay in autoclaved cracked kernels and surface-sterilized living kernels (Figure 3.4A and B). The results showed that ΔFvflbA2 and ΔFvflbA2/A1 produced significantly higher levels of FB1 compared with wild type or ΔFvflbA1 (Figure 3.4C and D). Significantly, the double mutant ΔFvflbA2/A1 produced a drastically higher FB1 level in contrast to ΔFvflbA2 mutant strain. However, ΔFvflbA1 produced similar levels of FB1 as the wild-type and complemented strains. This result suggested that FvFlbA2 serves as a negative regulator of FB1 biosynthesis, but the impact is more dramatic with double deletion of two FvFlbA paralogs.

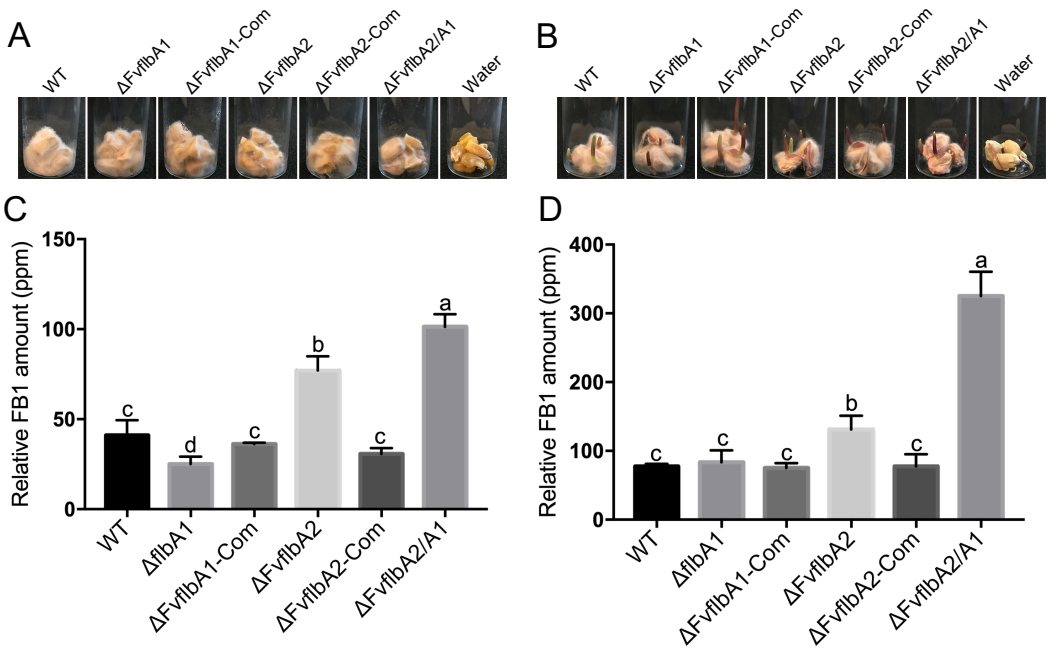

Figure 3.4 Colonization of two FvFlbA deletion mutants in kernels and FB1 assay. *F. verticillioides* WT, ΔFvflbA1, ΔFvflbA1, ΔFvflbA2, ΔFvflbA2/A1 and complemented strains were cultivated in (A) 2-g cracked autoclaved kernels and (B) four sterilized surface-sterilized kernels for seven days at room temperature. (C) FB1 production in WT, mutants and complemented strains cultured on nonviable kernels and (D) viable kernels after seven days incubation at room temperature. The relative FB1 production levels were normalized to fungal ergosterol.

Expression levels of genes associated with conidiation and FB1 biosynthesis

The expression of *brlA* mRNA was not detectable in *A. nidulans flbA* mutant, which indicated that AnFlbA is indispensable for *brlA* gene activation (Lee and Adams, 1994). In this study, we observed that ΔFvflbA2 produced a lower amount of conidia and germinated atypically in water in comparison to the wild type. To understand the impact of FvFlbA2 on asexual development of the molecular level, we performed qPCR to study

F. verticillioides putative *BRLA*, *ABAA* and *WETA* transcriptional expression in the wild-type and mutant strains. Our results showed that these three conidia related genes were highly down-regulated in ΔFvflbA2 and ΔFvflbA2/A1 but not in ΔFvflbA1 (Figure 3.5A). This result partially explains why FvFlbA1 does not completely correlate with conidiation production levels seen in *F. verticillioides*. To verify the role of the two paralogs in FB1 biosynthesis, we carried out qPCR analysis of three key FUM genes including *FUM1*, *FUM8* and *FUM21*. Consistent with our FB1 results in myro liquid cultures (Figure B-3), key FUM genes were greatly up-regulated in ΔFvflbA2 and ΔFvflbA2/A1 (Figure 3.5B). However, our results suggested that FlbA1 and FlbA2 regulate different signaling pathways, with FlbA2 playing a critical role in FB1 biosynthesis.

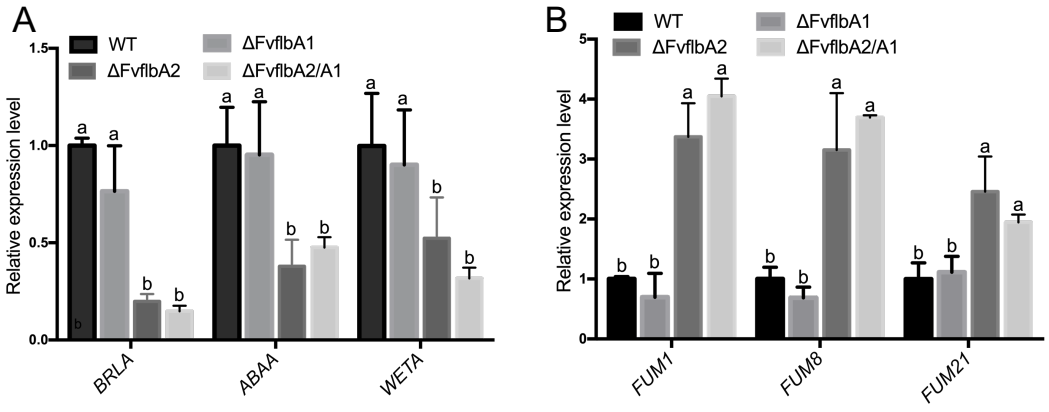

Figure 3.5 Effects of FvFlbA1 and FvFlbA2 on conidia related genes and key FUM gene transcription.
(A) Relative expression levels of putative Fv*BRLA* (FVEG_09661), Fv*ABAA* (FVEG_00646) and Fv*WETA* (FVEG_02891) in wild-type, ΔFvflbA1, ΔFvflbA2, ΔFvflbA2/A1 were normalized to *F. verticillioides* β-tubulin gene (FVEG_04081). (B) Relative mRNA expression level of three key FUM gene in deletion mutant strains in contrast to wild type.

F. verticillioides two FlbA paralogs are not required for stress responses, carbon utilization and virulence

We tested various carbon sources including sucrose, dextrose, fructose and xylose to test if there are deficiencies in carbon utilization. We observed only minor vegetative growth defects in ΔFvflbA2 and ΔFvflvA2/A1 mutants, suggesting that two FvFlbA paralogs are not critical for fungal growth (Figure 3.6A). Additionally, to determine whether FvFlbA1 and FvFlbA2 are required for response to cell wall integrity (SDS), oxidative (H_2O_2), and osmotic (NaCl) stresses, we investigated the vegetative growth of ΔFvflbA mutants in the presence of these agents in Czapek-Dox agar medium. We observed that ΔFvflbA2 and ΔFvflvA2/A1 mutants have slight defects in growth in all media tested (Figure 3.6B). However, ΔFvflbA2 and ΔFvflvA2/A1 mutants showed no significant difference in sensitivity to stresses agents (date not shown). We also determined that all mutant strains have similar capacities to cause seedling rot when compared to the wild type (Figure 3.7A and B). These results suggest that both FvFlbA1 and FvFlbA2 are dispensable for stress response, carbon utilization and virulence in *F. verticillioides*.

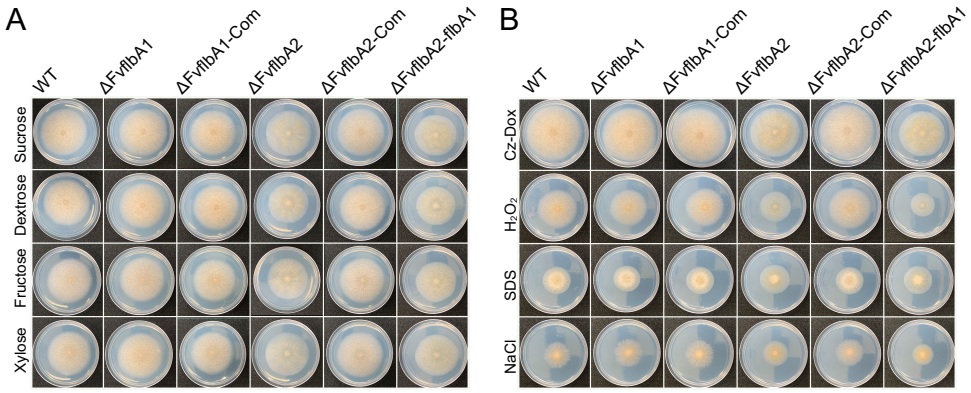

Figure 3.6 The influence of FvFlbA1 and FvFlbA2 on carbon utilization and stress response.
(A) The colony of wild-type, ΔFvflbA1, ΔFvflbA2, ΔFvflbA2/A1 and complemented strains grown on modified Czapek-Dox agar plates with different carbon sources for 8 days. (B) Strains were cultured on Czapek-Dox agar plates with various stress agents for 8 days.

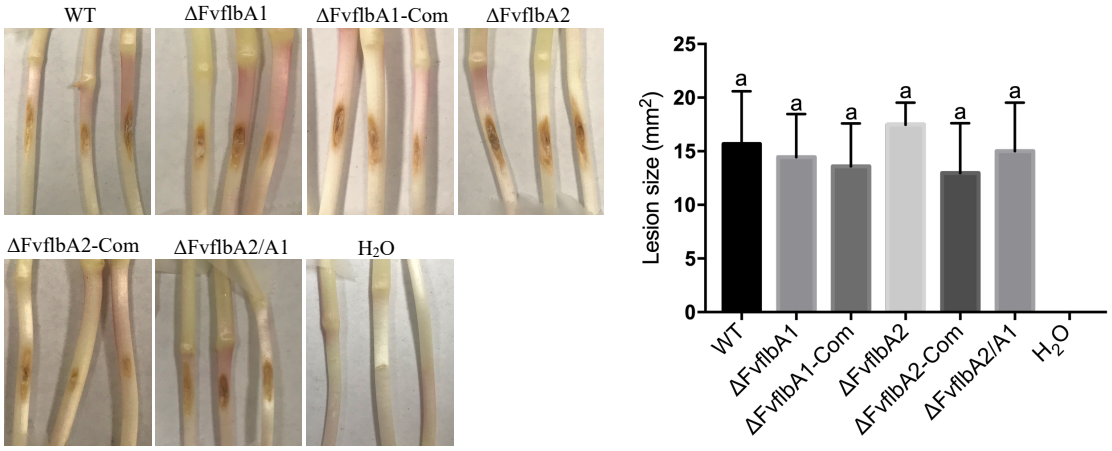

Figure 3.7 The pathogenicity of FvFlbA mutant strains in corn seedling rot assay.
(A) A syringe needle was used to created wounds on one-week old silver queen seedlings. Spore suspensions (5 µl, 10^6/ml) were inoculated on the wound sites. (B) The lesion size was quantified by Image J software after one-week incubation.

Discussion

Our previous study demonstrated that heterotrimeric G proteins and non-canonical Gβ components positively regulate the virulence and secondary metabolism (Yan and Shim, 2020). RGS proteins are well known as negative regulators of G protein signaling pathway. A further investigation showed that transcription of four putative RGS genes *FvFLBA1*, *FvFLBA2*, *FvRGSB* and *FvRGSC1* were significantly altered in ΔFvgbb1 Gβ deletion mutant background compared to the WT strain (Mukherjee et al., 2011). Further characterizations of *F. verticillioides* FvFlbA1 and FvFlbA2, two FvFlbA paralogs, showed FvFlbA2 is negatively associated with FB1 production (Mukherjee et al., 2011). Both FvFlbA1 and FvFlbA2 mRNA transcription levels are relatively low, which indicated these two gene functions are transient and may be degraded quickly after regulating Gα subunits (data not shown). In this study, our aim was to test the hypothesis that two FvFlbA paralogs play different roles that complement each other in *F. verticillioides.* Our study revealed that although FvFlbA1 is not critical for FB1 production, ΔFvflbA2 and ΔFvflbA2/A1 enhanced mycotoxin production and defects in aerial growth.

BrlA is a critical transcription factor involved in activating conidiophore development in both *A. nidulans* and *A. niger*. FlbA was demonstrated to be required for BrlA activation (Lee and Adams, 1994). The mutation of *flbA* in *A. nidulans* and *A. niger* resulted in the fluffier hyphal colony (Krijgsheld et al., 2013). But in *F. verticillioides*, the deletion

mutant ΔFvflbA2 showed a less fluffy phenotype similar to *M. oryzae* ΔMorgs1 while ΔFvflbA1 did not exhibit defects in growth (Ramanujam et al., 2012). ΔFvflbA2 mutant showed reduced conidia production while conidiation was completely blocked in *A. nidulans flbA* mutant. Both ΔFvflbA2 and ΔFvflbA2/A1 deletion mutants showed precocious germination. One possible explanation for this difference in two fungi could be due to distinct asexual production mechanisms between *A. nidulans* and *F. verticillioides*. *F. verticillioides* conidia are formed through monophialides in long chains and false heads, while *A. nidulans* is the model of conidia production through typical conidiophore, specialized asexual reproductive structures found in Ascomycetes (Leslie and Summerell, 2008). As described earlier, fungal asexual development had been proposed to be regulated by BrlA-AbaA-WetA transcription factor cascade (Yu, 2010). Our result in *F. verticillioides* raises the question of whether putative BrlA-AbaA-WetA cascade follows the same expression pattern in two FvFlbA paralogs deletion mutants. Our transcriptional expression study showed these three genes were produced significantly lower but not completely abolished. This result shows a strong correlation with actual conidia production.

In *A. nidulans*, the *flbA* mutant showed reduced sterigmatocystin production (Hicks et al., 1997b). Interestingly*, A. niger* is known to harbor the putative *FUM* gene cluster and is capable of synthesizing fumonisins (Aerts et al., 2018). Transcriptome analysis of *flbA* mutant in *A. niger* demonstrated highly down-regulated expression of *FUM21* which positively corresponds with other *FUM* genes expression and fumonisins production

(Aerts et al., 2018). In *F. verticillioides*, *FUM21* also functions as a putative $Zn(II)_2Cys_6$ transcription factor that controls *FUM* genes expression, including *FUM1* and *FUM8* (Brown et al., 2007). *FUM21* locates adjacent to *FUM1* that encodes a polyketide synthase responsible for the first step of FB1 production. To further understand how FvFlbA paralogs regulate *FUM* genes expression, we tested transcription of *FUM1*, *FUM8* and *FUM21*. Our results showed that these three key *FUM* genes were highly up-regulated in ΔFvflbA2 and ΔFvflbA/A1 mutants. This result is consistent with our elevated FB1 production in ΔFvflbA2 and ΔFvflbA2/A1 mutants. The same pattern of FlbA impacts on mycotoxin productions was also reported in deletion mutants of FlbA paralogs in *F. graminearum* (Park et al., 2012). FgflbA mutant strain produced significantly higher levels of mycotoxins including DON and ZEA compared to wild-type. However, FgFlbB mutant showed no obvious deficiencies in mycotoxin production similar to ΔFvflbA1 mutant strain (Park et al., 2012).

Inactivation of Rgs1 in *M. oryzae* led to appressorium formation in both non-inductive and inductive surfaces and no capacity to cause rice blast disease (Liu et al., 2007; Zhang et al., 2011a). Similar impacts were observed in the ΔMorgs1 complement DEP or the RGS domain mutant strains with drastically less of virulence on barley and rice compared to wild-type (Ramanujam et al., 2012). Similarly, FgFlbA was shown to be positively involved in wheat head pathogenicity in *F. graminearum*. However, our seedling rot assay revealed that FvFlbA1 and FvFlbA2 are not associated with virulence in *F. verticillioides* similar to the Gβ deletion mutant ΔFvgbb1. This result was consistent with our analyses

of stress response and carbon utilization assays, in which both FflbA1 and FvFlbA2 deletion mutants failed to exhibit defects.

FlbA is well known as a negative regulator of the G protein signaling pathway. One important question we need to clarify is the relationship between two FvFlbA paralogs with canonical G protein components in *F. verticillioides*. Fluorescence localization study, split luciferase complementation and yeast two hybrid assay will be performed to verify the interaction between two FvFlbA paralogs and G protein components. Experimental procedure for these assays are well established (Yan and Shim, 2020), and thus should not pose technical issues. Our previous study showed that FvGbb1 and FvGpa2 localized in the cell membranes and vacuoles (Yan and Shim, 2020). Here, we hypothesize that two FvFlbA paralogs share the same localization with canonical heterotrimeric G protein components. However, it is reasonable to anticipate that these interactions are transient and may only be observable under certain developmental or physiological stages of *F. verticillioides*. Additionally, we hope to identify the mechanisms of how *FLBA* paralogs are important for FB1 biosynthesis regulation while showing relatively low transcription levels. It is reasonable to hypothesize that these RGS proteins are transiently expressed and also differentially regulated at different fungal growth stages. In addition, the DEP domain in FlbA paralogs is well studies for membrane targeting. Our unpublished yeast two hybrid experimental data showed FvFlbA2 but not FvFlbA1 physically interacts with C terminus of one of the G protein-coupled receptors (GPCRs) (FVEG_10980). This raises the possibility that FvFlbA2 can work with GPCR and heterotrimeric G protein

components to regulate *F. verticillioides* FB1 production and asexual development. When two FvFlbA paralogs localization and protein interaction partner studies are completed, we will have a clearer understanding of how FvFlbA1 and FvFlbA2 differentially regulate FB1 biosynthesis in *F. verticillioides*.

Materials and methods

Fungal strains and growth study

F. verticillioides M3125 was used as the wild-type strain in this study (Yan and Shim, 2020). For growth and conidia production, all strains were grown on 0.2xPDA, myro, YEPD and V8 agar plates as described previously (Yan et al., 2019). Spore germination assay followed our previous descriptions (Yan and Shim, 2020). For carbon utilization assay, Czapek-Dox agar was modified with various carbon sources such as sucrose (10g/L), dextrose (10g/L), fructose (10g/L) and xylose (10g/L) (Yan et al., 2019). Fungal growth was determined by measuring colony diameter on agar plates after 8 days of incubation at room temperature. For mycelial weight assay, we inoculated 0.5 ml of WT and mutant conidia (10^6) into 100 ml YEPD with constant shaking before harvested at indicated time points. For stress assays, 4 μl (10^6) spore suspension was inoculated on 0.2xPDA agar plates and were grown with various stressors including 0.01% SDS, 2 mM H_2O_2, 0.6 M NaCl. All experiments had at least three replicates.

Gene deletion and complementation

Both ΔFvflbA1 and ΔFvflbA2 knockout mutants were generated in wild-type strain via split-marker approach (Yan and Shim, 2020). All knockout constructs were amplified using Q5 High-Fidelity DNA Polymerase (New England Biolabs) except the second step of joint PCR using Taq enzyme (New England Biolabs). To further characterize the function of two FvFlbA paralogs in *F. verticillioides*, we generated the ΔFvflbA2/A1 double mutants in the ΔFvflbA2 background. Complementation fragments were amplified by Phusion Flash High-Fidelity PCR Master Mix (Thermo Scientific). All transformants were screened by PCR using Phire Hot Start II DNA Polymerase and verified by qPCR (Thermo Scientific). All primers are listed in the Table B-1.

Fumonisin B1, virulence, and gene expression assays

To study the FB1 production, cracked autoclaved kernels (2 g) and four surface sterilized kernels were used as described previously (Christensen et al., 2012; Yan and Shim, 2020). These experiments were performed with three biological replicates. Seedling rot was assayed by inoculating spore (5 μL, 10^6/mL) and imaged after one-week growth in the dark room. For qPCR analysis of conidiation-related genes and key FUM genes, mycelia were harvested from 7-day-old culture grown in myro liquid medium at 150 rpm. Primers for three conidia related genes, *FUM1* and *FUM8* were from previous studies (Zhang et al., 2011b; Yan et al., 2019)

CHAPTER IV

A RAB GTPASE PROTEIN FVSEC4 IS NECESSARY FOR FUMONISIN B1 BIOSYNTHESIS AND VIRULENCE IN *FUSARIUM VERTICILLIOIDES*

Summary

Rab GTPases are responsible for a variety of membrane trafficking and vesicular transportation in fungi. But the role of Rab GTPases in *Fusarium verticillioides*, one of the key corn pathogens worldwide, remains elusive. These Small GTPases in fungi, particularly those homologous to *Saccharomyces cerevisiae* Sec4, are known to be associated with protein secretion, vesicular trafficking, secondary metabolism and pathogenicity. In this study, our aim was to investigate the molecular functions of FvSec4 in *F. verticillioides* associated with physiology and virulence. Interestingly, the FvSec4 null mutation did not impair the expression of key conidiation-related genes. Also, the mutant did not show any defect in sexual development, including perithecia production. Meanwhile, GFP-FvSec4 localized to growing hyphal tips and raised the possibility that FvSec4 is involved in protein trafficking and endocytosis. The mutant exhibited defect in corn stalk rot virulence and also significant alteration of fumonisin B1 production. The

* This chapter is reprinted with permission from "A Rab GTPase protein FvSec4 is necessary for fumonisin B1 biosynthesis and virulence in *Fusarium verticillioides*" by Yan, H.J., Huang J., Zhang, H. and Shim, W.B. 2020. Current Genetics 66, 205-216.

mutation led to higher sensitivity to oxidative and cell wall stress agents, and defects in carbon utilization. Gene complementation fully restored the defects in the mutant demonstrating that FvSec4 plays important roles in these functions. Taken together, our data indicate that FvSec4 is critical in *F. verticillioides* hyphal development, virulence, mycotoxin production and stress responses.

Introduction

Eukaryotic cells employ exocytosis and endocytosis to ensure proper cell physiology while interacting with ambient environment (Schultzhaus and Shaw, 2015). Vesicles mediate protein transport during exo- and endocytosis (Lazar et al., 1997), and Rab GTPases play important roles in each transport step (Lazar et al., 1997). This protein family, the largest subfamily of Ras superfamily, is involved in vesicular trafficking regulation in eukaryotes by cycling between inactive (GDP-bound) and active (GTP-bound) states (Novick, 2016). In *Saccharomyces cerevisiae*, 11 members of Rab GTPases have been identified and studied (Lazar et al., 1997). Sec4 was first identified in *S. cerevisiae* which was shown to be involved in both secretory vesicles and the plasma membrane (Salminen and Novick, 1987; Goud et al., 1988). A recent study also demonstrated that Sec4 is associated with the actin patches and endocytic internalization in yeast (Johansen et al., 2016). In host-pathogen interactions, pathogenic fungi such as *Fusarium* species utilize many virulence factors including cell-wall degrading enzymes, effectors and toxins by secreting these into the extracellular space or the host cytoplasm

to trigger a variety of responses in the host (Ma et al., 2013). Thus, it is reasonable to anticipate that exocyst complex plays an important role in fungal pathogenesis (Chen et al., 2015). And Sec4 is a crucial component during this process which is responsible for the transport of post-Golgi-derived secretory vesicles to the cell membrane (Salminen and Novick, 1987).

Fusarium verticillioides (teleomorph *Gibberella moniliformis* Wineland) is a fungal pathogen of corn causing ear rot and stalk rot, posing significant food safety and security risks. The fungus is a heterothallic ascomycete, but predominantly utilizes asexual spores, *i.e.* macroconidia and microconidia, to rapidly reproduce on infected seeds and plant debris (Leslie and Summerell, 2008). Most importantly, the fungus can produce various mycotoxins and biologically active metabolites including fusaric acid, fusarins, and fumonisins on infested corn ears. Fumonisin B1 (FB1) is the most prevalent and toxic form of fumonisins, a group of polyketide-derived mycotoxins structurally similar to sphinganine, and this mycotoxin is linked to devastating health risks in humans and animals, including esophageal cancer and neural tube defect (Alexander et al., 2009; Wu et al., 2014). Fumonisin biosynthesis gene cluster, also referred to as the *FUM* cluster, was first discovered by Proctor et al (1999). The cluster consists of a series of key genes encoding biosynthetic enzymes and regulatory proteins (Alexander et al., 2009), and molecular characterization of *FUM1*, a polyketide synthase (PKS) gene, and *FUM8*, an aminotransferase gene, showed their important roles in FB1 biosynthesis. FB1 production was significantly reduced in *fum1* and *fum8* knockout mutants suggesting that these two

key genes in the *FUM* cluster are critical for fumonisin biosynthesis (Proctor et al., 1999; Seo et al., 2001).

However, the regulatory mechanisms involved transport and secretion of FB1 in *F. verticillioides* remain obscure. But it is reasonable to hypothesize that key mycotoxigenic fungi employ similar mechanisms (Woloshuk and Shim, 2013). A study performed in *Aspergillus parasiticus* described how vesicles, not vacuoles, are primarily associated with aflatoxin biosynthesis and export (Chanda et al., 2009). The study also illustrated the development of mycotoxigenic vesicles under conditions conducive to mycotoxin biosynthesis. A follow-up study also demonstrated that these mycotoxigenic vesicles fuse with the cytoplasmic membrane to secrete and export aflatoxin (Chanda et al., 2010). In other pathogenic fungi, a number of studies have shown that Sec4 is associated with various cellular functions important for virulence. *CLPT1* in *Colletotrichum lindemuthianum* was the first Sec4-like Rab GTPase gene reported in a phytopathogenic fungus associated with intracellular vesicular trafficking (Dumas et al., 2001). Later, *CLPT1* was further demonstrated to be required for protein secretion and fungal pathogenicity (Siriputthaiwan et al., 2005). In *A. fumigatus*, Sec4 homolog SrgA was shown to be involved in stress response, virulence and phenotypic heterogeneity (Powers-Fletcher et al., 2013). *Magnaporthe oryzae* ΔMosec4 mutant exhibited defects in extracellular proteins secretion and consequently hyphal development and pathogenicity in the rice blast fungus (Zheng et al., 2016). Exocytosis relies on a exocyst complex which has eight proteins, including Exo70p, Exo84p, Sec3p, Sec5p, Sec6p, Sec8p, Sec10p and

Sec15p (TerBush et al., 1996; Chen et al., 2015). And Sec4 was recognized as the key component regulating the exocyst assembly (Guo et al., 1999). We hypothesize that Sec4-like Rab GTPases in *F. verticillioides* is important for FB1 synthesis and transport. To test this, we identified a *S. cerevisiae* Sec4 homolog FvSec4 and characterized its roles in *F. verticillioides* vegetative growth, virulence and FB1 biosynthesis.

Results

Identification of the Sec4 homolog in *F. verticillioides*

We used the Sec4 protein sequence from the *S. cerevisiae* genome database (http://www.yeastgenome.org/) to conduct a search into NCBI *F. verticillioides* database. This search identified FVEG_06175 locus, a 990-bp gene encoding a putative 203-amino-acid protein, which was designated as *FvSEC4* gene. To identify Sec4 homolog in other fungal species, the predicted FvSec4 amino acid sequence from the *F. verticillioides* genome database was used for our BLAST search. Multiple sequences alignment (Figure 4.1) and phylogenetic analyses (Figure C-1A) indicated that Sec4-like proteins share high amino acid identity in fungi, such as *S. cerevisiae* Sec4 (YFL005W, 64 % identity), *A. fumigatus* AfSrgA (Afu4g04810, 87% identity), *M. oryzae* MoSec4 (MGG_06135, 88% identity), *C. lindemuthianum* CLPT1 (AJ272025, 95% identity) and *C. orbiculare* CoSec4 (Cob_13201, 95% identity). The predicted ScSec4 protein structure was obtained from PDB (PDB ID: 1G16) and modified into alignment by ESPript (Stroupe and Brunger,

2000; Robert and Gouet, 2014).

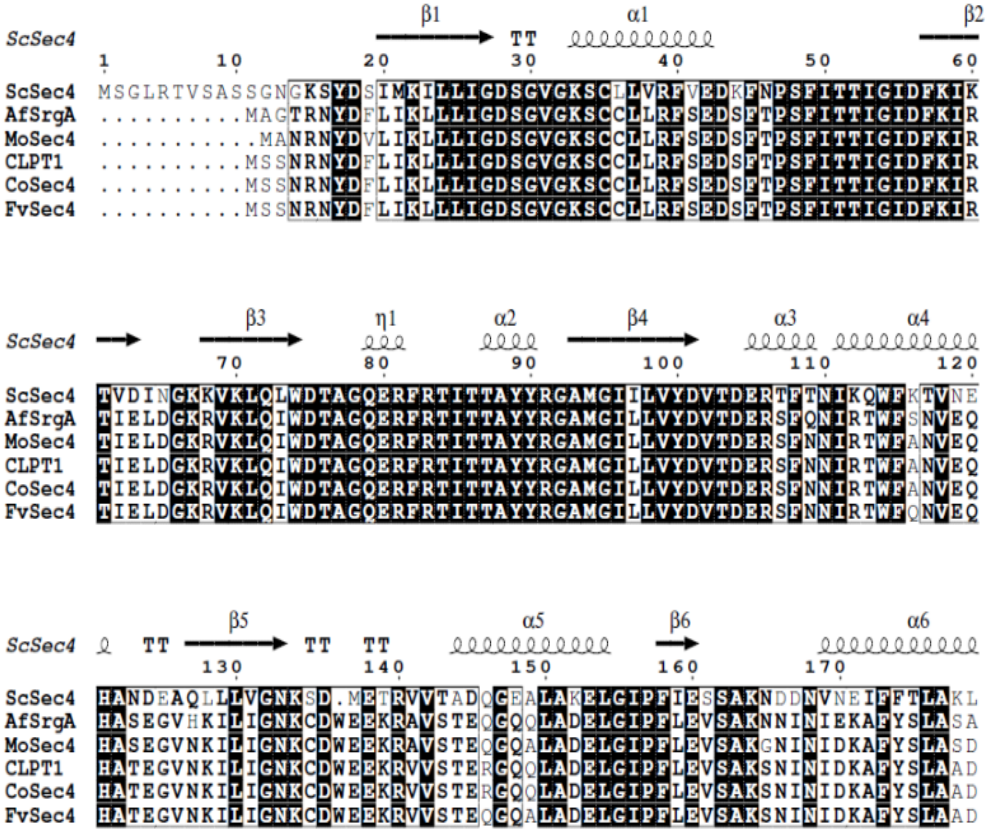

Figure 4.1 FvSec4 protein sharing high similarity with other fungal species.
Protein sequence alignment of *S. cerevisiae* Sec4, *F. verticillioides* FvSec4, *A. fumigatus* AfSrgA, *M. oryzae* MoSec4. *C. lindemuthianum* CLPT1. White characters with black background and black characters in a box indicate identical and similar sequences, respectively. Sec4 is predicted to have six alpha helices and six beta strands.

Loss of FvSec4 impairs hyphal growth and conidiation

To investigate the function of FvSec4, we generated deletion mutants by replacing the entire gene with a hygromycin-resistance marker (Figure C-2A). The gene-replacement mutants were confirmed by Southern blot (Figure C-2B). The wild-type strain showed a 2.4-kb hybridizing band and all three putative mutants had a 6.5-kb band, as expected when using the ORF 5' flanking probe for Southern blot (Figure C-2B). These results suggested that the three mutant strains had a single-copy insertion of the hygromycin-resistance marker and had no ectopic insertion events. We selected the first mutant, which was designated ΔFvsec4, to perform further experiments, including qPCR and phenotypic analyses in this study (Figure C-2C). We also generated a gene complementation strain ΔFvsec4-Com and a GFP-tagged complementation strain ΔFvsec4-GFP-FvSec4.

To study the role of FvSec4 protein in *F. verticillioides* vegetative growth, we cultivated wild-type, ΔFvsec4, ΔFvsec4-Com and ΔFvsec4-GFP-FvSec4 strains on V8, 0.2xPDA, myro agar media. The ΔFvsec4 mutant showed a drastic reduction in growth and less fluffy mycelia on all agar media tested. Both ΔFvsec4-Com and ΔFvsec4-GFP-FvSec4 strains exhibited full recovery of growth defects (Figure 4.2A). Moreover, ΔFvsec4 displayed hyphal hyperbranching under microscopic examination (Figure 4.2B). In addition, ΔFvsec4 mutant produced a significantly lower quantity of conidia when compared with wild-type and complemented strains (Figure 4.3A). However, conidia germination rate in the mutant and wild-type did not show a significant difference when

all strains were cultivated in 0.2xPDB liquid culture (Figure 4.3B). Also, mycelial fresh weight did not differ between wild-type and mutants after growing in YEPD liquid medium for 3 days (Figure 4.3C).

To further characterize the basis for conidia production deficiency in ΔFvsec4, we used qPCR to test transcription levels of key conidia regulation genes, including *BRLA*, *WETA*, *ABAA* and *STUA.* Total RNA samples were extracted from strains cultured in myro broth for 7 days and in YEPD broth for 20 h. The qPCR data suggested that conidia regulation genes are not impacted by the FvSec4 deletion both in myro and YEPD culture, except *ABAA* expression that showed 40% reduction when the mutant was cultured in myro broth (Figure C-3C and C-3D). We also tested whether FvSec4 is important for sexual reproduction, but all strains showed no defect perithecia production (Figure C-3E).

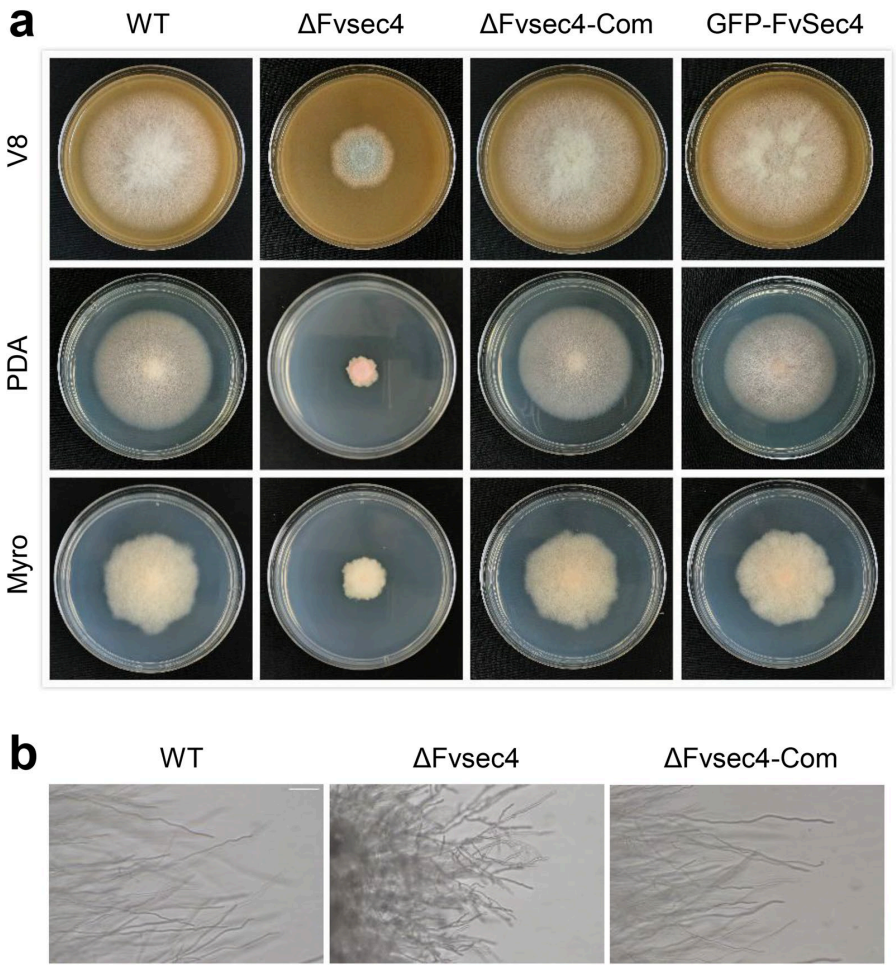

Figure 4.2 Vegetative growth of wild-type (WT), ΔFvsec4, ΔFvsec4-Com and ΔFvsec4-GFP-FvSec4 (GFP) strains.
(A) Strains were cultured on the V8, 0.2xPDA, myro agar plates for 8 days at room temperature. (B) ΔFvsec4 mutant enhanced hyphal branching compared to WT, ΔFvsec4-Com after 3 days on 0.2xPDA agar plates. Bar = 100 μm

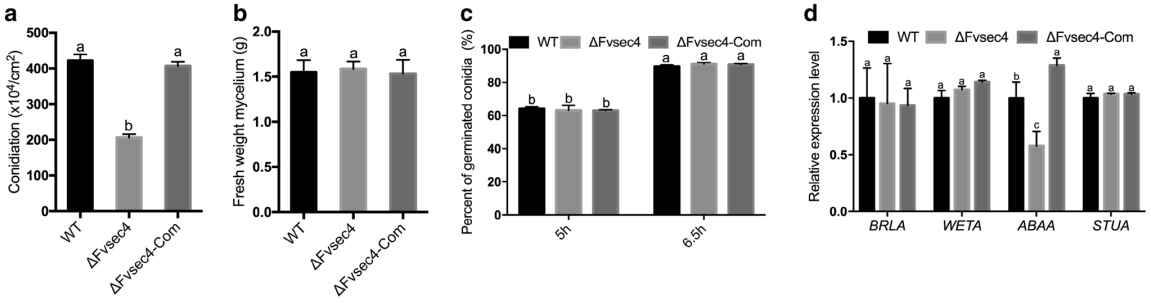

Figure 4.3 Impacts of FvSec4 on conidia production

(A) Conidia production in wild-type (WT), ΔFvsec4, ΔFvsec4-Com strains were measured after incubation on V8 agar medium at room temperature for 8 days. (B) Conidia germination rate in WT, ΔFvsec4, and ΔFvsec4-Com on 0.2xPDB were examined under a microscope after 5 and 6.5h incubation with gentle shaking. (C) Mycelium samples (fresh weight) were assayed after 3-day incubation in YEPD liquid medium. (D) Transcript differences of conidia-related genes in ΔFvsec4 were compared to WT and ΔFvsec4-Com strains. Three biological replicates were performed independently. Error bars in this study all represent the standard deviations for three replicates. Lowercase letters in this study on the bar top suggest significant differences among various strains. (Student T-test, $P < 0.05$). All data in this study were analyzed by Prism software.

Subcellular localization of FvSec4 suggests its role in vesicle trafficking

Since Sec4 is known as a key component that regulates the exocyst assembly, we studied the localization of FvSec4 in *F. verticillioides*. We used the native promoter and fused GFP to the N-terminus of *FvSEC4* coding sequence, and subsequently transformed the *FvSec4*$_{pro}$*-GFP-FvSec4* construct into ΔFvsec4 strain. After confirming construct insertion through PCR, we performed a live-cell imaging study of GFP-FvSec4 protein subcellular localization. The FvSec4 green fluorescent signal accumulated mainly in the tips of hyphae, which was consistent with the predicted Sec4 protein role in the tip vesicle transport and growth (Figure 4.4A).

In addition to exocytosis, a previous study revealed that Sec4 is also important for endocytosis (Kean et al., 1993). To further test whether FvSec4 is associated with endocytosis, we stained the mycelia of wild-type, ΔFvsec4, and ΔFvsec4-Com with FM4-64, which is frequently used to study endocytosis and vesicle trafficking in the fungal hyphae (Fischer-Parton et al., 2000). Highly concentrated fluorescent signals were detected in the Spitzenkörper region in both WT and ΔFvsec4-Com, while the ΔFvsec4 mutant showed a broader diffused staining at the mycelial tip (Figure 4.4B). In the mutant, FM4-64 staining was generally localized to the growing hyphal tip but no clear Spitzenkörper structure staining was observed. In addition, when we monitored FM4-64 staining in wild-type and ΔFvsec4 hypha in time course, we were able to observe higher intensity of endomembrane staining in the wild type (Figure C-4), which suggests that

ΔFvsec4 is either not properly functioning in the uptake of FM4-64 or defective in recycling dyes to hyphal tip by exocytosis.

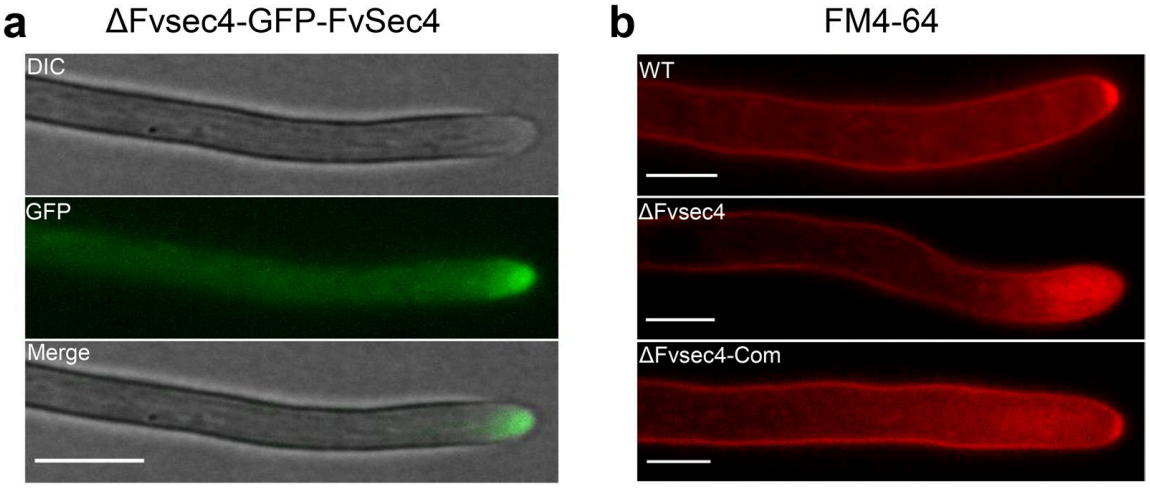

Figure 4.4 FvSec4 protein localization assay.
(A) GFP-Sec4 protein driven by its native promoter mainly localized to the apical area of growing hyphae. Bar = 5 μm (B) Hyphal growth of wild-type (WT), ΔFvsec4, ΔFvsec4-Com were examined under a microscope after 10 min of FM4-64 staining. The Spitzenkörper region in ΔFvsec4 was compared with WT and ΔFvsec4-Com. Bar = 5 μm

FvSec4 is important for corn seedling rot virulence

To test whether FvSec4 plays a role in *F. verticillioides* virulence, we inoculated wild-type, ΔFvsec4, ΔFvsec4-Com spore suspensions, with sterilized distilled water as the negative control, on one-week-old corn (silver queen hybrid) seedlings. After one week of incubation, we observed significantly reduced rot symptoms in ΔFvsec4 mutant when compared to the wild-type strain (Figure 4.5A and 4.5B). Gene complementation strain ΔFvsec4-Com showed fully recovered stalk rot symptoms in our assay. These results

demonstrated that FvSec4 plays an important role in *F. verticillioides* corn stalk rot virulence.

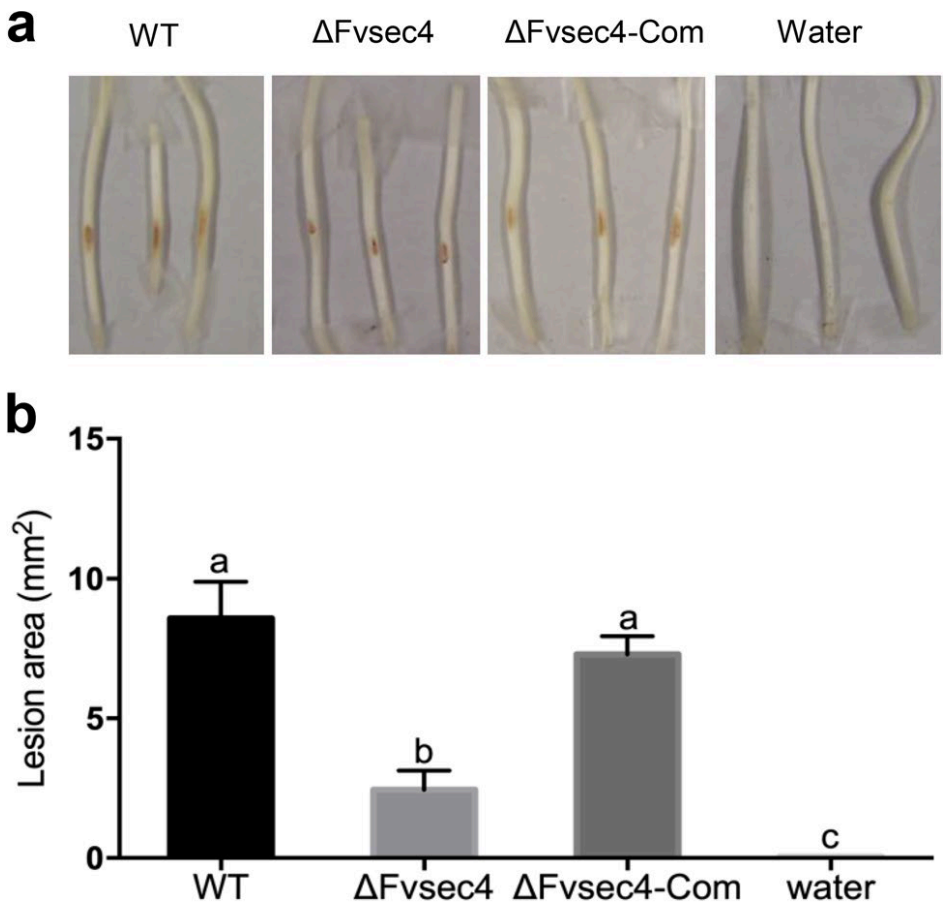

Figure 4.5 Role of FvSec4 in corn seedling rot severity.
(A) We inoculated 10 µl of wild-type (WT), ΔFvsec4, and ΔFvsec4-Com spore suspension (10^7/ml) on one-week old silver queen seedlings. Symptoms were observed after 7 days of incubation. (B) Lesion sizes were quantified using Image J.

FvSec4 is essential for FB1 production

We tested FB1 production in *F. verticillioides* strains on both corn kernels (silver queen hybrid) and in myro liquid medium after a one-week incubation. The ΔFvsec4 growth was reduced on corn kernels but not in myro liquid medium (Figure 4.6A and C-3B). When FB1 production was normalized to fungal growth, the results showed that ΔFvsec4 produces dramatically lower levels of FB1 than the wild-type progenitor in both growth conditions (Figure 4.6B and 4.6C). To further understand how FvSec4 impacts FB1 production at the molecular level, we used qPCR to study the expression of two key FUM cluster genes *FUM1* and *FUM8*. RNA samples were collected from 7 day-post-inoculation myro cultures. Both *FUM1* and *FUM8* expressions were significantly altered with the three-fold reduction in ΔFvsec4 strain when compared to the wild-type and ΔFvsec4-Com (Figure 4.6D). Additionally, to determine functions of FvSec4 associated the exocyst complex and secreted protein gene transcription, we also tested expression of three exocyst complex *SEC5*, *EXO70*, *SYN1* genes and one secreted protein *LCP1* gene in 7 day-post-inoculation myro and 20h YEPD liquid media. Our data showed selected genes associated with exocytosis were not altered but *LCP1* transcription level was suppressed in the ΔFvsec4 deletion mutants (Figure 6D and C-3D). Taken together, our results indicate that FvSec4 is positively associated with key *FUM* gene expression and ultimately FB1 production.

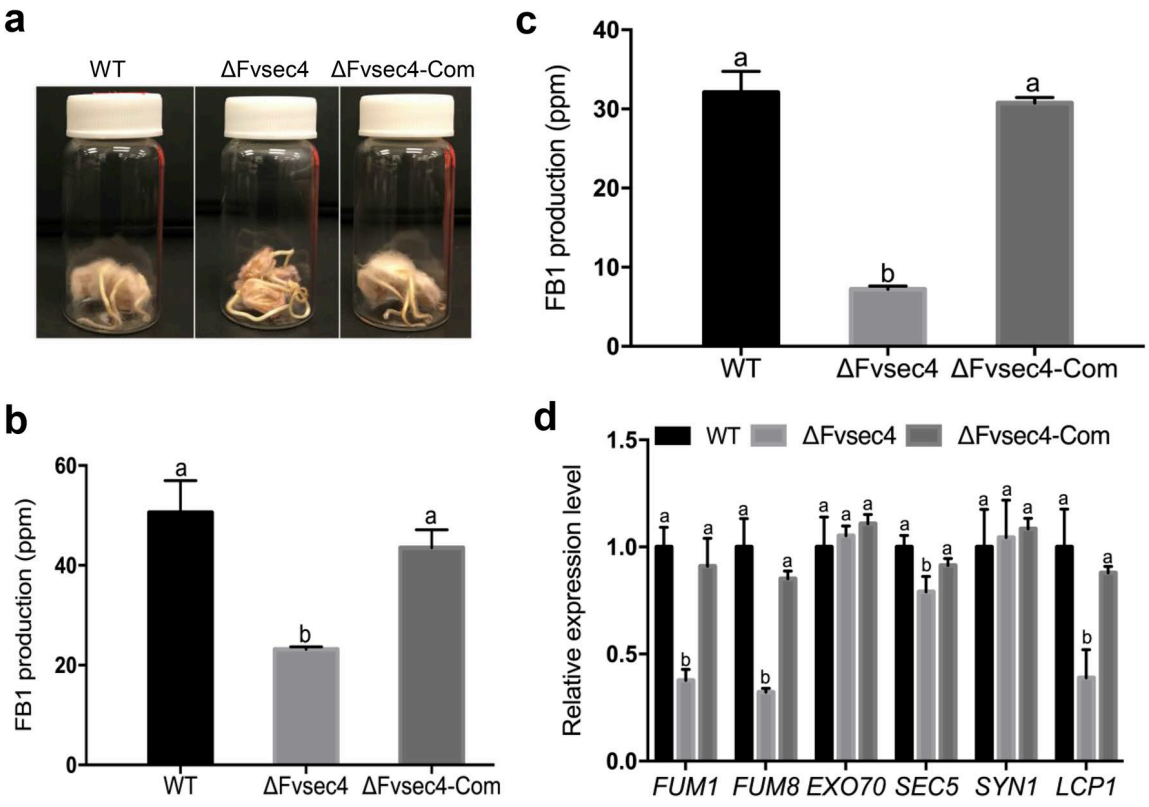

Figure 4.6 Influence of FvSec4 in FB1 production and key *FUM* gene transcription. (A) Surface sterilized silver queen corn seeds were inoculated with wild-type (WT), ΔFvsec4, ΔFvsec4-Com and incubated for 7 days. Sterile water was used as a negative control. (B) FB1 and ergosterol were quantified by HPLC. Ergosterol level in each sample was used to normalize FB1 levels, thus resulting in relative FB1 production in corn seeds. (C) Myro liquid medium was inoculated with WT, ΔFvsec4, and ΔFvsec4-Com for 7 days at room temperature with agitation. FB1 levels were analyzed by HPLC. (D) Transcriptional analyses of key FUM genes, exocyst-related genes, and FvLcp1 in WT, ΔFvsec4, ΔFvsec4-Com after 7-day incubation in the myro liquid medium. Transcripts were normalized against WT gene expression. Three biological replicates were performed independently. Error bars in this study all represent the standard deviations for three replicates. Lowercase letters in this study on the bar top suggest significant differences among various strains.

FvSec4 plays an important role in response to various stressors and differential carbon utilization

To investigate whether FvSec4 is involved in response to environmental stress agents, we tested vegetative growth of strains on minimal media amended with SDS (cell membrane stress), Congo red (cell wall stress) and H_2O_2 (oxidative stress) (Figure 4.7A). The mutant growth rate was significantly inhibited by these stress agents when compared to the wild-type strain, especially under the oxidative stress with H_2O_2 (Figure 4.7B). This outcome suggests that FvSec4 plays a role in response to stress-related to cell wall integrity and tolerance to oxidative stress.

To determine if FvSec4 is important for the utilization of different carbon nutrients, we cultivated wild-type, ΔFvsec4, ΔFvsec4-Com strains on Czapek-Dox agar medium containing different carbon sources, *i.e.* sucrose, dextrose, fructose and sorbitol (Figure 7C). We learned that the mycelial growth of ΔFvsec4 mutant exhibits significant restriction when grown on Czapek-Dox agar containing dextrose or fructose but not sorbitol, when compared to the growth observed with sucrose as the sole carbon source (Figure 4.7D). Further studies are needed to determine if this deficiency is due to carbon nutrient import into the fungal cell or secretion defect in extracellular catabolic enzymes.

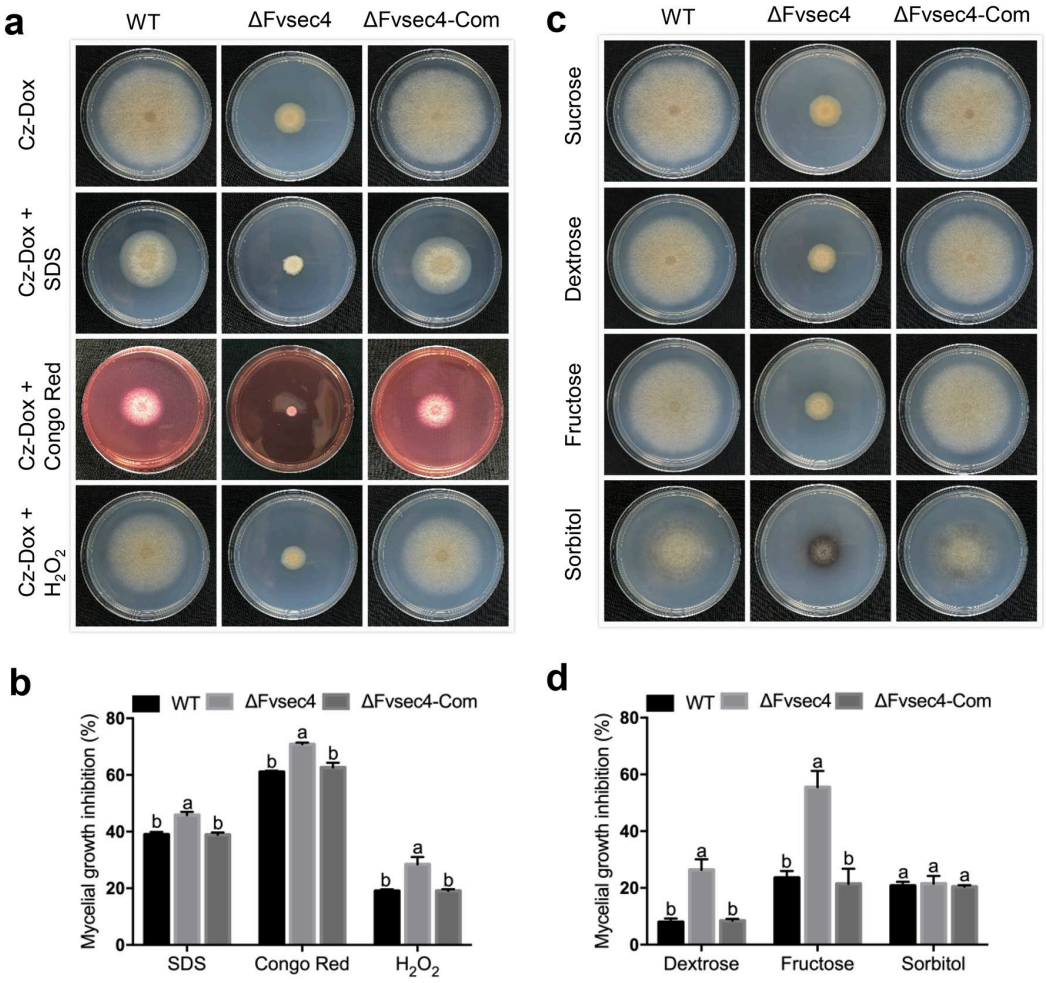

Figure 4.7 Susceptibility against various stressors and deficiency in carbon utilization in ΔFvsec4 mutant.

(A) Strains were grown on Czapek-Dox agar amended with SDS, congo red and H_2O_2 for 8 days at room temperature. (B) Growth diameter of ΔFvsec4, ΔFvsec4-Com were subjected to statistical analyses. The growth inhibition rate (%) was measured by (sucrose growth diameter - designated stress growth) / sucrose growth diameter x 100. (C) Strains were grown on modified Czapek-Dox with dextrose, fructose or sorbitol as the sole carbon source for 8 days at room temperature. Czapek-Dox agar plates with sucrose was used as a control. (D) Inhibition rate of strains grown on the media containing different carbon sources. Three replicates were used in this assay. The growth inhibition rate (%) was measured by (diameter of growth on sucrose - designated carbon growth) / diameter of growth on sucrose x 100.

Discussion

Exocytosis plays important roles in diverse functions such as cell polarization, growth, morphology, and migration (He and Guo, 2009). Exocytosis is responsible for the secretion of cellular substances to the extracellular space. When pathogenic fungi colonize the living plants, these organisms employ various strategies to adapt the host environment, namely by activating signaling pathways associated with producing effectors, secondary metabolites and enzymes (van der Does and Rep, 2017). Previous studies indicate the Sec4 protein is a key regulator of multi-subunit exocyst complex function (Guo et al., 1999). Unlike in *S. cerevisiae* and *Candida albicans*, Sec4 protein does not appear to be essential for viability but its function is critical for other physiological functions in filamentous fungi(Salminen and Novick, 1987; Mao et al., 1999). Our study showed that FvSec4, a highly conserved Rab GTPase protein, is essential for the hyphal branching and growth, conidiation, stress responses and carbon utilization in *F. verticillioides*. Furthermore, FvSec4 was also critical for the virulence and mycotoxin production.

Similar to ΔMosec4 in *M. oryzae*, the virulence in ΔFvsec4 strain was significantly reduced in our seedling rot assay when compared with the wild-type progenitor. The reduced virulence in ΔMosec4 was partially due to appressoria abnormalities, particularly with lower turgor pressure which is crucial for host penetration. Misshapen invasive hyphae and mislocalization of the cytoplasmic effector in ΔMosec4 mutant could have also negatively impacted virulence. Infection structures such as appressoria are not

recognized in *F. verticillioides.* But it is also noteworthy that a mutation in a Sec4 homolog in wheat scab pathogen *F. graminearum*, a non-appressorium producing ascomycete, also led to a virulence defect (Zheng et al., 2015). Furthermore, the deletion of Sec4 homolog BcSas1 in *Botrytis cinerea* also showed reduced virulence, and this outcome could perhaps be explained by reduced growth rate and inadequate secretion of cell wall degrading enzymes (Zhang et al., 2014). While we cannot exclude slower vegetative growth as one of the factors for reduced virulence, we can also propose that FvSec4 is involved in regulating the expression of *F. verticillioides* secreted proteins. Consistent with this idea, we learned that the expression of *FvLCP1* gene was significantly decreased in ΔFvsec4. In our previous study, we characterized FvLcp1 as a secreted protein that is involved in host defense suppression and FB1 biosynthesis (Zhang et al., 2019).

Another possible reason for attenuated pathogenicity is due to the mutant exhibiting deficiencies in responding to various exogenously applied stress agents. In our study, ΔFvsec4 showed increased sensitivity to H_2O_2. It is well studied that reactive oxygen species (ROS) are accumulated in plant hosts as a response to biotic and abiotic stress, and *Fusarium* species are directly causing biotic stress on corn (Lehmann et al., 2015). However, there are contradicting studies that suggest ROS sensitivity may not be a key factor in fungal virulence. For instance, *B. cinerea* BcSas1 deletion mutants showed less sensitivity when compared to the wild-type (Zhang et al., 2014). In addition to ROS response, ΔFvsec4 exhibited growth deficiencies when utilizing different carbon sources such as dextrose and fructose when compared to sucrose. This result raises a question

whether FvSec4 is involved in secretion of enzymes important for specific carbon nutrient utilization. The hypersensitivity to H_2O_2 and the impairment in carbon nutrient utilization are consistent with the attenuated virulence in ΔFvsec4. Published studies show that Sec4 Rab GTPases were important for stress response and nutrient utilization (Zhang et al., 2014; Zheng et al., 2016). But, whether these two physiological processes are genetically linked needs further investigation.

Secondary metabolites are not required for conventional growth in *Fusarium* species but may offer advantages in certain circumstances (Ma et al., 2013). However, it is clear that mycotoxins produced by fungi have adverse effects on human health and food safety (Wu et al., 2014). There is an earlier study by Zheng et al (2015) describing how Rab GTPase FgRab8 and exocytosis are positively associated with *F. graminearum* mycotoxin DON production (Zheng et al., 2015). While DON has been recognized as a virulence factor in *F. graminearum*, FB1 is not a critical factor for plant pathogenesis in *F. verticillioides* (Proctor et al., 1995; Desjardins et al., 2002). In this study, ΔFvsec4 showed a significantly lower level of FB1 production when compared to the wild-type strain, implying that this protein is critical for regulating mycotoxin biosynthesis. To further understand how FvSec4 is impacting FB1 production, we tested the expression of key FUM genes *FUM1* and *FUM8*. Our qPCR result showed that the transcriptional expression of these two FUM genes were significantly suppressed in the mutant. It is reasonable to hypothesize that this Rab GTPase indirectly regulates transcriptional activities of FUM cluster through other transcription factors.

Sec4 protein is known to control exocyst assembly and involved in secretion of vesicles. We confirmed that FvSec4 is localized to the hyphal tip area which is consistent with the exocytosis function. To investigate the role of FvSec4 in regulating the exocyst complex and other downstream components, we identified three Sec4 downstream genes, *EXO70*, *SEC5* and *SYN1*, to study their gene expression levels. We found that ΔFvsec4 mutation is not crucial for exocyst-related gene expression except for *SEC5*, which showed 22% less expression when compared to wild-type progenitor after a 7-day incubation in myro medium. This outcome led us to conclude that Sec4 is not directly involved in the transcriptional regulation of its downstream genes associated with exocytosis.

Spitzenkörper is a subcellular structure found at the fungal hyphal tip that is associated with polar growth (Riquelme and Sanchez-Leon, 2014). A previous report also indicated that Spitzenkörper acts as a Vesicle Supply Center (VSC) where vesicles accumulate before being released to extracellular space (Bartnicki-Garcia et al., 1989). We stained mycelia with FM4-64, and the result showed that our wild-type strain harbors a recognizable Spitzenkörper at the hyphal tip. However, ΔFvsec4 exhibited accumulated fluorescence in both apical and subapical areas while the Spitzenkörper was absent after the same staining treatment. When we consider the important role of Spitzenkörper in delivering cell wall components to the sites of cell wall synthesis, perhaps this abnormal Spitzenkörper structure and distribution are impacting the response to SDS and congo red

cell wall stress agents in ΔFvsec4 (Riquelme, 2013). The lack of Spitzenkörper is possibly due to ΔFvsec4 showing a defect in maintaining the balance between exocytosis and endocytosis. We can further hypothesize that in the mutant insufficient number of vesicles are delivered to the hyphal tip, and perhaps this leads to significantly slower vegetative growth and hyper-branching.

Materials and methods

Fungal strains, culture media and growth conditions

F. verticillioides strain 7600 was used as the wild-type strains in this study (Zhang et al., 2018b). All strains were grown and evaluated on V8 juice agar (200 ml of V8 juice, 3 g of $CaCO_3$ and 20 g of agar powder per liter), potato dextrose agar (PDA, Difco) and myro agar (1g of $NH_4H_2PO_4$, 3 g of KH_2PO_4, 2 g of $MgSO_4 \cdot 7H_2O$, 5 g of NaCl, 40 g of sucrose and 20 g of agar powder per liter) at room temperature for 8 days. For the spore production, 5 ml sterile water was added into 8 days old V8 agar plates. Spore suspensions were harvested by passing through miracloth (EMD Millipore) and counted using the hemocytometer. Newly harvested microconidia were suspended in 0.2x potato dextrose broth (PDB) for 5h and 6.5 h with gentle shaking to assay spore germinations. For genomic DNA extraction, strains were grown in YEPD liquid medium (3 g yeast extract, 10 g peptone and 20 g dextrose per liter) at 25 °C in a rotatory shaker for 4 days. For stress assays, strains were cultured on Czapek-Dox agar (2 g/L $NaNO_3$, 0.5 g/L $MgSO_4$-$7H_2O$,

0.5 g/L KCl, 10 mg/L 14 $FeSO_4$-$7H_2O$, and 1 g/L K_2HPO_4, 30 g/L sucrose, pH 7) amended with 70 mg/L Congo red, 2 mmol/L H_2O_2 or 0.01% SDS.

For carbon utilization assay, 4 µl of 1×10^6 conidial suspension was inoculated on the center of Czapek-Dox agar plates with four different carbon sources, *i.e.* sucrose (30 g/L), dextrose (10 g/L), fructose (10 g/L) and sorbitol(91 g/L), and incubating 8 days at room temperature. For the mating study, conidia from wild-type, ΔFvsec4, ΔFvsec4-com strains were harvested from culture grown on V8 agar for 7 days, and subsequently spread onto *F. verticillioides* strain 7598, which was grown on carrot plates following our standard protocol (Sagaram and Shim, 2007).

Gene deletion and complementation, polymerase chain reaction (PCR), and transformation

The constructs for *F. verticillioides* transformation were generated following our laboratory standard procedures (Sagaram and Shim, 2007). Briefly, DNA fragments corresponding to 5' and 3' flanking regions of the gene were amplified from the wild-type genomic DNA. Meanwhile, hygromycin B phosphotransferase (*HPH*) gene in pBP15 plasmid was used to obtain the HP and PH fragments. 5' and 3' flanking region fragments were fused with PH and HP fragments by single-joint PCR respectively (Yu et al., 2004; Sagaram and Shim, 2007). We used protoplast preparation and transformation protocols previously described in Zhang et al (2018). We used PCR to verify targeted gene deletion

mutations using primers OF/OR, UAF/YG/F, UAR/HY/R (Table S1), followed by Southern blot and qPCR for further validation (Yun et al., 2019).

For gene complementation, wild-type *FvSEC4* gene with its native promoter was co-transformed with a geneticin-resistant gene (*GEN*) into mutant protoplasts. All transformants were screened by PCR. All primers used in this study are presented in Table S1. To construct the GFP-FvSec4 plasmid, *FvSEC4* coding region from *F. verticillioides* cDNA was amplified. *FvSEC4* native promoter and terminator were amplified from wild-type DNA. GFP was amplified from pKNTG plasmid (Yang et al., 2018). These four purified products were introduced to the *Hind*III and *BamH*I sites of pKNTG using In-Fusion-HD cloning kit (Takara Bio USA). The plasmid was then sequenced and introduced into the ΔFvsec4 strain for genetic complementation and localization study.

Nucleic acid manipulation and Southern blot

Bacterial plasmid DNA was isolated with Wizard miniprep DNA purification system (Promega). Fungal genomic DNA isolation and Southern blot analysis were performed following standard procedures (Sambrook, 2001). Briefly, 10 μg genomic DNA of each strain was completely digested with *Cla*I and probed with a ^{32}P-labelled DNA fragment amplified from *F. verticillioides* genomic DNA with primers FvAF1 and FvAR1 (Table S1).

Corn infection and fumonisin B1 assays

Infection assays on corn seedling were conducted as previously described with minor modifications (Kim et al., 2018a). In this study, we used silver queen hybrid seeds (Burpee) for seedling inoculation with fungal spore suspensions. The seedlings were collected and analyzed after a one-week growth period in the dark room. At least three biological and three technical replicates were performed for each fungal strain.

For FB1 and ergosterol extraction, four silver queen seeds were surface sterilized using the method previously described (Christensen et al., 2012) with a minor modification. Sodium hypochlorite (6%) was replaced with 10% bleach. Next, sterilized kernels were put on autoclaved 90-mm Whatman filter paper. A scalpel was used to create wounds on the endosperm area, and these seeds were placed in 40-ml borosilicate glass vials. Fungal spore suspensions (200 µl, 10^7/ml) were inoculated into each vial, and these samples were incubated in room temperature for 7 days. FB1 extraction and sample purification methods were described previously (Christensen et al., 2012). HPLC analyses of FB1 and ergosterol were performed as described (Shim and Woloshuk, 1999). FB1 levels were then normalized to ergosterol contents. The experiment was repeated twice with three biological replicates.

RNA extraction and gene expression study

A 1ml fungal spore suspension (10^6 spores/ml) was inoculated in 100 ml YEPD for 3 days at room temperature with agitation (150 rpm). Then, mycelium from each flask was filtered through Miracloth and weighed (0.3 g) before transferred to 100 ml myro liquid medium. Samples were collected after 7 days incubation at room temperature with agitation (150 rpm). In addition, 2 ml of spore suspension (10^6 spores/ml) were added into 100 ml YEPD, incubated for 20 h at 28°C at 150rpm before being harvested for RNA extraction for qPCR assay. Three replicates were performed for each strain. Total RNA was extracted using Qiagen kit following the manufacturers' protocols. RNA samples were converted into cDNA using the Verso cDNA synthesis kit (Thermo Fisher Scientific), and qPCR analyses were performed with Step One plus real-time PCR system using the DyNAmo ColorFlash SYBR Green qPCR Kit (Thermo Fisher Scientific) with 0.5 µl cDNA as the template in per 10 µl reaction. Expression levels were normalized with *F. verticillioides* β-tubulin-encoding gene (FVEG_04081).

Microscopy and staining protocol

For hyphal growth imaging, strains were cultivated on 0.2xPDA for three days, and a block of agar containing the growing edge (approximately 1 cm diameter) was cut and placed on a glass slide. Next, water (10 µl) was added on the agar block, and subsequently a coverslip was gently placed on top. We incubated the sample at 28°C for additional 20

mins, and then observed hyphal growth under a microscope (Olympus BX60). For GFP assay, we followed a previous method with minor modifications (Schultzhaus et al., 2015) and with assistance from Dr. Brian Shaw (Department of Plant Pathology and Microbiology, TAMU). We used 16-18 h hypha to take images and water was added on the top of agar. Samples were incubated at 28°C for 20 mins. For FM4-64 staining, 16-18h growth of strains in 0.2xPDA were cut and put in the slide. Then, we added 10 µl of 5 µM FM4-64 on top of the medium and incubated at room temperature for 10 mins. We used 0.2xPDB broth to wash samples twice before taking images. Images were prepared using ImageJ software (Schneider et al., 2012).

CHAPTER V

CONCLUSION

Mycotoxins produced by fungi pose serious food safety and health risk to humans and animals. The major mycotoxins are produced by *Aspergillus*, *Penicillium* and *Fusarium* species including aflatoxins, zearalenone and fumonisins. Fumonisins are predominantly produced by *Fusarium verticillioides*. Much work has contributed to uncovering the components regulating fumonisin B1 (FB1) production. However, there remains a gap in our understanding of how *F. verticillioides* senses environmental cues and ultimately stimulates FB1 biosynthesis on the plant host. One of the critical sensory mechanisms in eukaryotic organisms is mediated by G protein-coupled receptors (GPCRs) and G-protein signaling pathway. GPCR is the largest group of transmembrane receptors in the cell, which serves important sensor functions. GPCR functions as a guanine nucleotide exchange factor to activate heterotrimeric G proteins that consist of α, β, and γ subunits. Regulators of G protein signaling (RGS) proteins contribute to promoting GTPase activities in Gα subunit and regulating G protein-coupled receptor pathway. In this dissertation research, I asked a series of questions that provided a deeper understanding of how G-proteins impact FB1 regulation in *F. verticillioides.*

I studied a noncanonical G protein component, Receptor for Activated C Kinase 1 (RACK1) homolog, FvGbb2 in *F. verticillioides.* The mutant exhibited severe defects not only in fumonisin B1 biosynthesis but also in other physiological aspects. Gene expression

studies in Fvgbb2 showed 15 polyketide synthase (PKS) genes were all significantly altered when compared to the wild-type strain. Notably, *PKS11* (*FUM1*) gene expression was not detected in Fvgbb1 and Fvgbb2 mutants. The combined PKS and FB1 results suggest that Gβ-like protein, FvGbb2 is a broader regulator of PKS-related secondary metabolism while Gβ protein FvGbb1 plays a more positively dominant role in FB1 biosynthesis. Additionally, although FvGbb1 and FvGbb2 share the similarity in domain structures, their localizations are different. FvGbb1 is expressed mainly in the vacuole and cell membrane while FvGbb2 is constitutively expressed in the cytoplasm. The reason for FvGbb1 and FvGbb2 distinct localization is still not completely understood. But we hypothesize that the diverse roles of FvGbb2 may be explained by broad localization in the cytoplasm. The mechanism remains to be further investigated. In terms of RGS proteins, our characterization of two FvFlbA orthologs, namely FvFlbA1 and FvFlbA2, showed that FvflbA2/A1 double mutation results in severe growth defects and elevated FB1 production than those observed in single mutants. This is in contrast to our Gβ and Gα subunits single deletion mutants that decreased FB1 production. This contradictory FB1 regulation further supports the idea that the negative regulation by RGS signaling on heterotrimeric G protein.

My effort to characterize 18 putative GPCR single deletion mutants did not result in FB1 biosynthesis-related phenotypes (data not shown). This may be due to the redundancy of GPCR proteins in the cell. Specifically, I identified 117 putative GPCR proteins in *F. verticillioides*. Stimuli sensing and initiation of signal transduction pathways by GPCR is

a complex mechanism, and I question any single putative GPCR serve a predominant role in *F. verticillioides*. However, my study of genetic components highly associated with GPCRs, i.e. G protein subunits and RGS orthologs, has demonstrated critical impacts on FB1 regulation. Identification and further characterization of putative interacting proteins of FvGbb2 and two FlbA paralogs will provide more insightful knowledge in *F. verticillioides* virulence and mycotoxin biosynthesis.

REFERENCES

Adams, T.H., and Yu, J.H. (1998) Coordinate control of secondary metabolite production and asexual sporulation in *Aspergillus nidulans*. *Curr Opin Microbiol* **1**: 674-677.

Aerts, D., Hauer, E.E., Ohm, R.A., Arentshorst, M., Teertstra, W.R., Phippen, C. et al. (2018) The FlbA-regulated predicted transcription factor Fum21 of *Aspergillus niger* is involved in fumonisin production. *Antonie Van Leeuwenhoek* **111**: 311-322.

Alexander, N.J., Proctor, R.H., and McCormick, S.P. (2009) Genes, gene clusters, and biosynthesis of trichothecenes and fumonisins in Fusarium. *Toxin reviews* **28**: 198-215.

Ballon, D.R., Flanary, P.L., Gladue, D.P., Konopka, J.B., Dohlman, H.G., and Thorner, J. (2006) DEP-domain-mediated regulation of GPCR signaling responses. *Cell* **126**: 1079-1093.

Bartnicki-Garcia, S., Hergert, F., and Gierz, G. (1989) Computer simulation of fungal morphogenesis and the mathematical basis for hyphal (tip) growth. *Protoplasma* **153**: 46-57.

Blacutt, A.A., Gold, S.E., Voss, K.A., Gao, M., and Glenn, A.E. (2018) *Fusarium verticillioides*: advancements in understanding the toxicity, virulence, and niche adaptations of a model mycotoxigenic pathogen of maize. *Phytopathology* **108**: 312-326.

Bloemendal, S., Bernhards, Y., Bartho, K., Dettmann, A., Voigt, O., Teichert, I. et al. (2012) A homologue of the human STRIPAK complex controls sexual development in fungi. *Mol Microbiol* **84**: 310-323.

Bluhm, B.H., and Woloshuk, C.P. (2006) Fck1, a C-type cyclin-dependent kinase, interacts with Fcc1 to regulate development and secondary metabolism in *Fusarium verticillioides*. *Fungal Genet Biol* **43**: 146-154.

Brown, D.W., Butchko, R.A., Busman, M., and Proctor, R.H. (2007) The *Fusarium verticillioides* FUM gene cluster encodes a Zn(II)2Cys6 protein that affects FUM gene expression and fumonisin production. *Eukaryot Cell* **6**: 1210-1218.

Brown, D.W., Butchko, R.A., Busman, M., and Proctor, R.H. (2012) Identification of gene clusters associated with fusaric acid, fusarin, and perithecial pigment production in *Fusarium verticillioides*. *Fungal Genet Biol* **49**: 521-532.

Cai, Z.-d., Chai, Y.-f., Zhang, C.-y., Qiao, W.-r., Sang, H., and Lu, L. (2015) The Gβ-like protein CpcB is required for hyphal growth, conidiophore morphology and pathogenicity in *Aspergillus fumigatus*. *Fungal Genetics and Biology* **81**: 120-131.

Chanda, A., Roze, L.V., and Linz, J.E. (2010) A possible role for exocytosis in aflatoxin export in *Aspergillus parasiticus*. *Eukaryot Cell* **9**: 1724-1727.

Chanda, A., Roze, L.V., Kang, S., Artymovich, K.A., Hicks, G.R., Raikhel, N.V. et al. (2009) A key role for vesicles in fungal secondary metabolism. *Proc Natl Acad Sci U S A* **106**: 19533-19538.

Chasse, S.A., Flanary, P., Parnell, S.C., Hao, N., Cha, J.Y., Siderovski, D.P., and Dohlman, H.G. (2006) Genome-scale analysis reveals Sst2 as the principal regulator of mating pheromone signaling in the yeast *Saccharomyces cerevisiae*. *Eukaryotic Cell* **5**: 330-346.

Chen, J.G., and Jones, A.M. (2004) AtRGS1 function in *Arabidopsis thaliana*. *Methods Enzymol* **389**: 338-350.

Chen, X., Ebbole, D.J., and Wang, Z. (2015) The exocyst complex: delivery hub for morphogenesis and pathogenesis in filamentous fungi. *Curr Opin Plant Biol* **28**: 48-54.

Cheng, Z., Li, J.-F., Niu, Y., Zhang, X.-C., Woody, O.Z., Xiong, Y. et al. (2015) Pathogen-secreted proteases activate a novel plant immune pathway. *Nature* **521**: 213-216.

Choi, Y.E., and Shim, W.B. (2008) Functional characterization of *Fusarium verticillioides CPP1*, a gene encoding a putative protein phosphatase 2A catalytic subunit. *Microbiology* **154**: 326-336.

Christensen, S., Borrego, E., Shim, W.B., Isakeit, T., and Kolomiets, M. (2012) Quantification of fungal colonization, sporogenesis, and production of mycotoxins using kernel bioassays. *J Vis Exp* **62**: e3727

Cox, K.L., Jr., Babilonia, K., Wheeler, T., He, P., and Shan, L. (2019) Return of old foes - recurrence of bacterial blight and Fusarium wilt of cotton. *Curr Opin Plant Biol* **50**: 95-103.

Coyle, S.M., Gilbert, W.V., and Doudna, J.A. (2009) Direct link between RACK1 function and localization at the ribosome in vivo. *Molecular and Cellular Biology* **29**: 1626-1634.

Delgado-Jarana, J., Martinez-Rocha, A.L., Roldan-Rodriguez, R., Roncero, M.I., and Di Pietro, A. (2005) *Fusarium oxysporum* G-protein β subunit Fgb1 regulates hyphal growth, development, and virulence through multiple signalling pathways. *Fungal Genet Biol* **42**: 61-72.

Desjardins, A.E., and Plattner, R.D. (2000) Fumonisin B_1-nonproducing strains of *Fusarium verticillioides* cause maize (*Zea mays*) ear infection and ear rot. *J Agric Food Chem* **48**: 5773-5780.

Desjardins, A.E., Munkvold, G.P., Plattner, R.D., and Proctor, R.H. (2002) *FUM1*--a gene required for fumonisin biosynthesis but not for maize ear rot and ear infection by *Gibberella moniliformis* in field tests. *Mol Plant Microbe Interact* **15**: 1157-1164.

Dettmann, A., Heilig, Y., Ludwig, S., Schmitt, K., Illgen, J., Fleissner, A. et al. (2013) HAM-2 and HAM-3 are central for the assembly of the *Neurospora* STRIPAK

complex at the nuclear envelope and regulate nuclear accumulation of the MAP kinase MAK-1 in a MAK-2-dependent manner. *Mol Microbiol* **90**: 796-812.

Dohlman, H.G. (2009) RGS proteins the early days. *Prog Mol Biol Transl Sci* **86**: 1-14.

Dumas, B., Borel, C., Herbert, C., Maury, J., Jacquet, C., Balsse, R., and Esquerre-Tugaye, M.T. (2001) Molecular characterization of *CLPT1*, a *SEC4*-like Rab/GTPase of the phytopathogenic fungus *Colletotrichum lindemuthianum* which is regulated by the carbon source. *Gene* **272**: 219-225.

Duncan, K.E., and Howard, R.J. (2010) Biology of maize kernel infection by *Fusarium verticillioides*. *Mol Plant Microbe Interact* **23**: 6-16.

Eaton, C.J., Cabrera, I.E., Servin, J.A., Wright, S.J., Cox, M.P., and Borkovich, K.A. (2012) The guanine nucleotide exchange factor RIC8 regulates conidial germination through Gα proteins in *Neurospora crassa*. *PLoS One* **7**: e48026.

Fischer-Parton, S., Parton, R.M., Hickey, P.C., Dijksterhuis, J., Atkinson, H.A., and Read, N.D. (2000) Confocal microscopy of FM4-64 as a tool for analysing endocytosis and vesicle trafficking in living fungal hyphae. *J Microsc* **198**: 246-259.

Flaherty, J.E., and Woloshuk, C.P. (2004) Regulation of fumonisin biosynthesis in *Fusarium verticillioides* by a zinc binuclear cluster-type gene, *ZFR1*. *Appl Environ Microbiol* **70**: 2653-2659.

Flaherty, J.E., Pirttila, A.M., Bluhm, B.H., and Woloshuk, C.P. (2003) *PAC1*, a pH-regulatory gene from *Fusarium verticillioides*. *Appl Environ Microbiol* **69**: 5222-5227.

Gelderblom, W.C., Jaskiewicz, K., Marasas, W.F., Thiel, P.G., Horak, R.M., Vleggaar, R., and Kriek, N.P. (1988) Fumonisins--novel mycotoxins with cancer-promoting activity produced by *Fusarium moniliforme*. *Appl Environ Microbiol* **54**: 1806-1811.

Goud, B., Salminen, A., Walworth, N.C., and Novick, P.J. (1988) A GTP-binding protein required for secretion rapidly associates with secretory vesicles and the plasma membrane in yeast. *Cell* **53**: 753-768.

Guo, J., Wang, S., Wang, J., Huang, W.D., Liang, J., and Chen, J.G. (2009) Dissection of the relationship between RACK1 and heterotrimeric G-proteins in Arabidopsis. *Plant Cell Physiol* **50**: 1681-1694.

Guo, W., Roth, D., Walch-Solimena, C., and Novick, P. (1999) The exocyst is an effector for Sec4p, targeting secretory vesicles to sites of exocytosis. *EMBO J* **18**: 1071-1080.

Hamel, L.P., Nicole, M.C., Duplessis, S., and Ellis, B.E. (2012) Mitogen-activated protein kinase signaling in plant-interacting fungi: distinct messages from conserved messengers. *Plant Cell* **24**: 1327-1351.

Hanlon, C.D., and Andrew, D.J. (2015) Outside-in signaling--a brief review of GPCR signaling with a focus on the Drosophila GPCR family. *J Cell Sci* **128**: 3533-3542.

Hansen, F.T., Gardiner, D.M., Lysoe, E., Fuertes, P.R., Tudzynski, B., Wiemann, P. et al. (2015) An update to polyketide synthase and non-ribosomal synthetase genes and nomenclature in Fusarium. *Fungal Genet Biol* **75**: 20-29.

He, B., and Guo, W. (2009) The exocyst complex in polarized exocytosis. *Current Opinion in Cell Biology* **21**: 537-542.

He, Z., Zhang, H., Gao, S., Lercher, M.J., Chen, W.H., and Hu, S. (2016) Evolview v2: an online visualization and management tool for customized and annotated phylogenetic trees. *Nucleic Acids Res* **44**: W236-241.

Hicks, J.K., Yu, J.H., Keller, N.P., and Adams, T.H. (1997a) Aspergillus sporulation and mycotoxin production both require inactivation of the FadA Gα protein-dependent signaling pathway. *EMBO Journal* **16**: 4916-4923.

Hicks, J.K., Yu, J.H., Keller, N.P., and Adams, T.H. (1997b) Aspergillus sporulation and mycotoxin production both require inactivation of the FadA Gα protein-dependent signaling pathway. *EMBO J* **16**: 4916-4923.

Hopwood, D.A., and Sherman, D.H. (1990) Molecular genetics of polyketides and its comparison to fatty acid biosynthesis. *Annu Rev Genet* **24**: 37-66.

Johansen, J., Alfaro, G., and Beh, C.T. (2016) Polarized exocytosis induces compensatory endocytosis by Sec4p-regulated cortical actin polymerization. *PLoS Biol* **14**: e1002534.

Kean, L.S., Fuller, R.S., and Nichols, J.W. (1993) Retrograde lipid traffic in yeast: identification of two distinct pathways for internalization of fluorescent-labeled phosphatidylcholine from the plasma membrane. *J Cell Biol* **123**: 1403-1419.

Keller, N.P. (2019) Fungal secondary metabolism: regulation, function and drug discovery. *Nat Rev Microbiol* **17**: 167-180.

Kim, H.K., Cho, E.J., Jo, S., Sung, B.R., Lee, S., and Yun, S.H. (2012) A split luciferase complementation assay for studying in vivo protein-protein interactions in filamentous ascomycetes. *Curr Genet* **58**: 179-189.

Kim, M.S., Zhang, H., Yan, H., Yoon, B.-J., and Shim, W.B. (2018a) Characterizing co-expression networks underpinning maize stalk rot virulence in *Fusarium verticillioides* through computational subnetwork module analyses. *Scientific reports* **8**: 8310.

Kong, Q., Wang, L., Liu, Z., Kwon, N.-J., Kim, S.C., and Yu, J.-H. (2013) Gβ-like CpcB plays a crucial role for growth and development of *Aspergillus nidulans* and *Aspergillus fumigatus*. *Plos One* **8**.

Krijgsheld, P., Nitsche, B.M., Post, H., Levin, A.M., Muller, W.H., Heck, A.J. et al. (2013) Deletion of flbA results in increased secretome complexity and reduced secretion heterogeneity in colonies of *Aspergillus niger*. *J Proteome Res* **12**: 1808-1819.

Kroken, S., Glass, N.L., Taylor, J.W., Yoder, O.C., and Turgeon, B.G. (2003) Phylogenomic analysis of type I polyketide synthase genes in pathogenic and saprobic ascomycetes. *Proc Natl Acad Sci U S A* **100**: 15670-15675.

Kumar, S., Stecher, G., and Tamura, K. (2016) MEGA7: Molecular evolutionary genetics analysis version 7.0 for bigger datasets. *Mol Biol Evol* **33**: 1870-1874.

Kwon, N.J., Park, H.S., Jung, S., Kim, S.C., and Yu, J.H. (2012) The putative guanine nucleotide exchange factor RicA mediates upstream signaling for growth and development in Aspergillus. *Eukaryot Cell* **11**: 1399-1412.

Larkin, M.A., Blackshields, G., Brown, N.P., Chenna, R., McGettigan, P.A., McWilliam, H. et al. (2007) Clustal W and Clustal X version 2.0. *Bioinformatics* **23**: 2947-2948.

Lazar, T., Gotte, M., and Gallwitz, D. (1997) Vesicular transport: how many Ypt/Rab-GTPases make a eukaryotic cell? *Trends Biochem Sci* **22**: 468-472.

Lee, B.N., and Adams, T.H. (1994) Overexpression of flbA, an early regulator of Aspergillus asexual sporulation, leads to activation of brlA and premature initiation of development. *Mol Microbiol* **14**: 323-334.

Lee, M.J., and Dohlman, H.G. (2008) Coactivation of G protein signaling by cell-surface receptors and an intracellular exchange factor. *Curr Biol* **18**: 211-215.

Lehmann, S., Serrano, M., L'Haridon, F., Tjamos, S.E., and Metraux, J.P. (2015) Reactive oxygen species and plant resistance to fungal pathogens. *Phytochemistry* **112**: 54-62.

Leslie, J.F., and Summerell, B.A. (2008) *The Fusarium laboratory manual*: John Wiley & Sons.

Letunic, I., and Bork, P. (2018) 20 years of the SMART protein domain annotation resource. *Nucleic Acids Res* **46**: D493-D496.

Letunic, I., Doerks, T., and Bork, P. (2015) SMART: recent updates, new developments and status in 2015. *Nucleic Acids Res* **43**: D257-260.

Li, G., Zhang, X., Tian, H., Choi, Y.E., Tao, W.A., and Xu, J.R. (2017) *MST50* is involved in multiple MAP kinase signaling pathways in *Magnaporthe oryzae*. *Environ Microbiol* **19**: 1959-1974.

Li, L., Wright, S.J., Krystofova, S., Park, G., and Borkovich, K.A. (2007) Heterotrimeric G protein signaling in filamentous fungi. In *Annual Review of Microbiology*, pp. 423-452.

Li, Y., Yan, X., Wang, H., Liang, S., Ma, W.B., Fang, M.Y. et al. (2010) MoRic8 Is a novel component of G-protein signaling during plant infection by the rice blast fungus *Magnaporthe oryzae*. *Mol Plant Microbe Interact* **23**: 317-331.

Lind, A.L., Lim, F.Y., Soukup, A.A., Keller, N.P., and Rokas, A. (2018) An LaeA- and BrlA-dependent cellular network governs tissue-specific secondary metabolism in the human pathogen *Aspergillus fumigatus*. *mSphere* **3**.

Liu, H., Suresh, A., Willard, F.S., Siderovski, D.P., Lu, S., and Naqvi, N.I. (2007) Rgs1 regulates multiple Gα subunits in *Magnaporthe* pathogenesis, asexual growth and thigmotropism. *EMBO J* **26**: 690-700.

Liu, X., Nie, X., Ding, Y., and Chen, J. (2010) Asc1, a WD-repeat protein, is required for hyphal development and virulence in *Candida albicans*. *Acta Biochimica Et Biophysica Sinica* **42**: 793-800.

Ma, L.J., Geiser, D.M., Proctor, R.H., Rooney, A.P., O'Donnell, K., Trail, F. et al. (2013) *Fusarium* pathogenomics. *Annu Rev Microbiol* **67**: 399-416.

Ma, L.J., van der Does, H.C., Borkovich, K.A., Coleman, J.J., Daboussi, M.J., Di Pietro, A. et al. (2010) Comparative genomics reveals mobile pathogenicity chromosomes in *Fusarium*. *Nature* **464**: 367-373.

Mao, Y.X., Kalb, V.F., and Wong, B. (1999) Overexpression of a dominant-negative allele of *SEC4* inhibits growth and protein secretion in *Candida albicans*. *Journal of Bacteriology* **181**: 7235-7242.

Marchese, A., Paing, M.M., Temple, B.R., and Trejo, J. (2008) G protein-coupled receptor sorting to endosomes and lysosomes. *Annu Rev Pharmacol Toxicol* **48**: 601-629.

Marin, S., Ramos, A.J., Cano-Sancho, G., and Sanchis, V. (2013) Mycotoxins: occurrence, toxicology, and exposure assessment. *Food Chem Toxicol* **60**: 218-237.

Miller, K.G., Emerson, M.D., McManus, J.R., and Rand, J.B. (2000) RIC-8 (Synembryn): a novel conserved protein that is required for $G_q\alpha$ signaling in the *C. elegans* nervous system. *Neuron* **27**: 289-299.

Mochlyrosen, D., Khaner, H., and Lopez, J. (1991) Identification of intracellular receptor proteins for activated protein kinase C. *Proceedings of the National Academy of Sciences of the United States of America* **88**: 3997-4000.

Mukherjee, M., Kim, J.E., Park, Y.S., Kolomiets, M.V., and Shim, W.B. (2011) Regulators of G-protein signalling in *Fusarium verticillioides* mediate differential host-pathogen responses on nonviable versus viable maize kernels. *Mol Plant Pathol* **12**: 479-491.

Mukhopadhyay, R., Ho, Y.S., Swiatek, P.J., Rosen, B.P., and Bhattacharjee, H. (2006) Targeted disruption of the mouse Asna1 gene results in embryonic lethality. *FEBS Lett* **580**: 3889-3894.

Munk, C., Isberg, V., Mordalski, S., Harpsoe, K., Rataj, K., Hauser, A.S. et al. (2016) GPCRdb: the G protein-coupled receptor database - an introduction. *Br J Pharmacol* **173**: 2195-2207.

Nelson, P.E., Desjardins, A.E., and Plattner, R.D. (1993) Fumonisins, mycotoxins produced by fusarium species: biology, chemistry, and significance. *Annu Rev Phytopathol* **31**: 233-252.

Neves, S.R., Ram, P.T., and Iyengar, R. (2002) G protein pathways. *Science* **296**: 1636-1639.

Nishimura, M., Park, G., and Xu, J.R. (2003) The G-beta subunit *MGB1* is involved in regulating multiple steps of infection-related morphogenesis in *Magnaporthe grisea*. *Molecular Microbiology* **50**: 231-243.

Novick, P. (2016) Regulation of membrane traffic by Rab GEF and GAP cascades. *Small GTPases* **7**: 252-256.

Nunez, A., Franco, A., Madrid, M., Soto, T., Vicente, J., Gacto, M., and Cansado, J. (2009) Role for RACK1 orthologue Cpc2 in the modulation of stress response in fission yeast. *Molecular Biology of the Cell* **20**: 3996-4009.

Ortiz, C.S., and Shim, W.B. (2013) The role of MADS-box transcription factors in secondary metabolism and sexual development in the maize pathogen *Fusarium verticillioides*. *Microbiology* **159**: 2259-2268.

Palmer, D.A., Thompson, J.K., Li, L., Prat, A., and Wang, P. (2006) Gib2, a novel Gβ-like/RACK1 homolog, functions as a Gβ subunit in cAMP signaling and is essential in *Cryptococcus neoformans*. *Journal of Biological Chemistry* **281**: 32596-32605.

Park, A.R., Cho, A.R., Seo, J.A., Min, K., Son, H., Lee, J. et al. (2012) Functional analyses of regulators of G protein signaling in *Gibberella zeae*. *Fungal Genet Biol* **49**: 511-520.

Powers-Fletcher, M.V., Feng, X., Krishnan, K., and Askew, D.S. (2013) Deletion of the *sec4* homolog *srgA* from *Aspergillus fumigatus* is associated with an impaired stress response, attenuated virulence and phenotypic heterogeneity. *Plos One* **8**.

Proctor, R.H., Hohn, T.M., and McCormick, S.P. (1995) Reduced virulence of *Gibberella zeae* caused by disruption of a trichothecene toxin biosynthetic gene. *Mol Plant Microbe Interact* **8**: 593-601.

Proctor, R.H., Desjardins, A.E., Plattner, R.D., and Hohn, T.M. (1999) A polyketide synthase gene required for biosynthesis of fumonisin mycotoxins in *Gibberella fujikuroi* mating population A. *Fungal Genet Biol* **27**: 100-112.

Proctor, R.H., Van Hove, F., Susca, A., Stea, G., Busman, M., van der Lee, T. et al. (2013) Birth, death and horizontal transfer of the fumonisin biosynthetic gene cluster during the evolutionary diversification of *Fusarium*. *Mol Microbiol* **90**: 290-306.

Rachfall, N., Schmitt, K., Bandau, S., Smolinski, N., Ehrenreich, A., Valerius, O., and Braus, G.H. (2013) RACK1/Asc1p, a ribosomal node in cellular signaling. *Molecular & Cellular Proteomics* **12**: 87-105.

Ramanujam, R., Xu, Y., Hao, L., and Naqvi, N.I. (2012) Structure-function analysis of Rgs1 in *Magnaporthe oryzae*: role of DEP domains in subcellular targeting. *Plos One* **7**.

Ramanujam, R., Calvert, M.E., Selvaraj, P., and Naqvi, N.I. (2013) The late endosomal HOPS complex anchors active G-protein signaling essential for pathogenesis in *magnaporthe oryzae*. *PLoS Pathog* **9**: e1003527.

Rheeder, J.P., Marasas, W.F., and Vismer, H.F. (2002) Production of fumonisin analogs by *Fusarium* species. *Appl Environ Microbiol* **68**: 2101-2105.

Ridenour, J.B., and Bluhm, B.H. (2017) The novel fungal-specific gene *FUG1* has a role in pathogenicity and fumonisin biosynthesis in *Fusarium verticillioides*. *Mol Plant Pathol* **18**: 513-528.

Riquelme, M. (2013) Tip growth in filamentous fungi: a road trip to the apex. In *Annual Review of Microbiology, Vol 67*. Gottesman, S. (ed), pp. 587-609.

Riquelme, M., and Sanchez-Leon, E. (2014) The Spitzenkorper: a choreographer of fungal growth and morphogenesis. *Current Opinion in Microbiology* **20**: 27-33.

Robert, X., and Gouet, P. (2014) Deciphering key features in protein structures with the new ENDscript server. *Nucleic Acids Res* **42**: W320-324.

Ron, D., Chen, C.H., Caldwell, J., Jamieson, L., Orr, E., and Mochly-Rosen, D. (1994) Cloning of an intracellular receptor for protein kinase C: a homolog of the β subunit of G proteins. *Proc Natl Acad Sci U S A* **91**: 839-843.

Rosen, S., Yu, J.H., and Adams, T.H. (1999) The *Aspergillus nidulans sfaD* gene encodes a G protein β subunit that is required for normal growth and repression of sporulation. *EMBO J* **18**: 5592-5600.

Sagaram, U.S., and Shim, W.B. (2007) *Fusarium verticillioides GBB1*, a gene encoding heterotrimeric G protein β subunit, is associated with fumonisin B biosynthesis and hyphal development but not with fungal virulence. *Mol Plant Pathol* **8**: 375-384.

Sagaram, U.S., Butchko, R.A., and Shim, W.B. (2006) The putative monomeric G-protein *GBP1* is negatively associated with fumonisin B production in *Fusarium verticillioides*. *Mol Plant Pathol* **7**: 381-389.

Salminen, A., and Novick, P.J. (1987) A ras-like protein is required for a post-Golgi event in yeast secretion. *Cell* **49**: 527-538.

Sambrook, J.a.R., D. W. (2001) Molecular cloning : a laboratory manual. Cold Spring Harbor, N.Y.: Cold Spring Harbor Laboratory press.

Schneider, C.A., Rasband, W.S., and Eliceiri, K.W. (2012) NIH Image to ImageJ: 25 years of image analysis. *Nat Methods* **9**: 671-675.

Schuldiner, M., Metz, J., Schmid, V., Denic, V., Rakwalska, M., Schmitt, H.D. et al. (2008) The GET complex mediates insertion of tail-anchored proteins into the ER membrane. *Cell* **134**: 634-645.

Schultzhaus, Z., Yan, H., and Shaw, B.D. (2015) *Aspergillus nidulans* flippase DnfA is cargo of the endocytic collar and plays complementary roles in growth and phosphatidylserine asymmetry with another flippase, DnfB. *Mol Microbiol* **97**: 18-32.

Schultzhaus, Z.S., and Shaw, B.D. (2015) Endocytosis and exocytosis in hyphal growth. *Fungal Biology Reviews* **29**: 43-53.

Seo, J.A., Proctor, R.H., and Plattner, R.D. (2001) Characterization of four clustered and coregulated genes associated with fumonisin biosynthesis in *Fusarium verticillioides*. *Fungal Genet Biol* **34**: 155-165.

Seo, S., Pokhrel, A., and Coleman, J.J. (2020) The genome sequence of five genotypes of *Fusarium oxysporum f. sp. vasinfectum*: a resource for studies on Fusarium Wilt of Cotton. *Mol Plant Microbe Interact* **33**: 138-140.

Shen, J., Hsu, C.M., Kang, B.K., Rosen, B.P., and Bhattacharjee, H. (2003) The *Saccharomyces cerevisiae* Arr4p is involved in metal and heat tolerance. *Biometals* **16**: 369-378.

Shim, W.B., and Woloshuk, C.P. (1999) Nitrogen repression of fumonisin B1 biosynthesis in *Gibberella fujikuroi*. *FEMS Microbiol Lett* **177**: 109-116.

Shim, W.B., and Woloshuk, C.P. (2001) Regulation of fumonisin B_1 biosynthesis and conidiation in *Fusarium verticillioides* by a cyclin-like (C-type) gene, *FCC1*. *Appl Environ Microbiol* **67**: 1607-1612.

Shim, W.B., Sagaram, U.S., Choi, Y.E., So, J., Wilkinson, H.H., and Lee, Y.W. (2006) *FSR1* is essential for virulence and female fertility in *Fusarium verticillioides* and *F. graminearum*. *Molecular Plant-Microbe Interactions* **19**: 725-733.

Shin, J.H., Kim, J.E., Malapi-Wight, M., Choi, Y.E., Shaw, B.D., and Shim, W.B. (2013) Protein phosphatase 2A regulatory subunits perform distinct functional roles in the maize pathogen *Fusarium verticillioides*. *Mol Plant Pathol* **14**: 518-529.

Siriputthaiwan, P., Jauneau, A., Herbert, C., Garcin, D., and Dumas, B. (2005) Functional analysis of *CLPT1*, a Rab/GTPase required for protein secretion and pathogenesis in the plant fungal pathogen *Colletotrichum lindemuthianum*. *Journal of Cell Science* **118**: 323-329.

Smith, T.F., Gaitatzes, C., Saxena, K., and Neer, E.J. (1999) The WD repeat: a common architecture for diverse functions. *Trends Biochem Sci* **24**: 181-185.

Song, Z., Cox, R.J., Lazarus, C.M., and Simpson, T.T. (2004) Fusarin C biosynthesis in *Fusarium moniliforme* and *Fusarium venenatum*. *Chembiochem* **5**: 1196-1203.

Staunton, J., and Weissman, K.J. (2001) Polyketide biosynthesis: a millennium review. *Nat Prod Rep* **18**: 380-416.

Stroupe, C., and Brunger, A.T. (2000) Crystal structures of a Rab protein in its inactive and active conformations. *J Mol Biol* **304**: 585-598.

Studt, L., Humpf, H.U., and Tudzynski, B. (2013) Signaling governed by G proteins and cAMP is crucial for growth, secondary metabolism and sexual development in *Fusarium fujikuroi*. *PLoS One* **8**: e58185.

Tall, G.G., Krumins, A.M., and Gilman, A.G. (2003) Mammalian Ric-8A (synembryn) is a heterotrimeric Gα protein guanine nucleotide exchange factor. *J Biol Chem* **278**: 8356-8362.

Tang, G., Chen, Y., Xu, J.R., Kistler, H.C., and Ma, Z. (2018) The fungal myosin I is essential for *Fusarium* toxisome formation. *PLoS Pathog* **14**: e1006827.

TerBush, D.R., Maurice, T., Roth, D., and Novick, P. (1996) The exocyst is a multiprotein complex required for exocytosis in *Saccharomyces cerevisiae*. *Embo Journal* **15**: 6483-6494.

van der Does, H.C., and Rep, M. (2017) Adaptation to the host environment by plant-pathogenic fungi. *Annu Rev Phytopathol* **55**: 427-450.

Voth, W., Schick, M., Gates, S., Li, S., Vilardi, F., Gostimskaya, I. et al. (2014) The protein targeting factor Get3 functions as ATP-independent chaperone under oxidative stress conditions. *Mol Cell* **56**: 116-127.

Wang, C., Dong, X., Han, L., Su, X.D., Zhang, Z., Li, J., and Song, J. (2016) Identification of WD40 repeats by secondary structure-aided profile-profile alignment. *J Theor Biol* **398**: 122-129.

Wang, P., Perfect, J.R., and Heitman, J. (2000) The G-protein β subunit GPB1 is required for mating and haploid fruiting in *Cryptococcus neoformans*. *Molecular and Cellular Biology* **20**: 352-362.

Wang, Y., Shen, G., Gong, J., Shen, D., Whittington, A., Qing, J. et al. (2014) Noncanonical Gβ Gib2 is a scaffolding protein promoting cAMP signaling through functions of Ras1 and Cac1 proteins in *Cryptococcus neoformans*. *Journal of Biological Chemistry* **289**: 12202-12216.

Warman, N.M., and Aitken, E.A.B. (2018) The movement of *Fusarium oxysporum f.sp. cubense* (sub-tropical race 4) in susceptible cultivars of Banana. *Front Plant Sci* **9**: 1748.

Woloshuk, C.P., and Shim, W.B. (2013) Aflatoxins, fumonisins, and trichothecenes: a convergence of knowledge. *FEMS Microbiol Rev* **37**: 94-109.

Wu, F., Groopman, J.D., and Pestka, J.J. (2014) Public health impacts of foodborne mycotoxins. *Annu Rev Food Sci Technol* **5**: 351-372.

Wu, J., Liu, Y., Lv, W., Yue, X., Que, Y., Yang, N. et al. (2015) *FgRIC8* is involved in regulating vegetative growth, conidiation, deoxynivalenol production and virulence in *Fusarium graminearum*. *Fungal Genet Biol* **83**: 92-102.

Xu, C., and Min, J. (2011) Structure and function of WD40 domain proteins. *Protein Cell* **2**: 202-214.

Xue, C., Hsueh, Y.-P., and Heitman, J. (2008) Magnificent seven: roles of G protein-coupled receptors in extracellular sensing in fungi. *FEMS microbiology reviews* **32**: 1010-1032.

Yan, H., and Shim, W.B. (2020) Characterization of non-canonical Gβ-like protein FvGbb2 and its relationship with heterotrimeric G proteins in *Fusarium verticillioides*. *Environ Microbiol* **22**: 615-628.

Yan, H., Huang, J., Zhang, H., and Shim, W.B. (2019) A Rab GTPase protein FvSec4 is necessary for fumonisin B1 biosynthesis and virulence in *Fusarium verticillioides*. *Curr Genet*:1-12

Yang, P., Chen, Y., Wu, H., Fang, W., Liang, Q., Zheng, Y. et al. (2018) The 5-oxoprolinase is required for conidiation, sexual reproduction, virulence and deoxynivalenol production of *Fusarium graminearum*. *Curr Genet* **64**: 285-301.

Yin, Z., Zhang, X., Wang, J., Yang, L., Feng, W., Chen, C. et al. (2018) MoMip11, a MoRgs7-interacting protein, functions as a scaffolding protein to regulate cAMP signaling and pathogenicity in the rice blast fungus *Magnaporthe oryzae*. *Environ Microbiol* **20**: 3168-3185.

Yu, H.Y., Seo, J.A., Kim, J.E., Han, K.H., Shim, W.B., Yun, S.H., and Lee, Y.W. (2008a) Functional analyses of heterotrimeric G protein Gα and Gβ subunits in *Gibberella zeae*. *Microbiology* **154**: 392-401.

Yu, J.H. (2010) Regulation of Development in *Aspergillus nidulans* and *Aspergillus fumigatus*. *Mycobiology* **38**: 229-237.

Yu, J.H., Hamari, Z., Han, K.H., Seo, J.A., Reyes-Dominguez, Y., and Scazzocchio, C. (2004) Double-joint PCR: a PCR-based molecular tool for gene manipulations in filamentous fungi. *Fungal Genet Biol* **41**: 973-981.

Yun, Y., Zhou, X., Yang, S., Wen, Y., You, H., Zheng, Y. et al. (2019) *Fusarium oxysporum f. sp. lycopersici* C_2H_2 transcription factor FolCzf1 is required for conidiation, fusaric acid production, and early host infection. *Curr Genet* **65**: 773-783.

Zeller, C.E., Parnell, S.C., and Dohlman, H.G. (2007) The RACK1 ortholog Asc1 functions as a G-protein β subunit coupled to glucose responsiveness in yeast. *Journal of Biological Chemistry* **282**: 25168-25176.

Zhang, D., Wang, Y., Shen, J., Yin, J., Li, D., Gao, Y. et al. (2018a) *OsRACK1A*, encodes a circadian clock-regulated WD40 protein, negatively affect salt tolerance in rice. *Rice* **11**: 45.

Zhang, H., Mukherjee, M., Kim, J.E., Yu, W., and Shim, W.B. (2018b) Fsr1, a striatin homologue, forms an endomembrane-associated complex that regulates virulence in the maize pathogen *Fusarium verticillioides*. *Mol Plant Pathol* **19**: 812-826.

Zhang, H., Kim, M.S., Huang, J., Yan, H., Yang, T., Song, L. et al. (2019) FvLcp1, a type-D fungal LysM protein with Chitin-binding domains, is a secreted protein involved in host recognition and fumonisin production in *Fusarium verticillioides*-maize kernel interaction. *bioRxiv*: 789925.

Zhang, H., Tang, W., Liu, K., Huang, Q., Zhang, X., Yan, X. et al. (2011a) Eight RGS and RGS-like proteins orchestrate growth, differentiation, and pathogenicity of *Magnaporthe oryzae*. *PLoS Pathog* **7**: e1002450.

Zhang, X., Jain, R., and Li, G. (2016) Roles of rack1 proteins in fungal pathogenesis. *Biomed Res Int* **2016**: 4130376.

Zhang, Y., Choi, Y.E., Zou, X., and Xu, J.R. (2011b) The *FvMK1* mitogen-activated protein kinase gene regulates conidiation, pathogenesis, and fumonisin production in *Fusarium verticillioides*. *Fungal Genet Biol* **48**: 71-79.

Zhang, Z., Qin, G., Li, B., and Tian, S. (2014) Knocking out Bcsas1 in *Botrytis cinerea* impacts growth, development, and secretion of extracellular proteins, which decreases virulence. *Molecular Plant-Microbe Interactions* **27**: 590-600.

Zheng, H., Zheng, W., Wu, C., Yang, J., Xi, Y., Xie, Q. et al. (2015) Rab GTPases are essential for membrane trafficking-dependent growth and pathogenicity in *Fusarium graminearum*. *Environmental Microbiology* **17**: 4580-4599.

Zheng, H.K., Chen, S.M., Chen, X.F., Liu, S.Y., Dang, X., Yang, C.D. et al. (2016) The small GTPase MoSec4 is involved in vegetative development and pathogenicity by regulating the extracellular protein secretion in *Magnaporthe oryzae*. *Frontiers in Plant Science* **7**. 1458

APPENDIX A

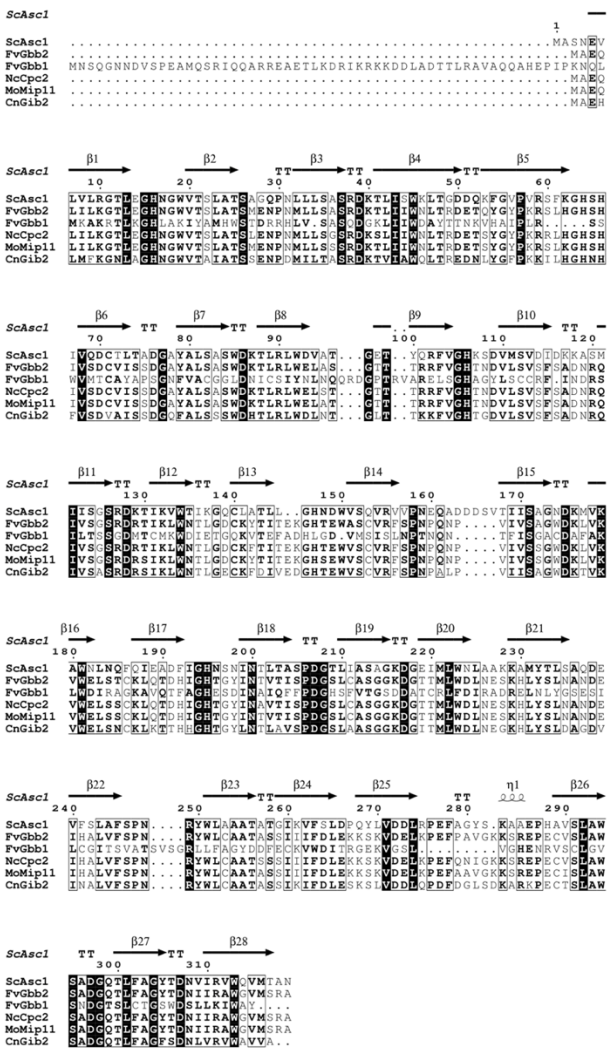

Figure A-1. Sequence alignment and domain analysis of Gβ-like proteins in fungal species.

We aligned amino acid sequences of *Saccharomyces. cerevisiae* ScAsc1, *Fusarium verticillioides* FvGbb2, *F. verticillioides* FvGbb1, *Magnaporthe oryzae* MoMip11, *Neurospora crassa* NcGnb1, and *Cryptococcus neoformans* CnGib2. Identical and similar sequences were indicated in white characters with black backgrounds and black characters in a white box, respectively. FvGbb2 is predicted to have 28 beta strands. ScAsc1 protein structure was from PDB (ID:3FRX) (Coyle et al., 2009).

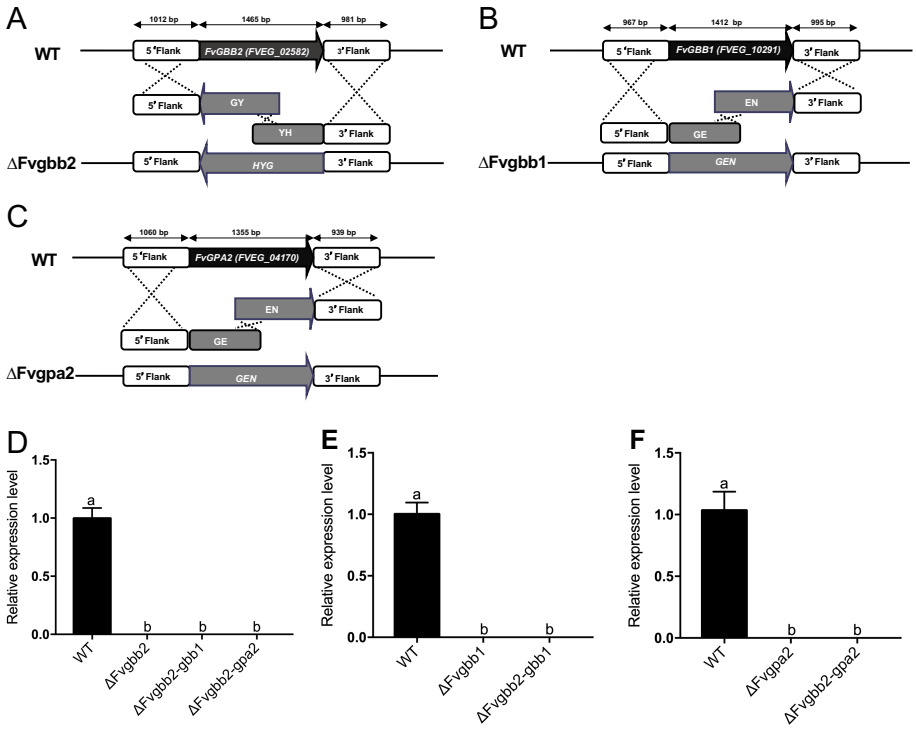

Figure A-2. Schematic description of split marker approach for generating gene deletion mutants ΔFvgbb2, ΔFvgbb1, and ΔFvgpa2 in *F. verticillioides.*
(A) Hygromycin gene (*HYG*) was used to replace the *FvGBB2* gene and generate ΔFvgbb2 mutant. (B) Geneticin gene (*GEN*) was used to replace the *FvGBB1 gene* and generate ΔFvgbb1 mutant. (C) Geneticin gene (*GEN*) was used to replace the *FvGPA2 gene* and generate ΔFvgpa2 mutant. (D) Total RNA samples were extracted from mycelia from 7-day myro liquid culture. Mutants ΔFvgbb2, ΔFvgbb2-gbb1, ΔFvgbb2-gpa2 were subject to qPCR using *FvGBB2* gene primer. *FvGBB2* transcript was not detectable in ΔFvgbb2, ΔFvgbb2-gbb1, ΔFvgbb2-gpa2 mutants when compared to the wild-type (WT) progenitor. (E) *FvGBB1* gene expression was assayed in WT, ΔFvgbb1, and ΔFvgbb2-gbb1. (F) *FvGPA2* gene expression was assayed in WT, ΔFvgpa2, and ΔFvgbb2-gpa2.

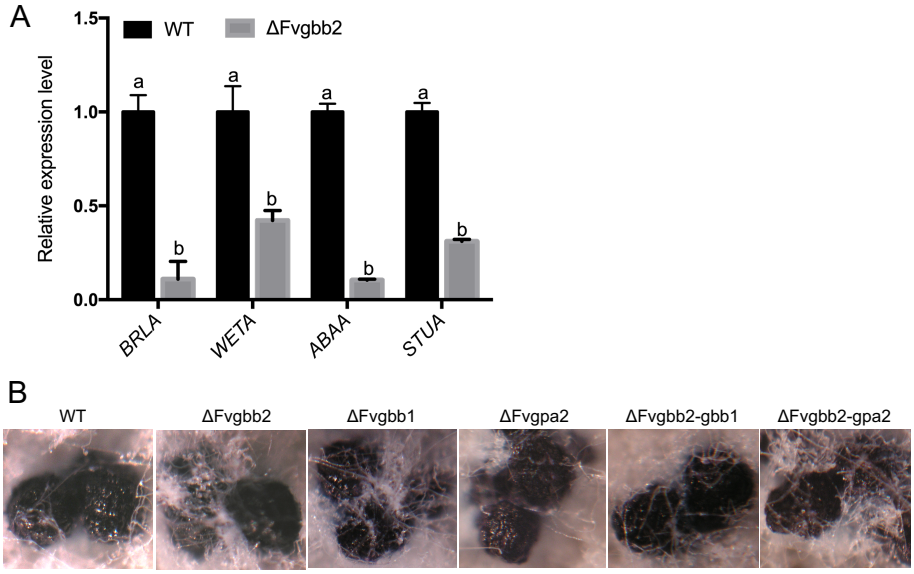

Figure A-3. Perithecia formation inf wild-type (WT) and deletion mutant strains. (A) Expression levels of conidia related genes in ΔFvgbb2 were compared to the WT in YEPD liquid medium. (B) (B) WT, ΔFvgbb2, ΔFvgbb1, ΔFvgpa2, ΔFvgbb2-gbb1and ΔFvgbb2-gpa2 strains, which all have MAT-1 mating type, were crossed to *F. verticillioides* m3120 strain (MAT-2) in carrot medium. After 3-week incubation, perithecia formation was observed.

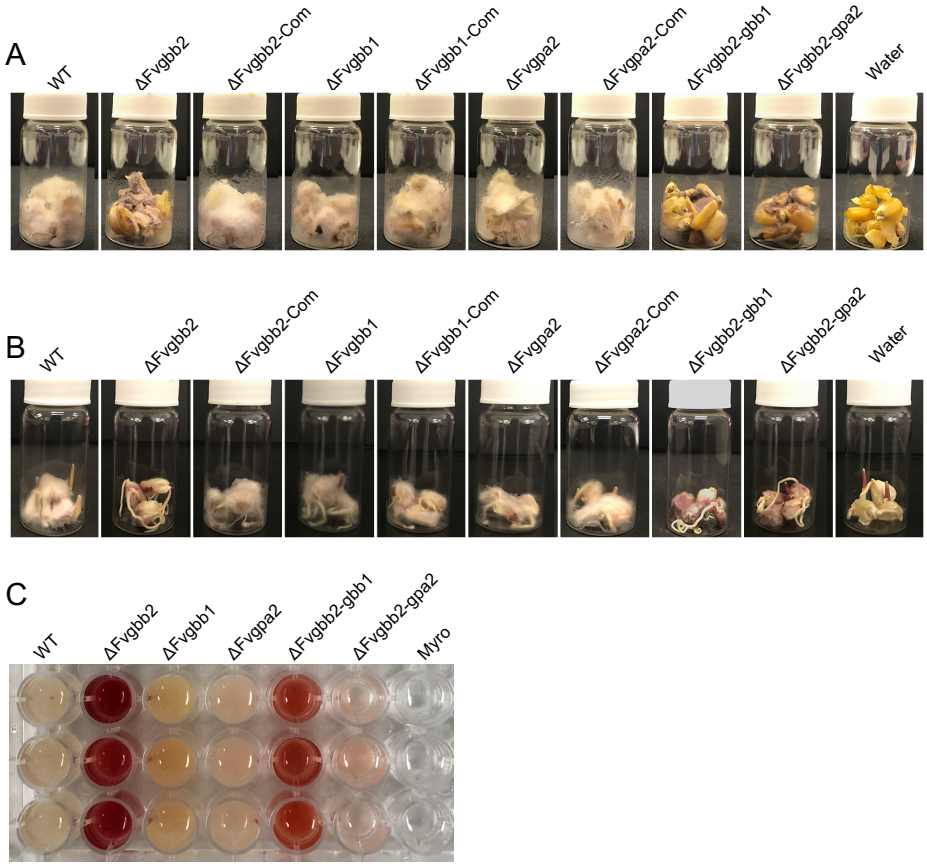

Figure A-4. ***Fusarium verticillioides*** **colonization in autoclaved cracked kernels and surface sterilized kernels.** Wild-type (WT), ΔFvgbb2, ΔFvgbb1, ΔFvgpa2, ΔFvgbb2-gbb1, ΔFvgbb2-gpa2 and complementation strains were cultured in (A) 2-g cracked autoclaved (non-viable) kernels and (B) four sterilized surface-sterilized (viable) kernels after 8 days of incubation at room temperature. (C) Pigment production when strains are grown in myro liquid medium. Two mutants ΔFvgbb2 and ΔFvgbb2-gbb1 exhibited dramatic alteration in pigmentation when cultured for 7 days with shaking.

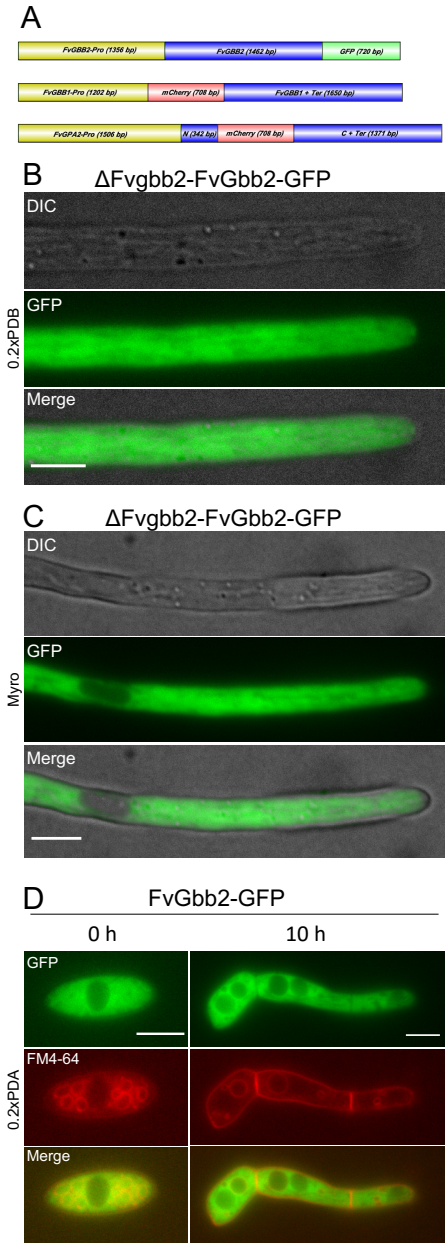

Figure A-5. FvGbb2 protein localization assays. (A) Schematic representation of FvGbb2-GFP, mCherry-FvGbb1, FvGpa2-mCherry constructs. (B) FvGbb2-GFP was expressed in the ΔFvgbb2 mutant in (B) FB1 non-inducing 0.2xPDB medium and in (C) FB1-inducing myro medium. Bar = 5 µm. (D) FvGbb2-GFP was expressed in the WT and with 10 µM FM4-64 stain after a 30-min incubation. Bar = 5 µm.

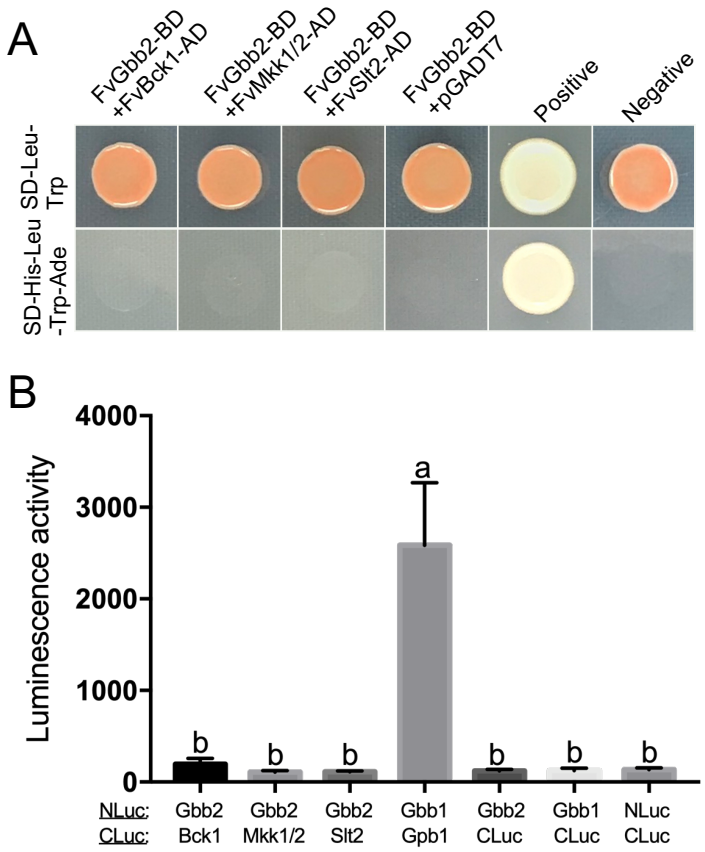

Figure A-6. Interaction between FvGbb2 and MAPK kinase cascade proteins.
(A) FvGbb2 did not show interaction with three MAPK cascade proteins when tested by yeast two-hybrid assay. FvGbb2 was co-transformed with FvBck1, FvMkk1/2 or FvSlt2 into AH109 strain. pGBKT7–53 and pGADT7-T were used as a positive control. pGBKT7–Lam and pGADT7-T were used as a negative control. (B) The split luciferase complementation analysis was performed to confirm yeast two-hybrid assays. FvGbb1-FvGpa2 complementation was used as a positive control.

Table A-1. Relative mRNA expression level of 15 PKS gene in deletion mutant strains

	Relative transcriptional level					
Gene	WT	ΔFvgbb2	ΔFvgbb1	ΔFvgpa2	ΔFvgbb2-gbb1	ΔFvgbb2-gpa2
PKS1	1[a]	0.24 ± 0.01	0.45 ± 0.19	0.58 ± 0.14	0.10 ± 0.09	0.28 ± 0.13
PKS2	1	ND	0.31 ± 0.15	0.62 ± 0.28	1.16 ± 0.46	0.46 ± 0.13
PKS3	1	762.42 ±168	1.89 ± 0.06	6.78 ± 2 79	0.47 ± 0.16	23.37 ± 10.26
PKS4	1	ND	1.28 ± 0.12	1.64 ± 0.67	ND	ND
PKS5	1	0.25 ± 0.01	0.86 ± 0.19	0.99 ± 0.01	0.75 ± 0.15	ND
PKS6	1	208.70 ± 28.52	1.32 ± 1.17	12.05 ± 4.15	131.84 ± 42.62	54.22 ± 22.75
PKS7	1	0.48 ± 0.21	0.65 ± 0.26	0.83 ± 0.42	1.14 ± 0.50	0.59 ± 0.15
PKS8	1	0.10 ± 0.02	0.23 ± 0.10	0.31 ± 0.20	0.06 ± 0.04	0.72 ± 0.18
PKS9	1	0.003 ± 0.001	0.82 ± 0.10	1.50 ± 0.10	ND	0.08 ± 0.01
PKS10	1	0.02 ±0.001	3.53 ± 1.19	1.51 ± 0.44	0.29 ± 0.01	0.08 ± 0.02
PKS11	1	ND	ND	0.86 ± 0.34	ND	ND
PKS12	ND	ND	ND	ND	ND	ND
PKS13	1	0.42 ± 0.12	0.95 ± 0.12	1.44 ± 0.55	2.46 ± 0.69	0.58 ± 0.14
PKS14	1	1.36 ± 0.15	0.76 ± 0.20	ND	0.55 ± 0.24	0.55 ± 0.02
PKS15	1	0.15 ± 0.02	0.17 ± 0.04	0.23 ± 0.10	0.43 ± 0.14	5.48 ± 0.56

Strains mycelium were harvested from 7 days of incubation on myro liquid medium. Then, total RNA samples were extracted. qPCR analysis of gene expressional levels on was conducted with SYBR-Green. Each gene expression was normalized to β-tubulin gene (FVEG_04081) expression level. Gene expressions were calculated using $2^{-\Delta\Delta Ct}$. Wild-type expression level was standardized to 1.0. Three replicates were performed for each test. *PKS5*, *PKS14*, *PKS15* expression levels were very low.

Table A-2. Primers used in this study

Primer	Primer sequence (5'-3')	Application
Gbb2_LF. F2	GCT CAG TGG ACA ACC AGA CAA A	validation of *FvGBB2* 5' deletion
Gbb2_LF. F1	TCC TTC TTC CTT TCC CGA CTT TC	amplify *FvGBB2* 5' flank sequence
Gbb2_LF. F/N	CGC AAG CAG AAA GAG GTC AAG AA	nested primer for amplify *FvGBB2-LF + YG*
Gbb2_LF. R1	TAG ATG CCG ACC GGG AAC GTT TGC GGT GAC GAG GCG AT	amplify *FvGBB2* 5' flank sequence
Gbb2_RF. F1	CCA CTA GCT CCA GCC AAG ATT GCT CTA CCC TAA AAA AGA GGC	amplify *FvGBB2* 3' flank sequence
Gbb2_RF. RN	TCT CTT ATT CAC CAG CGG ACA	nested primer for amplify *FvGBB2-RF + HY*
Gbb2_RF. R1	GTT GGG CGA TCA CCA TAA CTA	amplify *FvGBB2* 3' flank sequence
Gbb1/LF/F2	GTG TTT GGG TGA GCG GAT G	validation of *FvGBB1* 5' deletion
Gbb1-LF/F1	CGG GTA CTT GAT GTT TGG TGG A	amplify *FvGBB1* 5' flank sequence
Gbb1-LF/FN	ACG GAT GAA CTG GAG TCG A	nested primer for amplify *FvGBB1-LF + GE*
Gbb1-LF/R1	GGC GTT ACC CAA CTT AAT CGA TCG ACC AGT CAA CTT TTG TTG T	amplify *FvGBB1* 5' flank sequence

Gbb1_RF/F1	TTC CAC ACA ACA TAC GAG CCT TGT TCT TTG CGA CTA TGA ACC TT	amplify *FvGBB1* 3' flank sequence
Gbb1_RF/RN	ACA CAC GTC CGA CAG CAA ATA	nested primer for amplify *FvGBB1-RF + EN*
Gbb1_RF/R1	ACG GGA TAA GTG CGG AAT GTT	amplify *FvGBB1* 3' flank sequence
Gpa2_ LF/F2	ACA TGG AGG CTT GTG AGG TTA T	validation of *FvGPA2* 5' deletion
Gpa2_LF/F1	ACC TTA CTT TCC CGT CCC TC	amplify *FvGPA2* 5' flank sequence
Gpa2_LF/FN	TTT GGC ATT ACT TCC GCT TGC	nested primer for amplify *FvGPA2-LF + GE*
Gpa2_LF/R1	GGC GTT ACC CAA CTT AAT CGT GTG GCG GAT CAC AAA ATA GCT	amplify *FvGPA2*5' flank sequence
Gpa2_ RF/F1	TTC CAC ACA ACA TAC GAG CCT AGC GAA TCA CTG CTC ATT TGA	amplify *FvGPA2*3' flank sequence
Gpa2_ RF/RN	GTC ATT TAC GCC AAG CGA CTA T	nested primer for amplify *FvGPA2-RF + EN*
Gpa2_RF/R1	AAG CTC CAA TCC ACA TCC AGA	amplify *FvGPA2* 3' flank sequence
HYG/F	TTG GCT GGA GCT AGT GGA GGT CAA	amplify HY fragment
HY/R	GTA TTG ACC GAT TCC TTG CGG TCC GAA	amplify HY fragment
HYG/R	GTT CCC GGT CGG CAT CTA CTC TAT	amplify YG fragment
YG/F	GAT GTA GGA GGG CGT GGA TAT GTC CT	amplify YG fragment

GEN/F	CGA TTA AGT TGG GTA ACG CCA G	amplify GE fragment
GE/R	ATC ACG GGT AGC CAA CGC TA	amplify GE fragment
EN/F	TCG ACC ACC AAG CGA AAC AT	amplify EN fragment
GEN/R	GGC TCG TAT GTT GTG TGG AAT T	amplify EN fragment
Gbb2-BD-F	CCG GAA TTC ATG GCC GAA CAA TTG ATC CTG AA	construction of pGBDT7-*FvGBB2*
Gbb2-BD-R	CCG GGA TCC TTA TGC CCT CGA CAT GAC ACC	construction of pGBDT7 -*FvGBB2*
Gpa1-AD-F	CCG GAA TTC ATG GGT TGC GGA ATG AGC	construction of pGADT7-*FvGPA1*
Gpa1-AD-R	CCG GGA TCC TTAGAT GAG ACC ACA GAG ACG CAG	construction of pGADT7 -*FvGPA1*
Gpa2-AD-F	CCG GAA TTC ATG GGC GCA TGC ATG AGC T	construction of pGADT7-*FvGPA2*
Gpa2-AD-R	CCG GGA TCC TCA AAG AAT GCC CGA GTC CTT AAG TG	construction of pGADT7 -*FvGPA2*
Gpa3-AD-F	CCG GAA TTC ATG CTG CAG AAA CAC ATG GCC	construction of pGADT7-FvGPA3
Gpa3-AD-R	CCG GGA TCC TTA GAG AAT GAG CTG CTT GAG GTT G	construction of pGADT7 -*FvGPA3*
Gpb1-AD-F	CCG GAA TTC ATG CCT CAG TAC ACT TCT CGC	construction of pGADT7-*FvGPB1*
Gpb1-AD-R	CCG GGA TCC TTA CAT GAC CAC ACA GCA GC	construction of pGADT7 -*FvGPB1*

Mkk1/2-AD-F	CGG AAT TCA TGG CCG ACC AAC AGC CT	construction of pGADT7-*FvMKK1/2*
Mkk1/2 -AD-R	TCC CCC GGG CTA AGA GTC CTT AGG TTG TTC ATC CC	construction of pGADT7 -*FvMKK1/2*
Slt2_AD-F	CGG AAT TCA TGT CGG ACC TTC AAG GAC G	construction of pGADT7-*FvSLT2*
Slt2_AD-R	CGG GAT CCT TAT CTC CTG GAG GCA TCC A	construction of pGADT7 -*FvSLT2*
Bck1-AD-F1	ACCAGATTACGCTCATATG ATGAAGGGTAGCGATAGCTTG	construction of pGADT7 -*FvBCK1*
Bck1-AD-R1	ATT TGG CGA ATC CAT GGG ATC	construction of pGADT7-*FvBCK1*
Bck1-AD-F2	TCCCATGGATTCGCCAAATACACCTCTCAA TGCCCCTG	construction of pGADT7 -*FvBCK1*
Bck1-AD-R2	CTA TTT CGT TGG ACA TCC TCG G	construction of pGADT7-*FvBCK1*
Bck1-AD-F3	CCG AGG ATG TCC AAC GAA ATA G	construction of pGADT7 -*FvBCK1*
Bck1-AD-R3	CAG CTC GAG CTC GAT GGATCC TTA TTT GAA CGA CTT GAT TTT GTG ATA CAG	construction of pGADT7 -*FvBCK1*
Gbb2_nLUC/F	AAG CTC GAG TAG TCG ACA TGG CCG ACC AAC AGC CTG AA	construction of pFNLuc *FvGBB2*
Gbb2_nLUC/R	CGT ACG AGA TCT GGT CGA CTG CCC TCG ACA TGA CAC CCCA	construction of pFNLuc *FvGBB2*

Gbb1_nLUC/F	AAG CTC GAG TAG TCG ACA TGA ACT CTC AAG GCA ACA ACG A	construction of pFNLuc-*FvGBB1*
Gbb1_nLUC/R	CGT ACG AGA TCT GGT CGA CGT AGG CCC AGA TTT TAA GCA G	construction of pFNLuc-*FvGBB1*
Gpa1_cLUC/F	CGT CCC GGG GCG GTA CCG GTT GCG GAA TGA GCA CAG A	construction of pFCLuc-*FvGPA1*
Gpa1_cLUC/R	TTG GAT CCC CGG GTA CCT TAG ATG AGA CCA CAG AGA CGC AG	construction of pFCLuc-*FvGPA1*
Gpa2_cLUC/F	CGT CCC GGG GCG GTA CCG GCG CAT GCA TGA GCT CG	construction of pFCLuc-*FvGPA2*
Gpa2_cLUC/R	TTG GAT CCC CGG GTA CCT CAA AGA ATG CCC GAG TCC TTA AGT G	construction of pFCLuc-*FvGPA2*
Gpa3_cLUC/F	CGT CCC GGG GCG GTA CCC TGC AGA AAC ACA TGG CCA	construction of pFCLuc-*FvGPA3*
Gpa3_cLUC/R	TTG GAT CCC CGG GTA CCT TAG AGA ATG AGC TGC TTG AGG TTG	construction of pFCLuc-*FvGPA3*
Gbb1_cLUC/F	CGT CCC GGG GCG GTA CCA ACT CTC AAG GCA ACA ACG A	construction of pFCLuc-*FvGBB1*
Gbb1_cLUC/R	TTG GAT CCC CGG GTA CCT TAG TAG GCC CAG ATT TTA AGC AG	construction of pFCLuc-*FvGBB1*
Mkk1/2_cLUC/F	CGT CCC GGG GCG GTA CCG CCG ACC AAC AGC CTC AAA GT	construction of pFCLuc-*FvMKK1/2*
Mkk1/2_cLUC/R	TTG GAT CCC CGG GTA CCC TAA GAG TCC TTA GGT TGT TCA TCC CAG	construction of pFCLuc-*FvMKK1/2*

Slt2_cLUC/F	CGT CCC GGG GCG GTA CCT CGG ACC TTC AAG GAC GGA	construction of pFCLuc-*FvSLT2*
Slt2_cLUC/R	TTG GAT CCC CGG GTA CCT TAT CTC CTG GAG GCA TCC A	construction of pFCLuc-*FvSLT2*
Bck1_cLUC/F	CGTCCCGGGGCGGTACC AAGGGTAGCGATAGCTTGC	construction of pFCLuc-*FvBCK1*
Bck1_cLUC/R	TTGGATCCCCGGGTACC TTA TTT GAA CGA CTT GAT TTT GTG ATA CAG	construction of pFCLuc-*FvBCK1*
cLUC_F:	GAT TGA CAA GGA TGG ATG GCT AC	screening paired with each gene cLUC/R
nLUC-R	GGT AGA TGA GAT GTG ACG AAC GTG	screening paired with each gene nLUC/F
Gbb2-GFP-F	AGG GAA CAA AAG CTG GGT ACC CGC TAC GAC GGC ACA ATG TT	construction of pKNTG-*FvGBB2*
Gbb2-GFP-R	GCC CTT GCT CAC CAT AAG CTT TGC CCT CGA CAT GAC ACC	construction of pKNTG-*FvGBB2*
Gbb1-pro-F	AGG GAA CAA AAG CTG GGT ACC GTG TTT GGG TGA GCG GAT G	amplify *FvGBB1* native promoter
Gbb1-pro-R	CTC CTC GCC CTT GCT CAC CAT CGT GAT CGA CCA GTC AAC TTTT	amplify *FvGBB1* native promoter
Gbb1-F	GGC ATG GAC GAG CTG TAC AAG ATG AAC TCT CAA GGC AAC AAC GA	amplify *FvGBB1* coding sequence
Gbb1-R	TCA GTA ACG TTA AGT GGA TCC GTA TAG CCG TCA ACT CCT ATG GA	amplify *FvGBB1* coding sequence

Gpa2-pro-F	AGG GAA CAA AAG CTG GGT ACC ACA TGG AGG CTT GTG AGG TTA T	amplify *FvGPA2* native promoter
Gpa2-pro-R	TGA TCC GCC TCC TCA TTG CT	amplify *FvGPA2* native promoter
Gpa2-N-F	AGCAATGAGGAGGCGGATCA	amplify *FvGPA2* partial coding sequence
Gpa2-N- R	CTC CTC GCC CTT GCT CAC CAT GGC TTG GTA TTC TAA TAG GAA CTC C	amplify *FvGPA2* partial coding sequence
Gpa2-C-F	GGC ATG GAC GAG CTG TAC AAG GAG TCT GGC CCT CAA GCG CAA AT	amplify *FvGPA2* partial coding sequence and terminal
Gpa2-Ter-R	TCA GTA ACG TTA AGT GGA TCC AAG GGA AGC CAT ACG CCT GTT CTC	amplify *FvGPA2* partial coding sequence and terminal
mCherry-F	ATGGTGAGCAAGGGCGAGGAG	amplify mCherry fragment
mCherry-R	CTT GTA CAG CTC GTC CAT GCC	amplify mCherry fragment
Gbb2-qpcr_F1	ATC GTC TCC GAC TGT GTC ATC TCC TCT GA	qPCR analysis
Gbb2-qpcr_R1	TAG TAC CGC TGG CAA GCT CCC AGA	qPCR analysis
Gbb1-qPCR_F1	TTC GTG GCT TGC GGT GGT CT	qPCR analysis
Gbb1-qPCR_R1	TCA CGG GCA ACA CGG GTA GG	qPCR analysis
Gpa2-qPCR-F1:	TGA GCA GGT CTC CGC TAG GCA A	qPCR analysis
Gpa2-qPCR-R1	TGT CGC TTG CGT CAA GTG GGG A	qPCR analysis
Tub2-F	CAG CGT TCC TGA GTT GAC CCA ACA G	qPCR analysis

Tub2-R	CTG GAC GTT GCG CAT CTG ATC CTC G	qPCR analysis

Underlined sequences represent overlaps with a DNA fragment, or a linearized vector used for joint PCR. Sequences in gray background represent restriction enzyme.

APPENDIX B

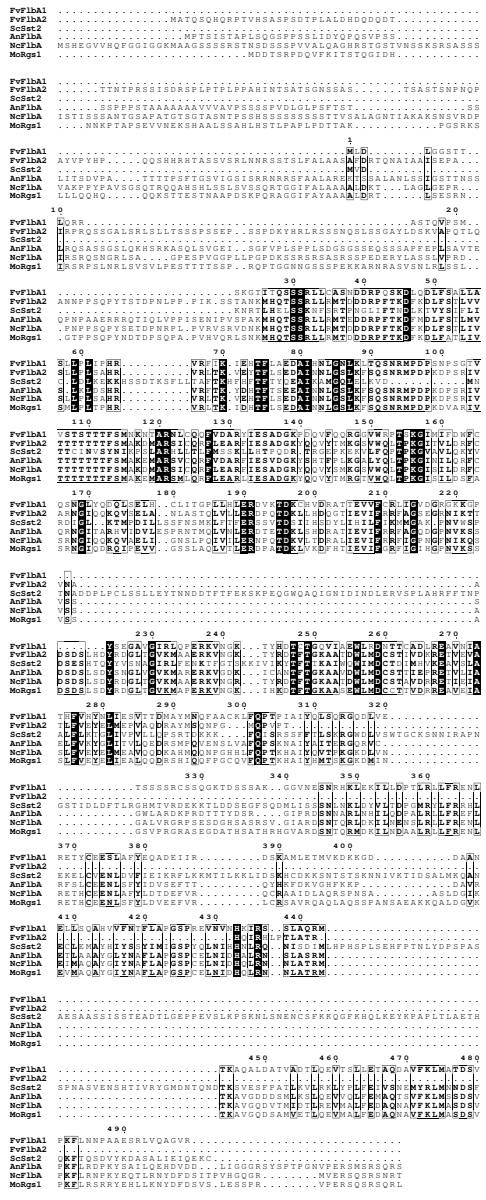

Figure B-1. Sequence alignment FlbA ortholog proteins in select fungal species. We aligned protein sequences of *Fusarium verticillioides* FvFlbA1, *F. verticillioides* FvFlbA2, *Saccharomyces cerevisiae* ScSst2, *A.nidulans* AnFlbA, *Neurospora crassa* NcFlbA, and *Magnaporthe oryzae* MoRgs1. Identical and similar sequences were displayed in the box.

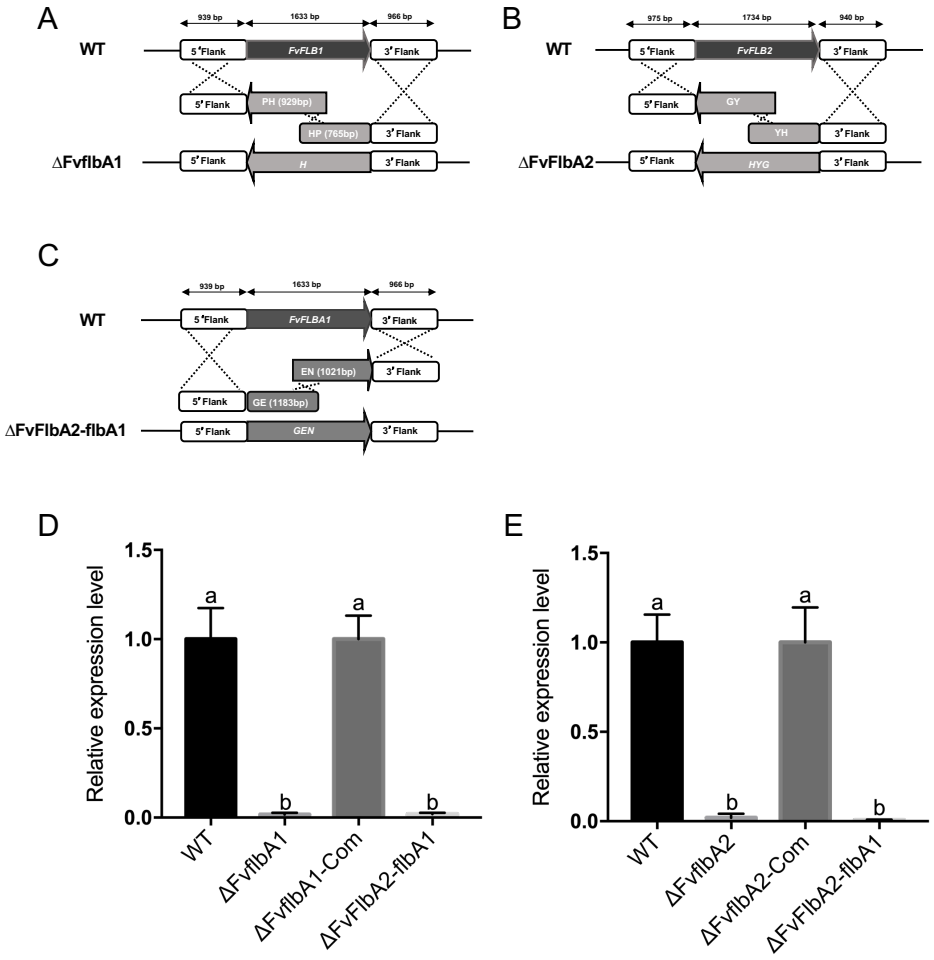

Figure B-2. Split marker approach employed in *FLBA* generating gene deletion mutants in *F. verticillioides*.

(A) ΔFvflbA1 mutant was generated by replacing *FLBA1* gene with a hygromycin B phosphotransferase gene (*HPH*). (B) *FvFLBA2 gene* was replaced by a hygromycin gene to generate a ΔFvflbA2 mutant. (C) ΔFvflbA2/A1*FvFLBA1* was generated by replacing *FLBA1* gene with a geneticin gene (*GEN*) in ΔFvflbA2 background. (D) Mutants ΔFvflbA1, ΔFvflbA1-Com, ΔFvflbA2/A1 were subject to qPCR using *FvFLBA1* gene primer. Relative expression was normalized to *F. verticillioides* β-tubulin gene (FVEG_04081). (E) *FvFLBA2* gene transcription level was examined in WT, ΔFvflbA2, ΔFvflbA2-Com, ΔFvflbA2/A1 strains.

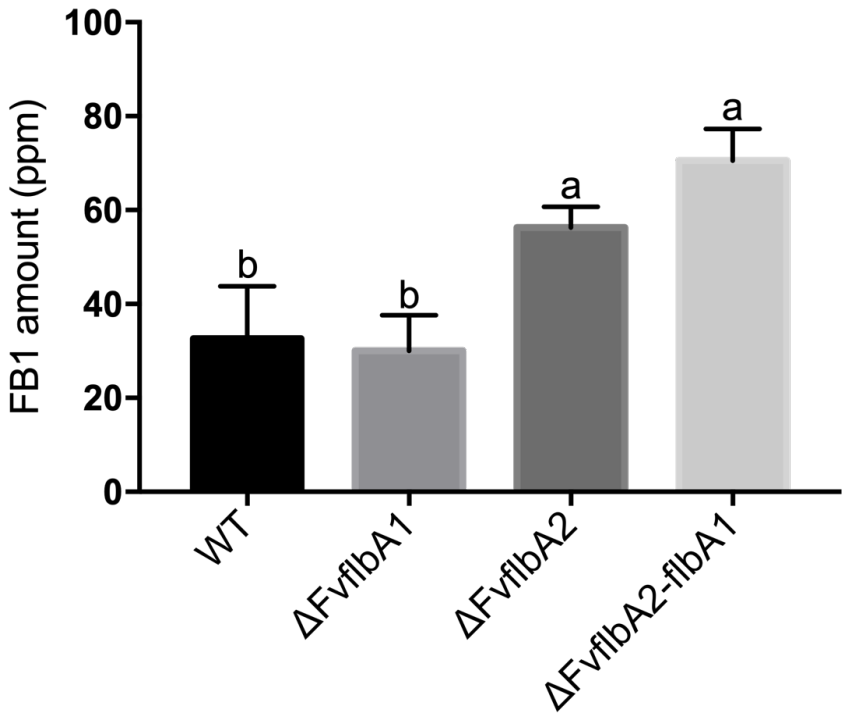

Figure B-2. Relative FB1 expression in wild-type and FvflbA mutants.
FB1 was extracted from supernatant (2ml) of 7-day incubation at 150 RPM in myro liquid culture. In details, YEPD mycelial samples (3 dpi) were harvested through Miracloth (EMD Millipore). Subsequently, mycelia (0.3g) were inoculated into 100 ml myro liquid medium at room temperature.

Table B-1. Primers used in this study

Primer	Primer sequence (5'-3')	Application
FlbA1_LF/F2	CAG TTG TCC CGC CGT TCT ACA T	validation of *FvFLBA1* 5' deletion
FlbA1_LF/F1	TAT CTC GTT TAG CCT CCT TGA GC	amplify *FvFLBA1* 5' flank sequence
FlbA1_LF/N	GAT GTT CGG TTC ATG TCC ATG C	nested primer for amplify *FvFLBA1-LF + YG or LF+GE*
FlbA1_LF/R1	TAG ATG CCG ACC GGG AAC ATG AAT GAA TGA AGC AGC ACA GC	amplify *FvFLBA1* 5' flank sequence
FlbA1_LF/R1-GE	GGC GTT ACC CAA CTT AAT CGA TGA ATG AAT GAA GCA GCA CAG C	amplify *FvFLBA1* 5' flank sequence for double knockout
FlbA1_RF. F1	CCA CTA GCT CCA GCC AAG GTT CGA TGT AAT ACA GCG AGC GA	amplify *FvFLBA1* 3' flank sequence
FlbA1-RF/F1-EN	TTC CAC ACA ACA TAC GAG CCG TTC GAT GTA ATA CAG CGA GCG A	amplify *FvFLBA1* 5' flank sequence for double knockout
FlbA1_RF/RN	GTT TAG CGT TCG GAC AGA TGG	nested primer for amplify *FvFLBA1-RF + HY and RF+EN*
FlbA1_RF/R1	TGC CAG GAA GTC AAC AAC ATA C	amplify *FvFLBA1* 3' flank sequence
FlbA2_LF/F2	GCT TCT CCA GCT TGT TGG TAT GT	validation of *FvFLBA2* 5' deletion

FlbA2_LF/F1	AGA CAG ACA AGC AAT TCA GGC	amplify *FvFLBA2* 5' flank sequence
FlbA2_LF/FN	CAA GCA AGC CCA CAT GGA ATA GA	nested primer for amplify *FvFLBA2-LF + YG*
FlbA2_LF/R1	TAG ATG CCG ACC GGG AAC CTA ACG GGA ACG AGA AAG GTC A	amplify *FvFLBA2* 5' flank sequence
FlbA2_RF/F1	CCA CTA GCT CCA GCC AAG GGA TCT TGT CAG TGG TGC TG	amplify *FvFLBA2* 3' flank sequence
FlbA2_RF/RN	GAG GCA GAT GAT GGA TGT GAG AA	nested primer for amplify *FvFLBA2-RF + HY*
FlbA2_RF/R1	GAA GCC GAG GCG ACA AAT AAA	amplify *FvFLBA2* 3' flank sequence
HYG/F	TTG GCT GGA GCT AGT GGA GGT CAA	amplify HY fragment
HY/R	GTA TTG ACC GAT TCC TTG CGG TCC GAA	amplify HY fragment
HYG/R	GTT CCC GGT CGG CAT CTA CTC TAT	amplify YG fragment
YG/F	GAT GTA GGA GGG CGT GGA TAT GTC CT	amplify YG fragment
GEN/F	CGA TTA AGT TGG GTA ACG CCA G	amplify GE fragment
GE/R	ATC ACG GGT AGC CAA CGC TA	amplify GE fragment
EN/F	TCG ACC ACC AAG CGA AAC AT	amplify EN fragment
GEN/R	GGC TCG TAT GTT GTG TGG AAT T	amplify EN fragment
FlbA1-qPCR-F	ATG CTT GAC CTA GGA GGT TCT AC	validation of *FvFLBA1* deletion
FlbA1- qPCR R	TCA TCG CAC GCC AGC CTG AA	validation of *FvFLBA1* deletion
FlbA2- qPCR-F	ATG GCC ACT CAG TCG CAA CC	validation of *FvFLBA1* deletion

FlbA2- qPCR-R	TTA CCG CGT TGC GAG AGT T	validation of *FvFLBA1* deletion
Fum21- qPCR-F	CGG TTT GCG AGG ATC TGT TCT TCT ATC	*FvFUM21* qPCR
Fum21- qPCR-R	ACC GAG CTT GCG CTA TAC TCA G	*FvFUM21* qPCR

APPENDIX C

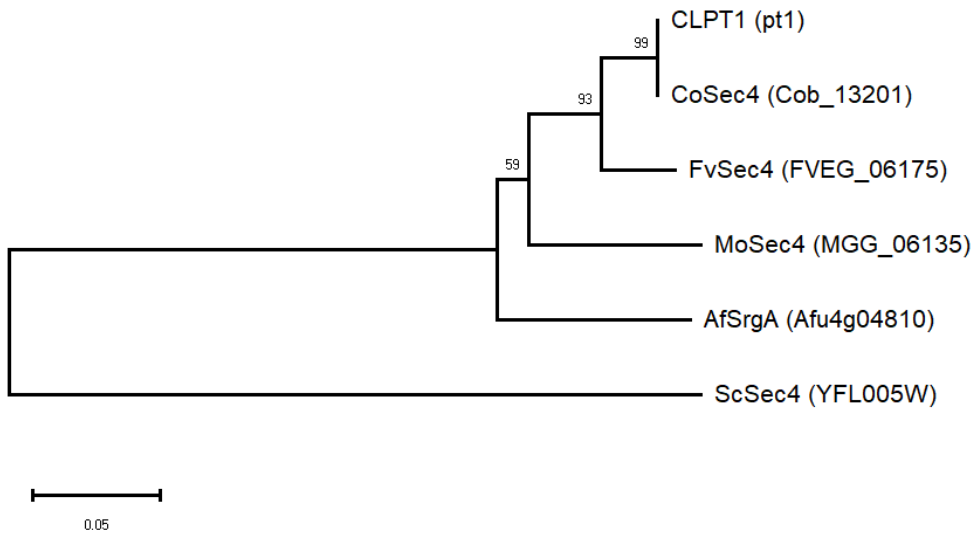

Figure C-1. Phylogenetic analysis for FvSec4 and other Sec4 orthologs.
Multiple sequences were aligned by ClusterX2. A neighbor-joining tree was constructed by MEGAX. The number at nodes indicates the percentage of replicate trees clustered together in 1000 bootstrap replications.

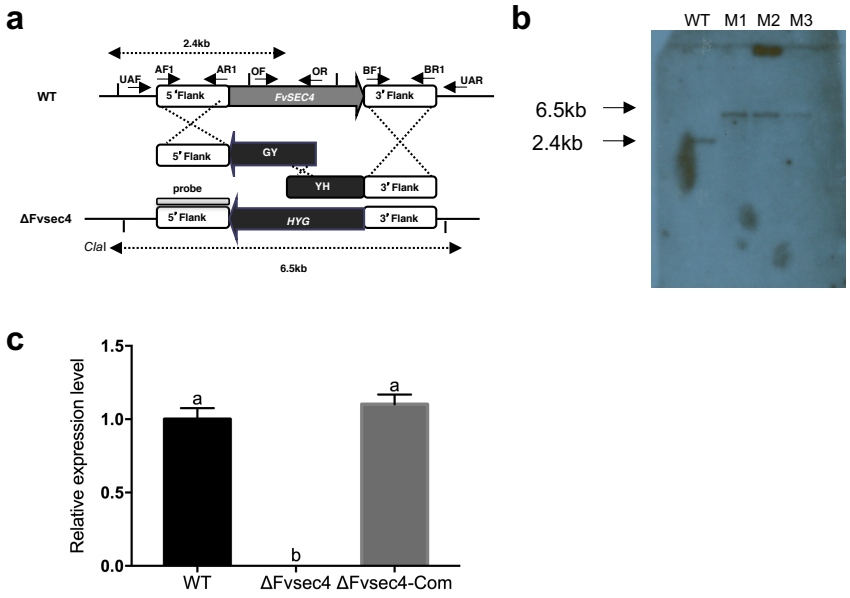

Figure C-2. ΔFvsec4 knockout schematic overview and verifications

(a) Homologous gene recombination approach used to construct ΔFvsec4 mutant in *F. verticillioides*. (b) Southern blot analyses of WT and three knockout candidates (M1, M2, M3). M1 was used in this study as ΔFvsec4. We used the 5'-flanking regions as a probe for Southern blot. (c) WT, ΔFvsec4 and ΔFvsec4-Com total RNAs were isolated after 7 days in myro liquid medium and reversed to cDNA. qPCR was employed to verify the ΔFvsec4 and ΔFvsec4-Com using a *FvSEC4* gene-specific primer set while WT was as a control. No detectable FvSec4 transcript in the ΔFvsec4 mutant by qPCR analysis and ΔFvsec4-Com fully recover the *FvSEC4* expression.

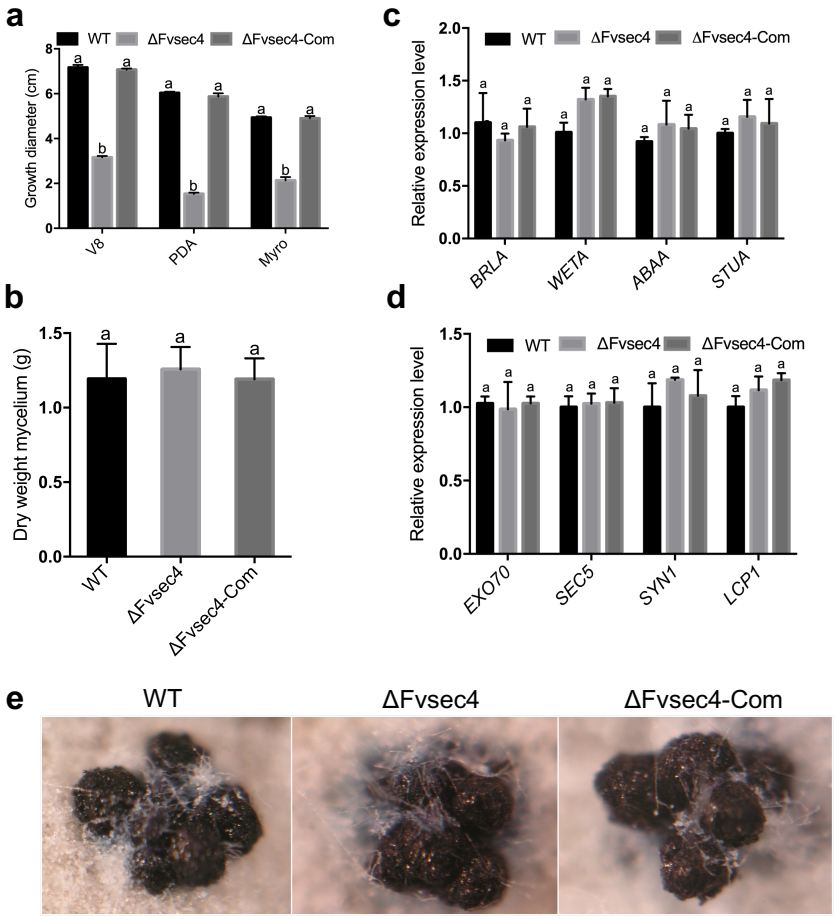

Figure C-3. Involvement of FvSec4 the vegetative growth but not perithecia in sexual mating. (a) Mycelia growth diameter on V8, 0.2xPDA and myro solid medium were assayed after 8 days at room temperature. (b) Same weight of mycelia from YEPD was transferred into myro liquid medium for constant shaking. Samples were collected after 7 days incubation in 100ml myro liquid medium. (c) qPCR study of putative *BRLA*, *WETA*, *ABAA* and *STUA* after 20 h incubation in YEPD liquid medium. (d) 20 h samples in YEPD medium was studied the expression of exocyst-related and FvLcp1 gene expression. (e) WT, ΔFvsec4 and ΔFvsec4-Com were crossed to M3120, an opposite mating type to assay fertility.

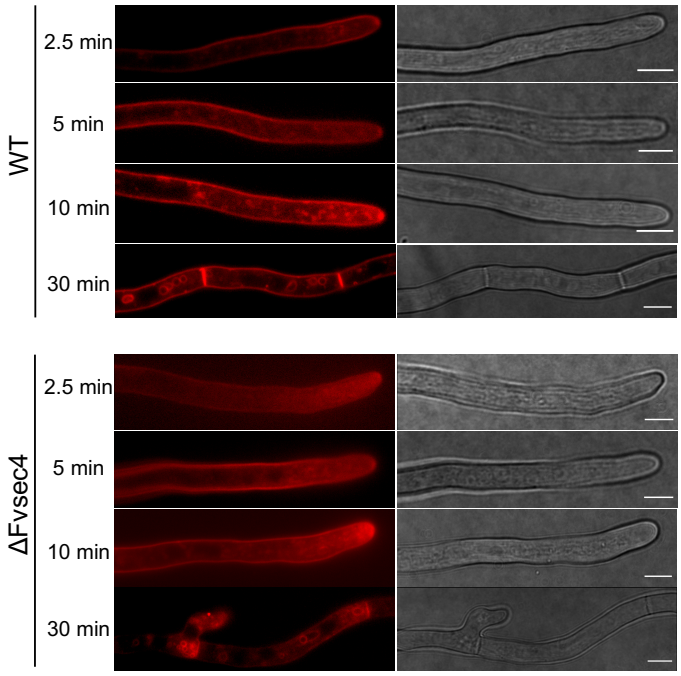

Figure C-4. FM4-64 staining with time course in WT and ΔFvsec4.
We inoculated 10 µl conidia (10^6/ml) of WT and ΔFvsec4 on 0.2x PDA agar plates overnight. WT and ΔFvsec4 were stained with 10 µl of 10 µM FM4-64 for 2.5, 5, 10 and 30 mins. Bars=10 µm.

Table C-1. Primers used in this study

Primer	Primer sequence (5'-3')	Application
UAF	TTCCTGCTCCCTATGGTGAT	amplify *FvSEC4* 5' flank sequence
AF1	GTG AAT GTG GTT GCC AGA ATG C	amplify *FvSEC4* 5' flank/probe sequence
AR1	TAG ATG CCG ACC GGG AACCGGGACTAATCCGTTTGC	amplify *FvSEC4* 5' flank/probe sequence
BF1	CCA CTA GCT CCA GCC AAGAGCGGTCGTTGTTGGAGTA	amplify *FvSEC4* 3' flank sequence
BR1	CTC TTG ACC CGA TAC CTA ATC G	amplify *FvSEC*4 3' flank sequence
UAR	GCCCTTCCTCCCTTTATTTC	amplify *FvSEC4* 3' flank sequence
HYG/F	TTGGCTGGAGCTAGTGGAGGTCAA	amplify HY fragment
HY/R	GTATTGACCGATTCCTTGCGGTCCGAA	amplify HY fragment
HYG/R	GTTCCCGGTCGGCATCTACTCTAT	amplify YG fragment
YG/F	GATGTAGGAGGGCGTGGATATGTCCT	amplify YG fragment
OF	AATCGCATCGCACTGTTGTC	*FvSEC4* ORF screening
OR	AGCGCATTGCTTTGTTGG	*FvSEC4* ORF screening
AF2	TCAAGTATCCCATGCCAGTTC	*FvSEC4* complementation
BR2	TGGCTGAGGGCTTTGGTT	*FvSEC4* complementation

SEC4-PF	gtcgacggtatcgataagctt TCAAGTATCCCATGCCAGTTC	amplify *FvSEC4* promoter sequence
SEC4-PR	CTC GCC CTT GCT CAC CAT GTT GAC CAA GAG TGA GAG TAG C	amplify *FvSEC4* promoter sequence
GFP-F	ATG GTG AGC AAG GGC GA	amplify GFP sequence
GFP-R	CTT GTA CAG CTC GTC CAT GC	amplify GFP sequence
ORF-F	cacggcatggacgagctgtacaagATG TCG AGT AAT CGC AAC TAT GAT	amplify *FvSEC4* cDNA sequence
ORF-R	GGA CTC CTT AGG GTA TTC GGT TTA GCA GCA CTT GCT	amplify *FvSEC4* cDNA sequence
Ter-F	ACC GAA TAC CCT AAG GAG TCC	amplify *FvSEC4* terminal sequence
Ter-R	tcagtaacgttaagtggatcc TAT GAC GGA GGA GAC GAG GT	amplify *FvSEC4* terminal sequence
BrlA-qpcr-F1	CGT CAC AAG CAA ACT TTC CAC GGT	qPCR analysis
BrlA-qpcr-R1	CGT GTA GCT TGC GGT GGT TGT T	qPCR analysis
WetA-qpcr-F1	GGC ATC CAC ACA CCA GCA GAA T	qPCR analysis
WetA-qpcr-R1	GAT GCT GCC AAG CTG ACT GAG GA	qPCR analysis
AbaA-qpcr-F1	TAC CGC AAC CGA CAA GCA CAC AA	qPCR analysis
AbaA-qpcr-R1	GTG AGG CAT GAG AAG AAC AGA GTC AAC A	qPCR analysis
StuA-qpcr-F1	TGT AGC ACG GAG AGA AGA TAA CCA CAT GA	qPCR analysis
StuA-qpcr-R1	ATC TTG ACG ACG TGG CGA ACC TTT	qPCR analysis
Exo70-qpcr-F1	GCT CTA GAT GAA GAA GCA AGG GCT GA	qPCR analysis
Exo70-qpcr-R1	ATC AAC GTT ATT TCC CAA TAT CTG CAG TCG	qPCR analysis
Sec5- qpcr -F1	TGA AGA AGA CGG AGG ACG ACT GGT TAAT	qPCR analysis
Sec5- qpcr_R1	CGA ATG TTT CTA TCC CCT GAG TCC AATGC	qPCR analysis

Syn1-qpcr-F1	CCC TCG TCG TTC AGC AAG AA	qPCR analysis
Syn1-qpcr-R1	AGC AAC ACA AAT ACC CAA GCA G	qPCR analysis
Lcp1-qpcr-F1	TAT GGA CCT GAG GAG GAC GAA TG	qPCR analysis
Lcp1-qpcr-R1	CAC CAA AGG TAC TCC CAG CAA TC	qPCR analysis
Sec4_qPCR_F1	GTG CGA CTG GGA GGA GAA GCG	qPCR analysis
Sec4_qPCR_R1	GCT GAG GGT TGG TCG TTC TTG G	qPCR analysis
Tub2-F	CAG CGT TCC TGA GTT GAC CCA ACA G	qPCR analysis
Tub2-R	CTG GAC GTT GCG CAT CTG ATC CTC G	qPCR analysis